DISSERTATION

EXPLORING MICROBIOME-TARGETED INTERVENTIONS IN THE MITIGATION OF ENDOTHELIAL DYSFUNCTION

Submitted by

Briana D. Risk (Greenlee)

Department of Food Science & Human Nutrition

In partial fulfillment of the requirements

For the Degree of Doctor of Philosophy

Colorado State University

Fort Collins, Colorado

Summer 2024

Doctoral Committee:

Advisor: Tiffany L. Weir
Co-Advisor: Christopher L. Gentile

Adam J. Chicco
Michelle T. Foster

ABSTRACT

EXPLORING MICROBIOME-TARGETED INTERVENTIONS IN THE MITIGATION OF ENDOTHELIAL DYSFUNCTION

Cardiovascular disease (CVD) has been the leading cause of mortality in the United States for more than seventy years eclipsing cancer and respiratory disease by more than 13%. Despite sincere efforts to decrease the incidence of CVD, various environmental and intrinsic factors contribute to CVD progression, making it challenging to mitigate this complex condition. However, the past decade has shown tremendous growth in understanding the connection between the gut microbiome in its protective, or pathogenic progression of CVD. The gut microbiome, or the consortia of microbial species, genes, and metabolites, that shapes the gastrointestinal environment has a profound impact on the vascular endothelium through mechanisms not yet entirely understood. Therefore, the purpose of the research in this dissertation was to: 1) Utilize next-generation sequencing and metabolomics to characterize microbial contribution to varied endothelial response after a dietary blueberry intervention in post-menopausal females; 2) Determine if a hypertensive microbiome after blueberry treatment confers gastrointestinal and endothelial phenotype in a humanized mouse model; 3) Evaluate the efficacy of a probiotic in reversing endothelial dysfunction in dietarily obese mice, while exploring the contribution to gut barrier integrity and vasoactive metabolite proliferation in a novel cell co-culture.

ACKNOWLEDGEMENTS

I would like to thank my rockstar advisors, Drs. Tiffany Weir and Christopher Gentile. Education is a challenging journey. It is an unknown path that we venture into, hoping to actualize our dreams and become better versions of ourselves. I firmly believe that it is impossible to reach your potential without mentorship and people who believe in your dreams as well. I only made it through graduate school with the support and guidance of both of my mentors. Although I am a bit unorthodox, they believed in my vision to create a better world through the lens of nutrition, and have fostered my development as a scientist and a critical thinker. I will never be able to fully repay them for their dedication to their students such as myself, but I hope to one day have a fraction of their poise, determination, and generosity.

I would also like to thank my committee members Dr. Adam Chicco and Dr. Michelle Foster. Dr. Chicco graciously allowed me to spend time in his lab which was no less during a pandemic when times were uncertain. To learn the fine art of qPCR and Western blotting and to be part of an interdisciplinary team with which I am still friends to this day. To Dr. Michelle Foster who has always been willing to share her scientific knowledge, resources, and style tips. Our hallway interactions will always be cherished. Outside my committee, I would like to thank Dr. Doreen Hyatt with whom I now have a thirteen-year relationship being her student for undergraduate work, then a teaching assistant, and friend. To work in tandem exploring the delicate work of microbes and petri dishes has been an absolute pleasure. To Dr. Matthew Hickey, who was always available to listen and offer sage advice on the intricacies of graduate school and to push me to think about the unknowns in human metabolism. Vive le tour, Dr. Hickey. To Dr. Josiane Broussard whose enthusiasm and approachability helped me to remember what I care about when times were uncertain. To Drs. Edit Szalai and Melinda Clark.

My friends that not only ride bikes but have given me perspective and guidance about what is truly important in life.

I owe a warm hug and thank you to my primary labmate Elliot Graham. We have worked in tandem over the years learning lab techniques from scratch and celebrating each other's successes and failures. It was on us to rewrite the script and I could not be more thankful for Elliot's gusto and fist bumps throughout this journey. To Mrs. Mingue Zhang, a beautifully intelligent woman who outworks even the most driven of us for her passion for creating a better world. To Natasha Williams for her honesty, no matter how brutal. To Lance Poehlein for his tenacity and willingness to work with impossibly small instruments. To the soon-to-be Dr. Raj Trikha that I may not have been able to start this adventure without. Lastly, to Dr. Caitlin Clark, Annika Webber, Paul Matthews, Scott Wrigley, Sylvia Lee, Emily Woolf, Nancy Ghanem, Ana Altares, Annie Campain, Viridiana Gonzalez, Natalie Mendez as the FSHN grad students who have all been part of my tribe to make the magic happen.

DEDICATION

"Discipline is remembering what you want"

I would like to dedicate this journey to my mother LeAnn, grandparents Elaine, Bonnie, Lynn and Dave, and my husband Jay for putting up with my insatiable desire to change the face of nutrition, and to be pillars throughout this eighteen-year journey. I have only been able to reach for the stars because of your love, generosity, and unwavering support.

TABLE OF CONTENTS

CHAPTER 1: MICROBIAL METABOLITE PRODUCTION AND ENDOTHELIAL DYSFUNCTION, REVIEW OF THE EVIDENCE

I. SUMMARY

Metabolites are small signaling molecules that facilitate chemical reactions in the human body. They are derived from a variety of sources including the food we eat and transformations via the gut microbiome. Accumulating evidence suggests that certain microbial metabolites either support cardiovascular homeostasis or contribute to the dysfunction of the inner lining of blood vessels, known as the endothelium, in the progression of cardiovascular disease (CVD). This narrative review highlights the scientific evidence of the contribution of the gut microbiome in producing diet-derived metabolites and the complex interactions of these compounds with endothelial dysfunction in the progression of CVD. Polyphenol-derived, phenyl-containing amino acids, and short-chain fatty acid metabolite production are dependent on members of the microbiome and have been studied in various human, rodent, and cell culture trials for their role in influencing endothelial inflammation and other processes related to endothelial dysfunction. Given the connection between diet, microbiome, and metabolites, dietary interventions aimed at modifying the production of microbial metabolites hold promise in mitigating endothelial dysfunction and serving as potential biomarkers for lifestyle and CVD progression. Future research on the translation from clinical results to community-based interventions may be the next step in implementing microbial metabolites in healthcare to reduce cardiovascular disease burden.

II. INTRODUCTION

From the Greek translation of “micro” meaning small, and “biome” meaning life, the microbiome is a collection of bacteria, archaea, fungi, and viruses, along with their genomes and the immediate environment surviving with a host.[1] The human gut microbiome, which will be referred to simply as the microbiome, is a complex and dynamic system that provides many functions to the host and has a crucial role in mediating metabolic processes that the host is unable to perform on its own. It is established that the microbiome is critical for host homeostasis and imbalances have associations with chronic health conditions such as cardiovascular disease (CVD).[2] Endothelial dysfunction is an independent risk factor for CVD, apart from established risk factors. It occurs due to altered signaling from the vascular endothelium, thereby limiting blood vessel dilation even under appropriate stimulus.[3] While the community of organisms that shapes the microbiome is critical, the question arises as to what features of a microbiome impact health or disease states. Specifically, the microbiome’s diverse array of metabolite signaling molecules plays a pivotal role in regulating various physiological processes and is the subject of extensive research to better understand the connection between the microbiome and human health and disease.

This review will focus on the microbial production of diet-derived metabolites and the known and proposed interactions to endothelial dysfunction related to CVD risk. Emphasis will be placed upon polyphenol-derived metabolites with ties to phenyl-containing amino acid metabolites, and short-chain fatty acids as these metabolites were examined in corresponding chapters included in this dissertation. Each metabolite will be classified by its dietary source, digestion process, and microbiome interaction, along with its unique impacts on endothelial dysfunction and CVD.

III. METABOLITES, MICROBIOME, AND ENDOTHELIAL FUNCTION

Metabolites are small chemical compounds that serve as signaling molecules, energy sources, and mediators of cellular redox reactions.[4] There are thousands of metabolites in the body that are produced and altered by both the host and microbes in various ways. For instance, they can be derived from microbial metabolism, produced by the host and modified by microbiota, or formed by microbes and transformed by the host. Metabolites directly reflect the biochemical activity of the system as a whole, and have profound effects on host metabolism, gut homeostasis, and vascular function.[5] Collectively, metabolites play an important role in host-microbiome-diet interactions that impact health and susceptibility to disease.[6] Thus, the advancement of metabolite research has the potential to provide mechanistic insight into links between the microbiome and host physiology.

One link that microbial metabolites have to host health, is their interplay with the vascular endothelium. The endothelium is made from a single layer of cells that lines blood vessels and comes in contact with the bloodstream and its components.[7] This semi-permeable organ is responsible for an infinite number of processes, but a primary function is its action as an endocrine organ by signaling the underlying smooth muscle in controlling vascular tone.[7] While a healthy endothelium properly signals the blood vessel to contract or relax to regulate blood pressure, endothelial dysfunction alters signaling pathways that limit proper vasodilation which has links to hypertension.[3] Furthermore, systemic inflammation can aggravate the endothelium increasing monocyte adhesion in foam cell formation and atherosclerosis prognosis.[8] A number of variables impact endothelial function, and recent research indicates that microbial metabolites, directly and indirectly, influence endothelial health.

Endothelial dysfunction and CVD incidence are strongly correlated to lifestyle factors such as nutrition.[9] As diet directly shapes the microbiome,[10] defining functional food and supplements that act upon the microbiome and its metabolites may be an alternative means for mitigating CVD risk. Despite a limited understanding of the bioavailability and bioactivity of

microbial metabolites, marked differences in microbiome profiles in healthy versus diseased states.[6] For example, a Western diet high in processed sugar and fat shifts microbial diversity and taxa that precede CVD development.[11] In contrast, epidemiological evidence suggests that diets high in plant-derived polyphenols may reduce the risk of CVD.[12,13] More specifically, microbial cleavage of polyphenolic compounds found in plants, increases the bioactivity of polyphenols that support endothelial health by limiting systemic inflammation and mediating endothelial signaling .[14] Therefore, exploring dietary interventions that aim to modify the microbiome can provide valuable insights into the role of microbial metabolites in influencing CVD, and serve as potential biomarkers for lifestyle and disease progression.

IV. PLANT POLYPHENOLS

A. INTRODUCTION

Polyphenols are a large family of plant metabolites containing hydroxylated phenyl groups present in various plant foods such as berries, green tea, spices, legumes, and nuts.[15] Plants produce polyphenols to protect against sun exposure, plants, animals, and other potential threats. To date, over 8000 polyphenols have been identified, with more to be discovered.[15] Their complex structure and high molecular weight, limit absorption of parent polyphenols to ~5%,[16] and is commonly called the 'low bioavailability/high bioactivity paradox'.[17] Very little of the parent polyphenols are absorbed in the small intestine,[18] rather microbial species liberate these polyphenols in the colon.[18] Despite the extensive transformation and low percentage that reaches the bloodstream, polyphenols still potently affect host metabolism. One area of great interest is the potential advantage of incorporating polyphenol-rich foods into the diet in mitigating CVD by targeting the endothelium.[19]

B. RESVERATROL

Resveratrol is a polyphenolic phytoalexin that is an antimicrobial extracted from the roots, stems, leaves, fruit, and seeds of plants.[20] It is highly concentrated in the skin of grapes

and found in a variety of other foods such as blueberries, peanuts, rhubarb, banana, guava, pineapple peach, apple, passion fruit, pear, potato, pistachio, and cucumber.[16] Resveratrol in its storage form is linked to glucose in the plant matrix as piceid (ie. polydatin).[21] Piceid is a glycoside and absorbed by the intestine to some extent,[22,23] although the microbiome is key to liberating the more bioactive resveratrol. Certain species of the *Lactobacillus* and *Bifidobacterium* genera contain β-glucosidases that deglycosylate piceid into resveratrol.[24] Additionally, secondary gut microbiota such as *Slackia equolifaciens* and *Adlercreutzia equolifaciens* contribute to resveratrol biotransformation through hydroxylation to dihydroresveratrol and other dihydroxyresveratrol derivatives that lend to conjugation for absorption.[25] It should be noted that *cis* and *trans*-isomers of piceid and resveratrol both exist. Yet, the *trans*-isomer is far more predominant and stable both in the plant and after extraction.[26] Although trans-resveratrol is lipophilic, which contributes to its low oral bioavailability, it is rapidly absorbed in the intestines after liberation from the microbiota through passive diffusion, or by complexing with transporters such as integrins, allowing it to enter circulation.[27,25] Circulating free trans-resveratrol binds to albumin or lipoproteins allowing for systemic transport for cellular offloading.[27] Resveratrol that passes through the liver can be glucuronidated and sulfated, carried out by uridine-5′-diphosphate-glucuronosyltransferases (UGT) and sulfotransferase (SULT) enzymes.[28] These secondary metabolites can then re-enter circulation or be transferred to the gut for recycling or elimination.[25]

The research behind trans-resveratrol has been focused on its antioxidant properties in limiting vascular oxidative stress. Systemic inflammation affects the endothelium, increasing monocyte adhesion and increasing the likelihood of foam cell formation and atherosclerotic plaque accrual.[8] At a transcriptional level, resveratrol inhibits proinflammatory cytokine production such as interleukin-1 and -6 (IL-1, IL-6), tumor necrosis factor-α (TNF-α) and suppresses the cytokine mediators nuclear factor kappa-light-chain-enhancer (NF-kB) and toll-like receptors, ultimately lowering chronic low-grade inflammation due to reactive oxygen

species (ROS) production.[29] Additionally, resveratrol quenches inflammatory preformed ROS, thereby protecting cellular membranes from lipid peroxidation while retaining the membrane potential of mitochondria and reducing cytochrome-C-induced apoptosis.[29] These additive effects of trans-resveratrol decrease the reactivity of the endothelium, thereby reducing the binding and extravasation of monocytes into the interstitial layer for foam cell development. Interestingly, trans-resveratrol may counteract the endothelial damaging effects of another microbiome-derived metabolite, trimethylamine oxidase (TMAO). Chen et. al showed that resveratrol shifted the composition of the microbiome in ApoE$^{-/-}$ mice reduced the presence of microbiota that produce the TMAO precursor TMA, and increased bile salt hydrolase-producing *Lactobacillus* and *Bifidobacterium,* ultimately decreasing circulating concentrations that contact the endothelium, and expediting bile acid synthesis in cholesterol turnover.[30] In humans, resveratrol's anti-inflammatory effects on the endothelium may have overall positive effects on the endothelium in CVD. A recent meta-analysis found that resveratrol reduced atherogenic TNF-α and c-reactive protein in patients with CVD.[31] In a clinical trial, 100mg of resveratrol for twelve weeks patients decreased arterial stiffness in patients with type II diabetes mellitus in which those with a more pronounced effect had poor endothelial function at baseline.[32] In another study, resveratrol treatment improved flow-mediated dilation in hypertensive females, but not males, with endothelial dysfunction suggesting sex-related differences in response to resveratrol.[33]

C. UROLITHINS

Ellagitannins and ellagic acid are the precursors for urolithin metabolites and are found in berries and other foods such as blackberry, raspberry, strawberry, pomegranate, and walnut.[16] Ellagitannins are hydrolyzed to ellagic acid in the small intestine via bacterial tannase enzymes, then converted to urolithin-A, B, C, or D by *Gordonibacter, Enterocloster, Bifidobacteria,* and *Ellagibacter* genera,[34–36] in the colon.[37,38] Phase II biotransformation of adding hydrophilic groups to urolithins in intestinal enterocyte cells results in glucuronidated,

methylated, or sulfonated urolithins.[39] The type of hydrophilic group that is added dictates the fate of tissue distribution.[39] For example, urolithin-A establishes a presence in the intestine, whereas glucuronidated urolithin-A predominantly resides in the liver.[38] There are many secondary metabolites of urolithins, making research difficult to pinpoint which types of urolithins affect specific organs. For this review, the focus will be on urolithin-A as it is the most conserved and aptly studied urolithin across species.[40]

Urolithin-A has been detected in a dose-response fashion in plasma after repeated ellagitannin exposure.[41] However, not all individuals have this dose-response production of urolithins from ellagitannins/ellagic acid intake.[42,43] There are three identified urolithin metabotypes (UM) that relate to urolithin production. Metabotype A (UM-A) individuals dominantly produce urolithin-A, metabotype B (UM-B) produce varying concentrations of urolithin-A and urolithin B, and metabotype O (UM-O) do not produce urolithins, despite consumption of ellagitannin and ellagic acid-rich foods.[44] After years of investigation into the intricacies of these metabotypes, evidence suggests that UM-A has antiinflammatory properties via modulation of the microbiome in response to ellagitannin degradation.[45,46] Furthermore, metabotype may be associated with age. In a human clinical trial, Cortez-Martin et. al demonstrated that the UM-A metabotype decreases from ages 20-40 years old with an increase in the UM-B metabotype after the age of 40.[47] The UM-B metabotype is associated with a higher risk for CVD in obese individuals, but preliminary evidence suggests this metabotype can shift based on dietary intervention.[46] For example, daily supplementation at the equivalent dose of 117ml or 467ml of pomegranate juice for 3 weeks between washout periods in the 'POMEcardio' study shifted UM-B individuals to the urolithin-producing UM-A metabotype.[46] This shift was correlated with an improvement in serum lipid profiles in those who initially started with a UM-B metabotype at the beginning of treatment, and the urolithin-A producer *Gordonibacter* was significantly elevated in all participants after supplementation, implicating modulation of the microbiome.[46]

The production of urolithin-A is dependent on a two-step process from ellagitannin conversion to ellagic acid, with subsequent transformation of ellagic acid to urolithin-A. The microbiota that initiates the first conversion of ellagitannins to ellagic acid in the human body has yet to be ascertained. However, *in vitro* studies have observed *Akkermansia muciniphila* produces ellagic acid in response to ellagatannin exposure[48] and certain *Lactobacillus* genera (*L. plantarum, L. plantarum, L. pentosus*) release tannase enzymes involved in ellagic acid production.[40] In 2014 *Gordonibacter urolithinfaciens* and *Gordonibacter palemaeae* were the first bacterial species found to produce urolithin-A both *in vivo* and in cell culture.[34,49] Further studies have since identified *Bifidobacterium pseudocatenulatum*[36] and *Enterococcus faecium*[50] bacterial species to generate urolithin-A. Interestingly, the *Gordonibacter* genus is part of the *Corioibacteriaceae* family that also liberates resveratrol and produces equol from isoflavone polyphenols, indicating a close relationship with this family of bacteria to generalized polyphenol biotransformation.[40]

Urolithin-A is known for its anti-inflammatory[51] and anti-atherogenic[46] properties. The link to transcriptional inflammation regulation was first noted in 2010 when rats with induced inflammatory bowel disease were treated with urolithin-A and exhibited downregulated mRNA concentrations of cyclooxygenase 2 (COX2), and decreased prostaglandin E2 (PGE2).[52] Further examination showed that urolithin-A blocked NF-κB of activated B-cells involved in cell proliferation and inflammation[53,54] and that urolithin-A induced selective autophagy and mitophagy in cellular turnover[55]. These processes recycle damaged organelles to maintain homeostasis and decrease inflammatory ROS, thereby limiting cellular senescence. Thus, the antioxidant mechanism of urolithin-A activation within the human body influences inflammatory signaling and cellular turnover, making it a potent agent for endothelial health and CVD. Urolithin-A treatment in human aortic endothelial cells (HAECs) after TNF-α inflammatory insult significantly decreases monocyte adhesion and endothelial cell migration implicated in atherosclerotic lesion progression.[56][57][56]In a small randomized crossover trial of ten

healthy male volunteers, flow-mediated dilation (as a proxy for endothelial function), significantly increased at two and twenty-four hours after raspberry consumption.[58] Plasma ellagic acid, urolithin A-3-glucuronide, and urolithin A-sulfate also correlated with flow-mediated dilation improvements, and eight of the participants were classified as UM-A.[58] Another trial in those with UM-B metabotype and poor flow-mediated dilation at baseline, showed trending improvement after 50mg/d of urolithin-A supplementation along with increased alpha diversity of the microbiome.[59]

D. ISOFLAVONES

Much like resveratrol, isoflavones are antimicrobial phytoalexins produced by plants as a defense mechanism against environmental attack.[60] The three main active isoflavones in human-consumed food are daidzein, genistein, and glycitein. These compounds are mainly stored in plants bound to sugars as glycoside conjugates (ie. daidzin, genistin, glycitin) in legumes such as peanuts,[61] and in fruits and nuts including currents, raisins, coconut, prunes, mango, dates, strawberries, cranberries, hazelnuts[62] and even the livestock feed clover and alfalfa[6062] However, the dominant food source of isoflavones stored in soybeans in concentrations of up to 2g/kg wet weight.[62] Soybean has been well-studied in its cardioprotective effects with the ability to lower LDL-C as observed by several meta-analyses.[63–66] The United States Food and Drug Administration issued the health claim that " the daily dietary intake level of soy protein that has been associated with reduced risk of coronary heart disease is 25 grams (g) or more per day of soy protein" per CFR title 21 section 101.82.[67] Recent meta-analyses have also shown the intake of 3mg per day of isoflavones significantly decreases the incidence of coronary heart disease among all populations.[68] Teasing apart the mechanisms of soybean intake, isoflavones may be the culprit due to their ability to mitigate chronic inflammation,[69] and limit oxidation of LDL-C that induces a reactive endothelium to produce atherosclerotic lesions via monocyte extravasation[8]. However, these positive benefits are

partially dependent on the individual microbiota and the dynamics that release isoflavones from their storage structure.

Plants store daidzin, genistin, and glycitin isoflavone functional units bound to a saccharide by a glycosidic linkage. These glycosides make it difficult for the body to absorb isoflavones, as the linkage must be broken before they can be absorbed by the GI tract.[70] Once ingested, β-glucosidase enzymes produced by the intestinal brush border and members of the *Lactococcus, Enterococcus, Lactobacillus*[16] microbiota genera break glycosidic bonds in the isoflavones, thereby releasing daidzein, genistein, and glycitein from their attached saccharide.[70,71] The resulting isoflavones are passively absorbed by the intestinal epithelial cells, mainly in the jejunum, or undergo further conjugation into secondary metabolites to enter the bloodstream or hepatic portal circulation.[16,70] In the liver, isoflavones conjugate with glucuronic or sulfonic hydrophilic groups that move into circulation before urinary excretion or reentry into the colon for further microbial transformation or elimination.[16] Despite these modifications to improved bioavailability, plasma isoflavone concentrations only reach 0.5-1.3% of absorbed isoflavone by weight, supporting the 'low bioavailability/high bioactivity paradox'.[72]

There are numerous isoflavone metabolites that are not discussed in this review. Yet, there is one crucial isoflavone-derived metabolite that solely relies on the microbiota residing in the colon. In 1932, equol was the first isoflavone to be discovered.[73] It is the only microbially produced metabolite produced from isoflavone daidzein and is considered a secondary metabolite, and not a polyphenol or phytoestrogen, as it is not pre-formed in plants and requires microbial enzymes for production.[60]

Equol exists in two forms, known as enantiomers, with a chiral carbon located at position C-3 in the furan ring.[74] These enantiomers are known as S-equol or R-equol, and only the former is produced by human GI microbiota.[74] Humans, unlike animals, cannot innately produce S-equol, and its presence solely depends on the composition of the microbiome, and diet.[60] The involvement of the microbiota has been confirmed as germ-free mice do not

manufacture S-equol[70], which will be referred to simply as equol for the remainder of this review. Furthermore, human infants only start producing equol at 4-6 months of age after the microbiome begins to develop.[75] Identifying bacteria that produce equol has proven challenging. However, researchers have identified a few select species in daidzein transformation to equol including *Eggerthella sp*. strain YY7918, *Adlercreutzia equolifaciens, Lactococcus garvieae,* and certain members of the *Slackia* genus.[76]

Equol production is not universal among humans due to intrinsic variations in the microbiome. Equol-producers are defined as individuals with plasma concentrations over 83nmol/L and non-equol producers lower than 40nmol/L.[60] The production of equol is influenced by diet, as evidenced by studies on bacterial fermentation of isoflavone-containing carbohydrates.[77] Equol-producers on a high carbohydrate diet manufacture large amounts of equol compared to those on a low carbohydrate diet. Extensive research conducted by Setchell et. al revealed that 60% of Vegetarians produce equol compared to 25% of non-vegetarians, and 50-60% of Asian populations compared to 20-30% of Western countries generate equol.[78] It has been hypothesized that those who do not produce equol may instead convert daidzein into O-desmethylanogolensin. This conversion is carried out by a distinctly different population of microbiota, such as *Eubacterium ramulus* and certain members from the *Clostridium* cluster XIVa that may be explained by interindividual variability.[79]

The mechanisms of how equol affects the cardiovascular system in certain demographics are not entirely clear, but it is hypothesized that equol triggers antioxidant pathways in the delicate endothelial cells that line the vasculature. Equol limits the negative effect of oxidized LDL-C by decreasing monocyte chemoattractant protein-1 (MCP-1), thereby reducing the adhesion of monocytes[80] and limiting ROS production in endothelial cells[81]. Additionally, equol directly impacts the endothelium by stimulating nitric oxide production to signal blood vessel dilation,[82] as demonstrated in rodent aortic ring and umbilical vein cell models.[82,83] The

endothelium contains multiple receptors that stimulate the endothelial nitric oxide release, and one such receptor of particular interest is estrogen receptorβ (ERβ).

Equol, and the other flavonoids such as quercetin and myricetin, are comprised of non-steroidal phenol rings that closely mimic the scaffolding of 17β estradiol (E2) estrogen.[84] This molecular mimicry gives isoflavones the ability to bind to α and β host estrogen receptors.[84] and binding affinity to estrogen receptor α (ERα) and/or ERβ receptor subtypes are distributed throughout tissues in different concentrations with different functions.[85] ERα is dominantly found in mammary glands, uterus, epididymis, kidneys, liver, and white adipose tissue[86] in which receptor binding promotes cell proliferation[87]. ERβ is distributed throughout the colon, salivary glands, vascular endothelium, lung, and bladder and inhibits the proliferative effect ERα signaling.[86] Isoflavones preferentially bind to ERβ with a 20- to 300-fold higher binding capacity over ERα.[87] This is in contrast to endogenously produced estradiol (E2) estrogen with approximately equal affinity for either α and β ER subtype.[88] Equol has the highest bioavailability of the isoflavones [75] and binds with greater affinity to ERβ than its precursor daidzein.[75,87] In endothelial cell culture models, equol that binds to ERβ rapidly activates the PI3K/AKT pathway that phosphorylates serine 1177 on endothelial nitric oxide synthase (eNOS) to produce the vasodilation molecule, nitric oxide.[83] In ovariectomized rats, long-term equol intake partially restored endothelial-mediated dilation and increased phosphorylation of eNOS.[89] Additionally, another study showed that equol induced acute relaxation of naive rat aortic rings,[82] suggesting that equol has profound endothelial stimulation in various models.

Observational studies and randomized control trials have demonstrated that equol production may be anti-atherogenic by limiting arterial stiffness and ultimately reducing the incidence of coronary artery disease (CHD) in select demographics.[90] Equol producers have less coronary artery calcification,[91] less carotid intima-media thickness progression,[92] reduced diastolic blood pressure,[93] decreased low-density lipoprotein cholesterol (LDL-C),[94] and reduced mean arterial pressure and pulse wave velocity[93]. Zhang et. al were the first to show that equol,

but not other isoflavones had a significant inverse relationship with CHD in females after soy intake.[95] In another prospective observational study, 10 mg/d of equol taken for a year significantly decreased arterial stiffness in middle-aged females with moderate to high risk for atherosclerosis.[96] Additionally, Usui et al. trialing 10 mg/d in overweight or obese individuals for twelve weeks found equol supplementation significantly reduced cardio-ankle vascular index as a measure of arterial stiffness and serum LDL-C, and this effect was more prominent in female non-equol producers.[94] In contrast, acute dosing of equol in men with moderate CVD risk significantly improved pulse wave velocity twenty-four hours after intake in equol-producers, but not in non-producers.[97] The discrepancies in these results are unclear but indicate that sex and equol-producer status may be variables that contribute to interindividual response and variation seen in equol research.

E. QUERCETIN

Quercetin is a commonly consumed flavonol recognized as a pigment in foods such as blueberries, lettuce, onion, tomato, broccoli, buckwheat, and apple.[16,98,99] The US population consumes approximately 15mg of quercetin isoforms daily from food,[100] with a 25-60 fold increase by individuals who supplement with quercetin.[101] Quercetin was first discovered by Nobel laureate Alber Szent Gyorgyi in 1938. He originally co-discovered vitamin C and vitamin P, in which the latter was coined rutin (ie. quercetin glycoside).[102] Quercetin in plants is bound to saccharide moieties such as rutin, or quercetin-3-*O* or 4-*O* glucosides and the processing of quercetin is complex and requires the involvement of intestinal enzymes and the microbiome. For example, rutin is a glycoside of quercetin complexed by a linkage to the disaccharide rutinose (comprised of rhamnose and glucose).[103] The rutinose functional group is first removed by microbial genera[104] such as *Bacillus, Veillnella, and Bacteroides*[105] or intestinal lactase phlorizin hydrolase enzymes[16] to become aglycone quercetin. Alternatively, sodium-dependent glucose transporter-1 (SGLT-1) transports rutin into the intestinal enterocyte, where cytosolic β-glucosidase hydrolyzes rutinose into its constituents.[106] When rutinose is removed, quercetin

easily crosses into small intestine enterocytes through passive diffusion. The phase II enzymes UGT, SULT, and catechol-O-methyltransferases (COMT) add functional groups to quercetin so that glucoronated, sulfated, and methylated forms of quercetin enter the bloodstream.[16] Or, quercetin that remains in the intestines may travel via the portal vein to the liver to be acted upon by UGT, SULT, or COMT as well before entering systemic circulation or into the biliary tract for excretion.[16,98] Quercetin secondary metabolite distribution and function in tissues is poorly understood. Still, it is thought that quercetin may accumulate in organs, and its half-life in the body is extended by continuous dietary consumption of quercetin[107] and enterohepatic recycling.[98] Quercetin metabolites further degraded by the microbiota are found in the urine mainly as 3-hydroxylacetic, benzoic, and hippuric acid[16] and fecal matter as short-chain fatty acids (SCFAs).[108]

There is a growing body of evidence that quercetin has profound effects on cardiovascular health. Several high-fat diet animal models with quercetin supplementation exhibited improved endothelial-mediated dilation, increased eNOS expression,[109] and reduced atherosclerotic plaque formation[110–113]. Quercetin supplemented in rats inhibits platelet aggregation in a dose-dependent response[114] which has also been observed in human blood.[115] In two human randomized control trials, quercetin significantly decreased atherogenic oxidized LDL.[116,117] Moreover, acute administration of 200 mg of quercetin in twelve healthy males resulted in reduction of the vasoconstrictive endothelin-1 as compared to the control.[118] Recent meta-analyses suggest that supplementation of 100mg/d of quercetin reduces overall systolic and diastolic blood pressure, decreases circulating triglycerides, and increases high-density lipoprotein (HDL) cholesterol when regularly administered for >8 weeks.[119] The effects of quercetin are evident in a dose-dependent mechanism where quercetin >500mg/d has been shown to decrease blood pressure in normotensive and hypertensive individuals.[120] Furthermore, in a double-blind, placebo-controlled, crossover trial, 160 mg/d of quercetin-3-

glucoside taken for one month reduced soluble endothelial selectin as a marker of endothelial inflammation in males and females with elevated blood pressure.[121]

The exact mechanisms of quercetin's effects on vascular health are not known, as there are various influences of quercetin at the endothelium. Quercetin's antioxidant properties of scavenging ROS (such as superoxide, hydroxyl radicals, and peroxynitrite) protect the endothelium that facilitates nitric oxide production to signal vasodilation.[122] Additionally, quercetin downregulates endothelial cell adhesion molecules ICAM-1 and VCAM-1[123–125] as shown in endothelial cell and rodent models, and interacts with the renin-angiotensin system by inhibiting angiotensin-converting enzyme (ACE) and facilitating bradykinin production to induce vasodilation.[122] As the microbiome degrades quercetin, specific taxa are responsible for the amount and types of quercetin that enter circulation. A novel study by We. et al observed that quercetin fed to $ApoE^{-/-}$ mice not only improved circulating lipoprotein profiles, but the quercetin-degrading *Phascolarctobacterium* and *Anerovibrio* genera that metabolize quercetin to endothelial-protective SCFA were elevated.[126] Lastly, along with isoflavones, quercetin acts as a phytoestrogen binding to ERα and ERβ,[127] located in multiple tissues including the vascular endothelium. Coupling to ERs stimulates eNOS to generate nitric oxide to relax the smooth muscle in the dilation of blood vessels.[128] However, to our knowledge, there is no research looking specifically at quercetin in ERα and ERβ stimulation of eNOS in endothelial dysfunction, especially in post-menopausal women, representing an opportunity to research quercetin ERα and ERβ stimulation in this demographic.

V. AMINO ACIDS

A. INTRODUCTION

Dietary protein comes from a wide range of plant and animal sources and consists of various amino acids linked by peptide bonds. Mechanical digestion of dietary protein begins in the mouth with gastric hydrochloric acid and pepsin enzymatically begin to denature and cleave the protein.[129] Pancreatic proteases released in the small intestine continue to break protein into

amino acids, consisting at a minimum of a carboxylic acid and amino group, that can be absorbed by the intestinal enterocytes into the bloodstream.[129] These amino acids are used by the human body for various physiological processes including muscle maintenance, immune function, synthesis of new proteins, energy production, and hormone generation. However, it is estimated that as much as 5-10% of total dietary protein escapes absorption via the small intestine and enters the colon[5] as a result of low protein digestibility or low host proteolytic capacity. Protein and amino acids that reach the colon are poorly absorbed[130] rendering them substrate for microbial digestion and subsequent production of amino acid-derived metabolites. This review will focus on two metabolites produced from phenylalanine and tyrosine and their impact on endothelial health, as they converge into phenylacetic acid (PAA) or its derivatives during metabolism. PAA is a central gut metabolite that is produced from these aromatic amino acids and polyphenols and can have either inflammatory or cardioprotective effects depending on hepatic transformation by the host,[131–133] implicating these amino acids for future research in CVD risk.

B. PHENYLACETYLGLUTAMINE (PAGln)

Phenylalanine is an essential amino acid that the body cannot synthesize on its own and hence must be obtained through the diet from foods such as meat, chicken, fish, eggs, dairy, nuts, and soybean.[134] Most phenylalanine is absorbed in the small intestine, yet a small portion reaches the large intestine where it is metabolized to phenylacetylglutamine (PAGln) in a multi-step, multi-organ fashion. Microbial species from various genera first deaminate phenylalanine into phenylpyruvic acid using the enzyme phenylalanine dehydrogenase[135], or other aminotransferases[136]. Phenylpyruvic acid is then converted into the convergent metabolite PAA, by oxidative or non-oxidative decarboxylation from *Bacteriodetes,*[137,138] *Pseudomonadota,*[139] and *Bacillota*[138] phyla. Notably, PAA is also a metabolite of polyphenol (ie. quercetin) degradation that can feed into anti-inflammatory pathways.[140] If PAA is transported to the liver via the portal vein, phenylacetylglutamine (PAGln) is dominantly formed by conjugation to the amino

glutamine[141] in humans, or conjugated to glycine to form phenylacetylglycine in rodents.[142] Relatively little is known about the bacterial species that produce phenylacetic acid, albeit *Clostridium sporogenes* being a target organism for its porA gene responsible for phenylalanine to PAA conversion.[143]

PAGln is associated with vascular disease and adverse events such as ischemic stroke and heart failure .[141,144,145] Increased levels of circulating PAGln heighten platelet hyperreactivity due to PAGln's structural similarity to catecholamines, which can bind to α2A,α2B, and β2-adrenergic receptors, potentially raising the threat of thrombosis.[141] Previously it was found that increased PAGln in 4,000 individuals with or without diabetes, was associated with CVD beyond glycemic dysregulation and conventional risk factors.[141] A retrospective study found that PAGln is independently associated with atherosclerotic burden in patients with suspected coronary heart disease after adjusting for confounding variables.[146] In a prospective cohort study, PAGln was also correlated with a higher risk of adverse cardiovascular events in those with pre-existing heart failure determinants.[147] In another study evaluating PAGln in American and European heart failure patients, circulating PAGln was dose-dependently associated with reduced ejection fraction and B-type natriuretic peptide independent of traditional CVD risk factors.[148] Since phenylalanine is the precursor of PAGln and is acquired through diet, a low phenylalanine diet may be applicable for individuals at risk of vascular disease who exhibit high PAGln. This diet has been well-documented in the treatment for those who suffer from the inborn error of metabolism disease, known as phenylketonuria to prevent neurological damage, and may be suited for those with elevated PAGln in CVD.[134]

C. PARA-CRESOL SULFATE (PCS)

Para-cresol sulfate (PCS) is derived from microbial degradation of the amino acid tyrosine from foods such as cheese, meat, nuts, eggs, dairy soybeans, and whole grains[149]. Members of the microbiome work sequentially to produce the paracresol precursor from tyrosine as Wikoff et. al demonstrated PCS was not detected in the plasma of germ-free mice.[150]

First, certain *Bacteroidaceae, Eubactericeae* families convert tyrosine into 4-hydroxyphenylacetic acid (4-HPAA).[138,151,152] Then, *Clostridia, Eubacteriaceae, Lachnospiraceae, Ruminococcaceae, Bifidobacteriaceae,* and *Veillonellacea*e remove a carboxyl group from 4-HPAA to form paracresol.[138,151,153] The primary gene involved in this multi-step process is *hpdBCA,* which is involved both in 4-HPAA and paracresol formation.[154,155] Once formed, paracresol moves across the intestinal enterocytes and travels in the bloodstream bound to albumin.[156] It is then mostly sulfated to PCS in the liver before entering back into circulation.[157,158]

PCS is a uremic toxin most commonly associated with endothelial dysfunction in renal disease as it accumulates in tissue due to its high protein-binding ratios.[159,160] Yet, recent research implicates this tyrosine-derived microbial metabolite beyond renal disease to those who exhibit CVD with preserved renal function and is independently associated with all-cause mortality.[152] PCS damages endothelial cells by elevating oxidative stress in vascular smooth muscle cells, inducing endothelial microparticle release,[161] activating apoptosis, and inhibiting a subset of P450 biotransformation enzymes to reduce xenobiotic clearance thus exacerbating cardiovascular disease.[6,162] The first *in vitro* study on PCS in 2007 showed that this metabolite increased oxidative burst from unstimulated leukocytes from the blood of healthy donors.[163] This was further validated in a rodent model that observed rapid leukocyte rolling in the rat peritoneal vascular bed.[164] Moreover, it was observed that vascular reactivity in mouse thoracic aortas was affected by PCS, as it increases the contractility of blood vessels when exposed to phenylephrine and resulted in eutrophic remodeling.[165] A groundbreaking study conducted by Nemet et al. utilized fecal metagenomics in a human discovery cohort to find the paracresol *hpdBCA* gene located in specific gut bacteria is independently linked to CVD.[152] Further confirmation was provided by genetically engineering bacteria to produce paracresol in germ-free mice, which induced a pro-thrombotic phenotype.[152] Prognostics in heart failure patients have observed that PCS was significantly raised and that 25.7% experienced and adverse

cardiovascular event or mortality within three years with concentrations ≥50μM.[166] Furthermore, PCS was the only independent predictor of adverse events as compared to asymmetric dimethylarginine, glomerular filtration rate, or B-type natriuretic peptide as assessed in a multivariate COX linear regression analysis.[166] Individuals with renal disease are at higher risk of cardiovascular mortality than the general population. As such, a handful of studies have correlated, higher baseline concentration of PCS was with n cardiovascular events in those with progressive renal disease .[167] High baseline concentrations of PCS were associated with adverse cardiovascular events in sixty-two out of four-hundred ninety-nine patients with mild-to-moderate renal disease within three years.[167] Another three-year observational study in dialysis patients correlated baseline PCS concentration to cardiovascular associated deaths in 50% of the subjects.[168] Across the various stages of renal disease (ie. stage 2-5), Liabeuf et al. studied PCS in vascular calcification, arterial stiffness, and mortality.[169] They found that PCS was inversely associated with vascular calcification and a predictor for cardiovascular complications were responsible for 58% of the thirty-eight patients that died.[169] As PCS can accumulate in tissues from poor renal excretion, and is poorly removed by hemodialysis, therapeutics to reduce its precursor paracresol in the intestines may reduce overall circulating concentrations. Saccharolytic bacteria primarily ferment carbohydrates where proteolytic bacteria metabolize protein, thus a diet lower in tyrosine-containing protein and higher in fiber could reduce this PCS. This notion has been supported by studies observing that vegetarians consuming 25% less protein and 69% more fiber than non-vegetarians have significantly less urinary PCS,[170] and that a vegan diet decreases serum and urinary paracresol[171]. While dietary interventions are not yet commonly used to treat PCS in endothelial dysfunction, they are a powerful example of how microbiome modulation can influence the endothelium.

VI. SCFAs

Short-chain fatty acids (SCFAs) are a group of organic compounds that are produced by the microbial fermentation of dietary carbohydrates, particularly fiber or polyphenols, which

cannot be fully digested by the human body. The two main types of fiber as a substrate for SCFA production are soluble-that can dissolve and hold water once extracted, and insoluble-does not dissolve, but attracts water to create bulk.[172,173] Types and concentrations vary in food, but fiber sources are generally from plants such as legumes, grains, vegetables, and fruit. The majority of soluble dietary fiber (ie. gums, mucilage, inulin, and pectins) escapes host digestion in the stomach and small intestine, but can be fermented by the microbiome in the colon.[172] The microbial processing of the diverse assortment of fibers can lead to numerous SCFAs primarily consisting of butyrate, propionate, and acetate, along with heat and gas as the main end products.[172,173]

Many microbial species are responsible for fermenting various fiber types,[174] although synthesis and overall ratios of SCFAs are highly dependent on bacteria present along with substrate from the diet.[175,176] In the human body, the most abundant and shortest SCFA is two-carbon acetate.[177] Acetate is produced via fiber fermentation by most enteric bacteria[178] via various pathways. It acts directly as an energy substrate, as it converts into acetyl-CoA that feeds into the tricarboxylic acid cycle to produce adenosine triphosphate (ATP).[179] While the human body can produce acetate on its own, the levels of acetate present in the body can be affected by the actions of microbes in altering the acetate pool.[180] In contrast, the three-carbon SCFA propionate is synthesized from the microbiome via three distinct pathways. Propionate can be produced by members of the *Bacteriodota* phylum through the succinate pathway, as well as through the propanediol pathway, which involves the use of fucose and rhamnose deoxy sugars found in fiber and polyphenols.[178,181] Additionally, bacteria such as *Clostridium propionicum* produce propionate via the acrylate pathway.[182] Interestingly, *Akkermansia muciniphilia* from the *Verrucomicrobia* phylum consumes mucin produced by the intestine instead of fiber as its primary fuel source and has been shown to produce propionate as a direct fermentation product.[183,184] Lastly, the four-carbon SCFA butyrate is formed by condensation of two acetyl-CoA molecules by microbes that synthesize butyrate from previous production of acetate and

lactate.[181] Butyrate is dominantly produced by members of the *Ruminococcaceae* and *Lachnospiraceae* families the *Bacillota* phylum, although other bacteria may possess the ability to produce butyrate in varying quantities.[185]

SCFAs indirectly impact cardiovascular health by altering the intestinal environment. Among all microbial metabolites in the intestines, butyrate and propionate are the most abundant, with concentrations of up to 50-130mM found in the proximal colon.[6,186] The metabolism of butyrate and propionate tends to consume oxygen, which creates a hypoxic environment in the colon. This happens through mitochondrial β-oxidation, leading to a sharp decline in oxygen levels from the lamina propria to the intestinal lumen. This oxygen gradient favors the presence of anaerobic microorganisms over aerobic ones within the gut, thereby promoting the growth of commensal microbes.[187] In addition, the low partial pressure of oxygen (pO_2) of the intestinal tissue as augmented by butyrate and propionate is far below other bodily tissues. This creates an environment to stabilize the hypoxia-inducible factor (HIF)[188] that promotes intestinal barrier function and the production of mucins to aid in microbial defense and clearance.[188] Apart from its role as a primary fuel source for enterocytes[2,188] through β-oxidation in the mitochondria,[189] butyrate is crucial in maintaining gut barrier function and aiding cellular turnover, thereby promoting overall gut health. Moreover, butyrate has the ability to alter the gene expression of local inflammatory cytokines by suppressing histone deacetylases (HDACs).[190] Inhibition of HDAC gene expression modulation induces the proliferation and differentiation of $Foxp3^+$ $CD4^+$ regulatory T cells that downregulate the inflammatory response in the gut.[191] This limits the permeability of the apical junction complex (AJC) that can occur when proinflammatory cytokines are present. In addition, butyrate influences the expression of transcription factors that promote modulation of the AJC that partially dictates the transit of molecules, such as the endothelial damaging metabolite lipopolysaccharide (LPS) from the intestinal lumen into the bloodstream.[192–194]

It has long been recognized that fiber in the diet has cardioprotective effects that, in part, may be due to SCFA production.[195] Besides the localized effects of SCFAs in the gut, these metabolites enter the bloodstream and protect against vascular inflammation and endothelial stress.[196,197] Most of the anti-inflammatory properties of SCFAs have been studies in animal and cell culture models. An *in vitro* study by Li. et al, showed that SCFAs modulate GPR 41/43 and HDAC3 in a HUVEC cell culture to reduce inflammatory cytokine release after stimulation of the gut-derived LPS or TNF-α insult.[196] In another study, when endothelial EA. hy926 cells were pretreated with butyrate, there was a lower uptake of oxidized LDL, reduced expression of cell adhesion molecules VCAM-1, CD36, CCL2, and decreased proinflammatory cytokines IL-6 and IL-1β. The same authors also found that ApoE$^{-/-}$ mice given 1% butyrate in their diets for ten weeks had decreased atherosclerotic lesions with reduced aortic atherosclerosis by 50% as compared to the controls. Moreover the aortic valves of the mice displayed lower cell adhesion molecules CCL2 and VCAM-1.[198]

SCFAs also have an impact on lipoprotein metabolism implicated in inhibition of arterial foam cell formation. Kashahara et al. demonstrated that gnotobiotic ApoE$^{-/-}$ mice inoculated with butyrate-producing *Roseburia intestinalis* had decreased athlerosclerotic lesions. The authors observed that the treated mice had lower metabolic endotoxemia via improved gut barrier function, and that an analog of butyrate (ie. tributyrin) supplemented to the diet also reduced lesions.[199] Several clinical trials have observed that fiber supplementation leads to a reduction in serum cholesterol with a subsequent increase in SCFA.[200–202] In healthy participants, 20 g of inulin fiber daily for six weeks resulted in a correlation between decreased in VLDL cholesterol and total cholesterol with increased butyrate production.[200] Importantly, improved d18:1/16:0, d18:0/24:0, d18:1/24:1 plasma ceramide ratios, shown to predict CVD adverse events and mortality, were associated with increased SCFA concentration.[200] Mildly hypercholesteremic participants consuming 80 grams of oats containing 3 g of β-glucan fiber for forty-five days exhibited lower total cholesterol and lower LDL cholesterol.[202] *Roseburia,*

Enterobacteriaceae, and *Faecalibacterium prausnitizii* in this group were also positively correlated with plasma butyric and valeric SCFAs.[202] A different group tested 6 g of oat β-glucan fiber in hypercholesteremic participant for six weeks and found that LDL cholesterol decreased and a subsequent model of intestinal fermentation validated that oat β-glucan fiber increased acetate, propionate, butyrate, and total SCFA production. [201]

Given that endothelial dysfunction is a key risk factor for hypertension and CVD, therapeutics such as SCFAs have been implicated in blood pressure regulation. Mechanistically, SCFAs modulate blood pressure via binding to endothelial GPR41 or Olfr78 receptors. The agonism of GPR41 lowers blood pressure[203] while Olfr78 agonism increases blood pressure.[204] These opposing effects of SCFA binding on these receptors indicate a balancing effect on blood pressure. Pluznick et al. demonstrated this effect in $OLFR^{-/-}$ mice that became hypotensive after propionate administration, whereas propionate increased blood pressure in wild-type mice.[204] Numerous studies have associated microbiome composition in relation to hypertension.[205–207] For example, a significant decrease in microbial diversity, richness, and evenness with depressed SCFA-producing bacteria is associated with spontaneously hypertensive rats and a similar pattern was found in hypertensive human subjects.[205] Furthermore, transplanting the microbiome from hypertensive humans to C57BL/6L germ-free mice transfers a hypertensive phenotype thereby implicating the microbiome in blood pressure control.[207] However, human studies evaluating just SCFAs on blood pressure regulation are limited and inconclusive.[208–210] Supplementation of sodium butyrate or sodium butyrate with the prebiotic fiber inulin for forty-five days significantly reduced diastolic blood pressure in sixty adults with type II diabetes mellitus.[209] Sodium restriction to 2000mg/d in untreated hypertensive individuals increased circulating SCFAs and decreased blood pressure after adjusting for age, sex, race, and BMI.[211] The researchers observed that the types and quantities of SCFAs varied between male and females, and that females responded to SCFA production more than males.[211] Tilves et. al leveraged SCFA data from the Survivorship Promotion in Reducing IGF-1 Trial to study SCFA

abundance in overweight cancer survivors with hypertension that were given weight loss programming or metformin treatment for one year.[210] Butyrate was inversely associated with hypertension as fecal and plasma butyrate correlated with decreased systolic blood pressure.[210] Yet, this association between SCFAs and blood pressure differed by sex as this effect was most present in males.[210] Other researchers have found that higher fecal butyrate excretion was found in males that generally consumed more fiber, total calories, had higher central obesity, and incidence of hypertension compared females in a Columbian observational study.[208] Although this study did not evaluate SCFA production or absorption, the results are conflicting as to SCFA concentration and blood pressure.[208] It is important to note that a multitude of variables exist in the type and quantities of SCFAs that reach the bloodstream and there is not a linear relationship between diet and the concentration of SCFA produced by colonic bacteria.[6] Furthermore, metabolic health, and pre-existing CVD risk factors can greatly impact the outcomes of SCFA intervention, presenting an important challenge in research design.

VII. CONCLUSIONS

The human microbiome has been shown to play a crucial role in mediating the progression of CVD in its interaction with the endothelium. In part, this is achieved through the production and modification of metabolites that act locally, within the gut itself, or systemically, influencing the physiology of the entire body. However, while the scientific community has made progress in understanding the role of these metabolites, our knowledge of their bioavailability and bioactivity is still limited. Nevertheless, studies have shown that there are marked differences in the metabolite profiles of healthy individuals versus those with CVD. This suggests that microbial metabolites have the potential to intercede in processes related to endothelial function and that further study of the microbiome could lead to new insights into the prevention and treatment of CVD.

REFERENCES

1. Marchesi JR, Ravel J. The vocabulary of microbiome research: a proposal. *Microbiome*. 2015;3:31.

2. Herrema H, Niess JH. Intestinal microbial metabolites in human metabolism and type 2 diabetes. *Diabetologia*. 2020;63(12):2533-2547.

3. Vanhoutte PM, Zhao Y, Xu A, Leung SWS. Thirty Years of Saying NO. *Circ Res*. Published online July 8, 2016. doi:10.1161/CIRCRESAHA.116.306531

4. Beckonert O, Keun HC, Ebbels TMD, et al. Metabolic profiling, metabolomic and metabonomic procedures for NMR spectroscopy of urine, plasma, serum and tissue extracts. *Nat Protoc*. 2007;2(11):2692-2703.

5. Krautkramer KA, Fan J, Bäckhed F. Gut microbial metabolites as multi-kingdom intermediates. *Nat Rev Microbiol*. 2021;19(2):77-94.

6. Zhang LS, Davies SS. Microbial metabolism of dietary components to bioactive metabolites: opportunities for new therapeutic interventions. *Genome Med*. 2016;8(1):46.

7. Krüger-Genge A, Blocki A, Franke RP, Jung F. Vascular Endothelial Cell Biology: An Update. *Int J Mol Sci*. 2019;20(18). doi:10.3390/ijms20184411

8. Batty M, Bennett MR, Yu E. The Role of Oxidative Stress in Atherosclerosis. *Cells*. 2022;11(23). doi:10.3390/cells11233843

9. Petersen KS, Kris-Etherton PM. Diet Quality Assessment and the Relationship between Diet Quality and Cardiovascular Disease Risk. *Nutrients*. 2021;13(12). doi:10.3390/nu13124305

10. Dahl WJ, Rivero Mendoza D, Lambert JM. Diet, nutrients and the microbiome. *Prog Mol Biol Transl Sci*. 2020;171:237-263.

11. Battson ML, Lee DM, Jarrell DK, et al. Suppression of gut dysbiosis reverses Western diet-induced vascular dysfunction. *Am J Physiol Endocrinol Metab*. 2018;314(5):E468-E477.

12. Rienks J, Barbaresko J, Nöthlings U. Association of Polyphenol Biomarkers with Cardiovascular Disease and Mortality Risk: A Systematic Review and Meta-Analysis of Observational Studies. *Nutrients*. 2017;9(4):415.

13. Zurbau A, Au-Yeung F, Blanco Mejia S, et al. Relation of Different Fruit and Vegetable Sources With Incident Cardiovascular Outcomes: A Systematic Review and Meta-Analysis of Prospective Cohort Studies. *J Am Heart Assoc*. 2020;9(19):e017728.

14. Del Rio D, Rodriguez-Mateos A, Spencer JPE, Tognolini M, Borges G, Crozier A. Dietary (poly)phenolics in human health: structures, bioavailability, and evidence of protective effects against chronic diseases. *Antioxid Redox Signal*. 2013;18(14):1818-1892.

15. Leri M, Scuto M, Ontario ML, et al. Healthy Effects of Plant Polyphenols: Molecular

Mechanisms. *Int J Mol Sci*. 2020;21(4). doi:10.3390/ijms21041250

16.Luca SV, Macovei I, Bujor A, et al. Bioactivity of dietary polyphenols: The role of metabolites. *Crit Rev Food Sci Nutr*. 2020;60(4):626-659.

17.Gowd V, Karim N, Shishir MRI, Xie L, Chen W. Dietary polyphenols to combat the metabolic diseases via altering gut microbiota. *Trends in Food Science & Technology*. 2019;93:81-93. doi:10.1016/j.tifs.2019.09.005

18. Faria A, Fernandes I, Norberto S, Mateus N, Calhau C. Interplay between anthocyanins and gut microbiota. *J Agric Food Chem*. 2014;62(29):6898-6902.

19.Costa C, Tsatsakis A, Mamoulakis C, et al. Current evidence on the effect of dietary polyphenols intake on chronic diseases. *Food Chem Toxicol*. 2017;110:286-299.

20. Tian B, Liu J. Resveratrol: a review of plant sources, synthesis, stability, modification and food application. *J Sci Food Agric*. 2020;100(4):1392-1404.

21. Zhao G, Yang L, Zhong W, et al. Polydatin, A Glycoside of Resveratrol, Is Better Than Resveratrol in Alleviating Non-alcoholic Fatty Liver Disease in Mice Fed a High-Fructose Diet. *Front Nutr*. 2022;9:857879.

22. Zhou S, Yang R, Teng Z, et al. Dose-dependent absorption and metabolism of trans-polydatin in rats. *J Agric Food Chem*. 2009;57(11):4572-4579.

23. Du QH, Peng C, Zhang H. Polydatin: a review of pharmacology and pharmacokinetics. *Pharm Biol*. 2013;51(11):1347-1354.

24. Basholli-Salihu M, Schuster R, Mulla D, Praznik W, Viernstein H, Mueller M. Bioconversion of piceid to resveratrol by selected probiotic cell extracts. *Bioprocess Biosyst Eng*. 2016;39(12):1879-1885.

25. Chaplin A, Carpéné C, Mercader J. Resveratrol, Metabolic Syndrome, and Gut Microbiota. *Nutrients*. 2018;10(11). doi:10.3390/nu10111651

26. Delmas D, Aires V, Limagne E, et al. Transport, stability, and biological activity of resveratrol. *Ann N Y Acad Sci*. 2011;1215:48-59.

27. Gambini J, Inglés M, Olaso G, et al. Properties of Resveratrol: In Vitro and In Vivo Studies about Metabolism, Bioavailability, and Biological Effects in Animal Models and Humans. *Oxid Med Cell Longev*. 2015;2015:837042.

28. Wang P, Sang S. Metabolism and pharmacokinetics of resveratrol and pterostilbene. *Biofactors*. 2018;44(1):16-25.

29. Galiniak S, Aebisher D, Bartusik-Aebisher D. Health benefits of resveratrol administration. *Acta Biochimica Polonica*. Published online 2019. doi:10.18388/abp.2018_2749

30. Chen ML, Yi L, Zhang Y, et al. Resveratrol Attenuates Trimethylamine-N-Oxide (TMAO)-Induced Atherosclerosis by Regulating TMAO Synthesis and Bile Acid Metabolism via Remodeling of the Gut Microbiota. *MBio*. 2016;7(2):e02210-e02215.

31.Teimouri M, Homayouni-Tabrizi M, Rajabian A, Amiri H, Hosseini H. Anti-inflammatory effects of resveratrol in patients with cardiovascular disease: A systematic review and meta-analysis of randomized controlled trials. *Complement Ther Med*. 2022;70:102863.

32. Imamura H, Yamaguchi T, Nagayama D, Saiki A, Shirai K, Tatsuno I. Resveratrol Ameliorates Arterial Stiffness Assessed by Cardio-Ankle Vascular Index in Patients With Type 2 Diabetes Mellitus. *Int Heart J*. 2017;58(4):577-583.

33. Marques BCAA, Trindade M, Aquino JCF, et al. Beneficial effects of acute trans-resveratrol supplementation in treated hypertensive patients with endothelial dysfunction. *Clin Exp Hypertens*. 2018;40(3):218-223.

34. Selma MV, Tomás-Barberán FA, Beltrán D, García-Villalba R, Espín JC. Gordonibacter urolithinfaciens sp. nov., a urolithin-producing bacterium isolated from the human gut. *Int J Syst Evol Microbiol*. 2014;64(Pt 7):2346-2352.

35. Iglesias-Aguirre CE, García-Villalba R, Beltrán D, et al. Gut Bacteria Involved in Ellagic Acid Metabolism To Yield Human Urolithin Metabotypes Revealed. *J Agric Food Chem*. 2023;71(9):4029-4035.

36. Bifidobacterium pseudocatenulatum INIA P815: The first bacterium able to produce urolithins A and B from ellagic acid. *J Funct Foods*. 2018;45:95-99.

37. Espín JC, Larrosa M, García-Conesa MT, Tomás-Barberán F. Biological significance of urolithins, the gut microbial ellagic Acid-derived metabolites: the evidence so far. *Evid Based Complement Alternat Med*. 2013;2013:270418.

38. García-Niño WR, Zazueta C. Ellagic acid: Pharmacological activities and molecular mechanisms involved in liver protection. *Pharmacol Res*. 2015;97:84-103.

39. Vini R, Azeez JM, Remadevi V, et al. Urolithins: The Colon Microbiota Metabolites as Endocrine Modulators: Prospects and Perspectives. *Front Nutr*. 2021;8:800990.

40. Tomás-Barberán FA, González-Sarrías A, García-Villalba R, et al. Urolithins, the rescue of "old" metabolites to understand a "new" concept: Metabotypes as a nexus among phenolic metabolism, microbiota dysbiosis, and host health status. *Mol Nutr Food Res*. 2017;61(1). doi:10.1002/mnfr.201500901

41. Singh A, D'Amico D, Andreux PA, et al. Direct supplementation with Urolithin A overcomes limitations of dietary exposure and gut microbiome variability in healthy adults to achieve consistent levels across the population. *Eur J Clin Nutr*. 2022;76(2):297-308.

42. Tomás-Barberán FA, García-Villalba R, González-Sarrías A, Selma MV, Espín JC. Ellagic acid metabolism by human gut microbiota: consistent observation of three urolithin phenotypes in intervention trials, independent of food source, age, and health status. *J Agric Food Chem*. 2014;62(28):6535-6538.

43. Ismail T, Calcabrini C, Diaz AR, et al. Ellagitannins in Cancer Chemoprevention and Therapy. *Toxins* . 2016;8(5). doi:10.3390/toxins8050151

44. Cortés-Martín A, Selma MV, Tomás-Barberán FA, González-Sarrías A, Espín JC. Where to Look into the Puzzle of Polyphenols and Health? The Postbiotics and Gut Microbiota

Associated with Human Metabotypes. *Mol Nutr Food Res*. 2020;64(9):e1900952.

45. García-Mantrana I, Calatayud M, Romo-Vaquero M, Espín JC, Selma MV, Collado MC. Urolithin Metabotypes Can Determine the Modulation of Gut Microbiota in Healthy Individuals by Tracking Walnuts Consumption over Three Days. *Nutrients*. 2019;11(10). doi:10.3390/nu11102483

46. González-Sarrías A, García-Villalba R, Romo-Vaquero M, et al. Clustering according to urolithin metabotype explains the interindividual variability in the improvement of cardiovascular risk biomarkers in overweight-obese individuals consuming pomegranate: A randomized clinical trial. *Mol Nutr Food Res*. 2017;61(5). doi:10.1002/mnfr.201600830

47. Cortés-Martín A, García-Villalba R, González-Sarrías A, et al. The gut microbiota urolithin metabotypes revisited: the human metabolism of ellagic acid is mainly determined by aging. *Food Funct*. 2018;9(8):4100-4106.

48. Henning SM, Summanen PH, Lee RP, et al. Pomegranate ellagitannins stimulate the growth of Akkermansia muciniphila in vivo. *Anaerobe*. 2017;43:56-60.

49. Selma MV, Beltrán D, García-Villalba R, Espín JC, Tomás-Barberán FA. Description of urolithin production capacity from ellagic acid of two human intestinal Gordonibacter species. *Food Funct*. 2014;5(8):1779-1784.

50. Zhang X, Fang Y, Yang G, et al. Isolation and characterization of a novel human intestinal FUA027 capable of producing urolithin A from ellagic acid. *Front Nutr*. 2022;9:1039697.

51. Piwowarski JP, Kiss AK, Granica S, Moeslinger T. Urolithins, gut microbiota-derived metabolites of ellagitannins, inhibit LPS-induced inflammation in RAW 264.7 murine macrophages. *Mol Nutr Food Res*. 2015;59(11):2168-2177.

52. Anti-inflammatory properties of a pomegranate extract and its metabolite urolithin-A in a colitis rat model and the effect of colon inflammation on phenolic metabolism. *J Nutr Biochem*. 2010;21(8):717-725.

53. Komatsu W, Kishi H, Yagasaki K, Ohhira S. Urolithin A attenuates pro-inflammatory mediator production by suppressing PI3-K/Akt/NF-κB and JNK/AP-1 signaling pathways in lipopolysaccharide-stimulated RAW264 macrophages: Possible involvement of NADPH oxidase-derived reactive oxygen species. *Eur J Pharmacol*. 2018;833:411-424.

54. Fu X, Gong LF, Wu YF, et al. Urolithin A targets the PI3K/Akt/NF-κB pathways and prevents IL-1β-induced inflammatory response in human osteoarthritis: in vitro and in vivo studies. *Food Funct*. 2019;10(9):6135-6146.

55. Ryu D, Mouchiroud L, Andreux PA, et al. Urolithin A induces mitophagy and prolongs lifespan in C. elegans and increases muscle function in rodents. *Nat Med*. 2016;22(8):879-888.

56. Giménez-Bastida JA, González-Sarrías A, Larrosa M, Tomás-Barberán F, Espín JC, García-Conesa MT. Ellagitannin metabolites, urolithin A glucuronide and its aglycone urolithin A, ameliorate TNF-α-induced inflammation and associated molecular markers in human aortic endothelial cells. *Mol Nutr Food Res*. 2012;56(5):784-796.

57. Urolithin A shows anti-atherosclerotic activity via activation of class B scavenger receptor and activation of Nef2 signaling pathway. *Pharmacol Rep*. 2018;70(3):519-524.

58. Istas G, Feliciano RP, Weber T, et al. Plasma urolithin metabolites correlate with improvements in endothelial function after red raspberry consumption: A double-blind randomized controlled trial. *Arch Biochem Biophys*. 2018;651:43-51.

59. Nishimoto Y, Fujisawa K, Ukawa Y, et al. Effect of urolithin A on the improvement of vascular endothelial function depends on the gut microbiota. *Front Nutr*. 2022;9:1077534.

60. Křížová L, Dadáková K, Kašparovská J, Kašparovský T. Isoflavones. *Molecules*. 2019;24(6). doi:10.3390/molecules24061076

61. Aboushanab SA, Khedr SM, Gette IF, et al. Isoflavones derived from plant raw materials: bioavailability, anti-cancer, anti-aging potentials, and microbiome modulation. *Crit Rev Food Sci Nutr*. 2023;63(2):261-287.

62. Liggins J, Bluck LJ, Runswick S, Atkinson C, Coward WA, Bingham SA. Daidzein and genistein content of fruits and nuts. *J Nutr Biochem*. 2000;11(6):326-331.

63. Tokede OA, Onabanjo TA, Yansane A, Gaziano JM, Djoussé L. Soya products and serum lipids: a meta-analysis of randomised controlled trials. *Br J Nutr*. 2015;114(6):831-843.

64. Barańska A, Błaszczuk A, Kanadys W, et al. Effects of Soy Protein Containing of Isoflavones and Isoflavones Extract on Plasma Lipid Profile in Postmenopausal Women as a Potential Prevention Factor in Cardiovascular Diseases: Systematic Review and Meta-Analysis of Randomized Controlled Trials. *Nutrients*. 2021;13(8). doi:10.3390/nu13082531

65. Moradi M, Daneshzad E, Azadbakht L. The effects of isolated soy protein, isolated soy isoflavones and soy protein containing isoflavones on serum lipids in postmenopausal women: A systematic review and meta-analysis. *Crit Rev Food Sci Nutr*. 2020;60(20):3414-3428.

66. Harland JI, Haffner TA. Systematic review, meta-analysis and regression of randomised controlled trials reporting an association between an intake of circa 25 g soya protein per day and blood cholesterol. *Atherosclerosis*. 2008;200(1):13-27.

67. CFR - Code of Federal Regulations Title 21. Accessed August 21, 2023. https://www.accessdata.fda.gov/scripts/cdrh/cfdocs/cfcfr/cfrsearch.cfm?fr=101.82

68. Naghshi S, Tutunchi H, Yousefi M, et al. Soy isoflavone intake and risk of cardiovascular disease in adults: A systematic review and dose-response meta-analysis of prospective cohort studies. *Crit Rev Food Sci Nutr*. Published online January 27, 2023:1-15.

69. Shrode RL, Cady N, Jensen SN, Borcherding N, Mangalam AK. Isoflavone consumption reduces inflammation through modulation of phenylalanine and lipid metabolism. *Metabolomics*. 2022;18(11):84.

70. Setchell KDR, Brown NM, Lydeking-Olsen E. The clinical importance of the metabolite equol-a clue to the effectiveness of soy and its isoflavones. *J Nutr*. 2002;132(12):3577-3584.

71. Zubik L, Meydani M. Bioavailability of soybean isoflavones from aglycone and glucoside forms in American women. *Am J Clin Nutr*. 2003;77(6):1459-1465.

72. Soukup ST, Helppi J, Müller DR, et al. Phase II metabolism of the soy isoflavones genistein and daidzein in humans, rats and mice: a cross-species and sex comparison. *Arch Toxicol*. 2016;90(6):1335-1347.

73. Setchell KDR, Clerici C. Equol: history, chemistry, and formation. *J Nutr*. 2010;140(7):1355S - 62S.

74. Setchell KDR, Clerici C, Lephart ED, et al. S-equol, a potent ligand for estrogen receptor beta, is the exclusive enantiomeric form of the soy isoflavone metabolite produced by human intestinal bacterial flora. *Am J Clin Nutr*. 2005;81(5):1072-1079.

75. Setchell KDR, Zhao X, Shoaf SE, Ragland K. The pharmacokinetics of S-(-)equol administered as SE5-OH tablets to healthy postmenopausal women. *J Nutr*. 2009;139(11):2037-2043.

76. Stevens JF, Maier CS. The Chemistry of Gut Microbial Metabolism of Polyphenols. *Phytochem Rev*. 2016;15(3):425-444.

77. Setchell KD, Brown NM, Desai P, et al. Bioavailability of pure isoflavones in healthy humans and analysis of commercial soy isoflavone supplements. *J Nutr*. 2001;131(4 Suppl):1362S - 75S.

78. Setchell KDR, Cole SJ. Method of defining equol-producer status and its frequency among vegetarians. *J Nutr*. 2006;136(8):2188-2193.

79. Frankenfeld CL. O-desmethylangolensin: the importance of equol's lesser known cousin to human health. *Adv Nutr*. 2011;2(4):317-324.

80. Nagarajan S, Burris RL, Stewart BW, Wilkerson JE, Badger TM. Dietary soy protein isolate ameliorates atherosclerotic lesions in apolipoprotein E-deficient mice potentially by inhibiting monocyte chemoattractant protein-1 expression. *J Nutr*. 2008;138(2):332-337.

81. Kamiyama M, Kishimoto Y, Tani M, Utsunomiya K, Kondo K. Effects of equol on oxidized low-density lipoprotein-induced apoptosis in endothelial cells. *J Atheroscler Thromb*. 2009;16(3):239-249.

82. Joy S, Siow RCM, Rowlands DJ, et al. The isoflavone Equol mediates rapid vascular relaxation: Ca2+-independent activation of endothelial nitric-oxide synthase/Hsp90 involving ERK1/2 and Akt phosphorylation in human endothelial cells. *J Biol Chem*. 2006;281(37):27335-27345.

83. Zhang T, Liang X, Shi L, et al. Estrogen Receptor and PI3K/Akt Signaling Pathway Involvement in S-(-)Equol-Induced Activation of Nrf2/ARE in Endothelial Cells. *PLoS One*. 2013;8(11):e79075.

84. Boutas I, Kontogeorgi A, Dimitrakakis C, Kalantaridou SN. Soy Isoflavones and Breast Cancer Risk: A Meta-analysis. *In Vivo*. 2022;36(2):556-562.

85. Mayo B, Vázquez L, Flórez AB. Equol: A Bacterial Metabolite from The Daidzein Isoflavone and Its Presumed Beneficial Health Effects. *Nutrients*. 2019;11(9). doi:10.3390/nu11092231

86. Vrtačnik P, Ostanek B, Mencej-Bedrač S, Marc J. The many faces of estrogen signaling.

Biochem Med . 2014;24(3):329-342.

87. Jiang Y, Gong P, Madak-Erdogan Z, et al. Mechanisms enforcing the estrogen receptor β selectivity of botanical estrogens. *FASEB J*. 2013;27(11):4406-4418.

88. Starkey NJE, Li Y, Drenkhahn-Weinaug SK, Liu J, Lubahn DB. 27-Hydroxycholesterol Is an Estrogen Receptor β-Selective Negative Allosteric Modifier of 17β-Estradiol Binding. *Endocrinology*. 2018;159(5):1972-1981.

89. Ohkura Y, Obayashi S, Yamada K, Yamada M, Kubota T. S-equol Partially Restored Endothelial Nitric Oxide Production in Isoflavone-deficient Ovariectomized Rats. *J Cardiovasc Pharmacol*. 2015;65(5):500-507.

90. Sekikawa A, Ihara M, Lopez O, et al. Effect of S-equol and Soy Isoflavones on Heart and Brain. *Curr Cardiol Rev*. 2019;15(2):114-135.

91.Ahuja V, Miura K, Vishnu A, et al. Significant inverse association of equol-producer status with coronary artery calcification but not dietary isoflavones in healthy Japanese men. *Br J Nutr*. 2017;117(2):260-266.

92. Zuo LSY, Tang XY, Xiong F, et al. Isoflavone biomarkers are inversely associated with atherosclerosis progression in adults: a prospective study. *Am J Clin Nutr*. 2021;114(1):203-213.

93. Curtis PJ, Potter J, Kroon PA, et al. Vascular function and atherosclerosis progression after 1 y of flavonoid intake in statin-treated postmenopausal women with type 2 diabetes: a double-blind randomized controlled trial. *Am J Clin Nutr*. 2013;97(5):936-942.

94. Usui T, Tochiya M, Sasaki Y, et al. Effects of natural S-equol supplements on overweight or obesity and metabolic syndrome in the Japanese, based on sex and equol status. *Clin Endocrinol* . 2013;78(3):365-372.

95. Zhang X, Gao YT, Yang G, et al. Urinary isoflavonoids and risk of coronary heart disease. *Int J Epidemiol*. 2012;41(5):1367-1375.

96. Yoshikata R, Myint KZ, Ohta H. Relationship between equol producer status and metabolic parameters in 743 Japanese women: equol producer status is associated with antiatherosclerotic conditions in women around menopause and early postmenopause. *Menopause*. 2017;24(2):216-224.

97. Hazim S, Curtis PJ, Schär MY, et al. Acute benefits of the microbial-derived isoflavone metabolite equol on arterial stiffness in men prospectively recruited according to equol producer phenotype: a double-blind randomized controlled trial. *Am J Clin Nutr*. 2016;103(3):694-702.

98. Murota K, Nakamura Y, Uehara M. Flavonoid metabolism: the interaction of metabolites and gut microbiota. *Biosci Biotechnol Biochem*. 2018;82(4):600-610.

99. Showing all polyphenols found in Highbush blueberry, raw - Phenol-Explorer. Accessed April 9, 2024. http://phenol-explorer.eu/contents/food/95

100. Sampson L, Rimm E, Hollman PCH, de Vries JHM, Katan MB. Flavonol and flavone intakes in US health professionals. *J Am Diet Assoc*. 2002;102(10):1414-1420.

101. Van der Woude H, Boersma MG, Vervoort J, Rietjens IMCM. Identification of 14 quercetin phase II mono- and mixed conjugates and their formation by rat and human phase II in vitro model systems. *Chem Res Toxicol*. 2004;17(11):1520-1530.

102. Grzybowski A, Pietrzak K. Albert Szent-Györgyi (1893-1986): the scientist who discovered vitamin C. *Clin Dermatol*. 2013;31(3):327-331.

103. Yang J, Lee H, Sung J, Kim Y, Jeong HS, Lee J. Conversion of Rutin to Quercetin by Acid Treatment in Relation to Biological Activities. *Prev Nutr Food Sci*. 2019;24(3):313-320.

104. Manach C, Morand C, Demigné C, Texier O, Régérat F, Rémésy C. Bioavailability of rutin and quercetin in rats. *FEBS Letters*. 1997;409(1):12-16. doi:10.1016/s0014-5793(97)00467-5

105. Chiou YS, Wu JC, Huang Q, et al. Metabolic and colonic microbiota transformation may enhance the bioactivities of dietary polyphenols. *Journal of Functional Foods*. 2014;7:3-25. doi:10.1016/j.jff.2013.08.006

106. Dabeek WM, Marra MV. Dietary Quercetin and Kaempferol: Bioavailability and Potential Cardiovascular-Related Bioactivity in Humans. *Nutrients*. 2019;11(10). doi:10.3390/nu11102288

107. Li Y, Yao J, Han C, et al. Quercetin, Inflammation and Immunity. *Nutrients*. 2016;8(3):167.

108. Juśkiewicz J, Milala J, Jurgoński A, Król B, Zduńczyk Z. Consumption of polyphenol concentrate with dietary fructo-oligosaccharides enhances cecal metabolism of quercetin glycosides in rats. *Nutrition*. 2011;27(3):351-357.

109. Sánchez M, Galisteo M, Vera R, et al. Quercetin downregulates NADPH oxidase, increases eNOS activity and prevents endothelial dysfunction in spontaneously hypertensive rats. *J Hypertens*. 2006;24(1):75-84.

110. Juźwiak S, Wójcicki J, Mokrzycki K, et al. Effect of quercetin on experimental hyperlipidemia and atherosclerosis in rabbits. *Pharmacol Rep*. 2005;57(5):604-609.

111.Li SS, Cao H, Shen DZ, et al. Effect of Quercetin on Atherosclerosis Based on Expressions of ABCA1, LXR-α and PCSK9 in ApoE Mice. *Chin J Integr Med*. 2020;26(2):114-121.

112. Lu XL, Zhao CH, Yao XL, Zhang H. Quercetin attenuates high fructose feeding-induced atherosclerosis by suppressing inflammation and apoptosis via ROS-regulated PI3K/AKT signaling pathway. *Biomed Pharmacother*. 2017;85:658-671.

113. Nie J, Zhang L, Zhao G, Du X. Quercetin reduces atherosclerotic lesions by altering the gut microbiota and reducing atherogenic lipid metabolites. *J Appl Microbiol*. 2019;127(6):1824-1834.

114. Ko EY, Nile SH, Jung YS, Keum YS. Antioxidant and antiplatelet potential of different methanol fractions and flavonols extracted from onion (L.). *3 Biotech*. 2018;8(3):155.

115. Bojić M, Debeljak Z, Tomičić M, Medić-Šarić M, Tomić S. Evaluation of antiaggregatory activity of flavonoid aglycone series. *Nutr J*. 2011;10:73.

116. Chopra M, Fitzsimons PE, Strain JJ, Thurnham DI, Howard AN. Nonalcoholic red wine extract and quercetin inhibit LDL oxidation without affecting plasma antioxidant vitamin and carotenoid concentrations. *Clin Chem*. 2000;46(8 Pt 1):1162-1170.

117. Egert S, Bosy-Westphal A, Seiberl J, et al. Quercetin reduces systolic blood pressure and plasma oxidised low-density lipoprotein concentrations in overweight subjects with a high-cardiovascular disease risk phenotype: a double-blinded, placebo-controlled cross-over study. *Br J Nutr*. 2009;102(7):1065-1074.

118. Loke WM, Hodgson JM, Proudfoot JM, McKinley AJ, Puddey IB, Croft KD. Pure dietary flavonoids quercetin and (-)-epicatechin augment nitric oxide products and reduce endothelin-1 acutely in healthy men. *Am J Clin Nutr*. 2008;88(4):1018-1025.

119. Huang H, Liao D, Dong Y, Pu R. Effect of quercetin supplementation on plasma lipid profiles, blood pressure, and glucose levels: a systematic review and meta-analysis. *Nutr Rev*. 2020;78(8):615-626.

120. Serban MC, Sahebkar A, Zanchetti A, et al. Effects of Quercetin on Blood Pressure: A Systematic Review and Meta-Analysis of Randomized Controlled Trials. *J Am Heart Assoc*. 2016;5(7). doi:10.1161/JAHA.115.002713

121. Dower JI, Geleijnse JM, Gijsbers L, Schalkwijk C, Kromhout D, Hollman PC. Supplementation of the Pure Flavonoids Epicatechin and Quercetin Affects Some Biomarkers of Endothelial Dysfunction and Inflammation in (Pre)Hypertensive Adults: A Randomized Double-Blind, Placebo-Controlled, Crossover Trial. *J Nutr*. 2015;145(7):1459-1463.

122. Patel RV, Mistry BM, Shinde SK, Syed R, Singh V, Shin HS. Therapeutic potential of quercetin as a cardiovascular agent. *European Journal of Medicinal Chemistry*. 2018;155:889-904. doi:10.1016/j.ejmech.2018.06.053

123. Bian Y, Liu P, Zhong J, et al. Quercetin Attenuates Adhesion Molecule Expression in Intestinal Microvascular Endothelial Cells by Modulating Multiple Pathways. *Dig Dis Sci*. 2018;63(12):3297-3304.

124. Kobuchi H, Roy S, Sen CK, Nguyen HG, Packer L. Quercetin inhibits inducible ICAM-1 expression in human endothelial cells through the JNK pathway. *Am J Physiol*. 1999;277(3):C403-C411.

125. Kondo M, Izawa-Ishizawa Y, Goda M, et al. Preventive Effects of Quercetin against the Onset of Atherosclerosis-Related Acute Aortic Syndromes in Mice. *Int J Mol Sci*. 2020;21(19). doi:10.3390/ijms21197226

126. Wu DN, Guan L, Jiang YX, et al. Microbiome and metabonomics study of quercetin for the treatment of atherosclerosis. *Cardiovasc Diagn Ther*. 2019;9(6):545-560.

127. Estrogenic biological activity and underlying molecular mechanisms of green tea constituents. *Trends Food Sci Technol*. 2020;95:247-260.

128. Arias-Loza PA, Jazbutyte V, Pelzer T. Genetic and pharmacologic strategies to determine the function of estrogen receptor alpha and estrogen receptor beta in cardiovascular system. *Gend Med*. 2008;5 Suppl A:S34-S45.

129. Dallas DC, Sanctuary MR, Qu Y, et al. Personalizing protein nourishment. *Crit Rev Food Sci Nutr*. 2017;57(15):3313-3331.

130. Macfarlane GT, Cummings JH, Allison C. Protein Degradation by Human Intestinal Bacteria. *Microbiology*. 1986;132(6):1647-1656.

131. Jiao M, He W, Ouyang Z, Shi Q, Wen Y. Progress in structural and functional study of the bacterial phenylacetic acid catabolic pathway, its role in pathogenicity and antibiotic resistance. *Front Microbiol*. 2022;13:964019.

132. Pourová J, Najmanová I, Vopršalová M, et al. Two flavonoid metabolites, 3,4-dihydroxyphenylacetic acid and 4-methylcatechol, relax arteries ex vivo and decrease blood pressure in vivo. *Vascul Pharmacol*. 2018;111:36-43.

133. Morita M, Yano S, Yamaguchi T, Yamauchi M, Sugimoto T. Phenylacetic acid stimulates reactive oxygen species generation and tumor necrosis factor-α secretion in vascular endothelial cells. *Ther Apher Dial*. 2011;15(2):147-150.

134. MacDonald A, van Wegberg AMJ, Ahring K, et al. PKU dietary handbook to accompany PKU guidelines. *Orphanet J Rare Dis*. 2020;15(1):171.

135. Asano Y, Nakazawa A, Endo K, et al. Phenylalanine dehydrogenase of Bacillus badius. Purification, characterization and gene cloning. *Eur J Biochem*. 1987;168(1):153-159.

136. Mavrides C, Orr W. Multispecific aspartate and aromatic amino acid aminotransferases in Escherichia coli. *J Biol Chem*. 1975;250(11):4128-4133.

137. Mayrand D. Identification of clinical isolates of selected species of Bacteroides: production of phenylacetic acid. *Can J Microbiol*. 1979;25(8):927-928.

138. Russell WR, Duncan SH, Scobbie L, et al. Major phenylpropanoid-derived metabolites in the human gut can arise from microbial fermentation of protein. *Mol Nutr Food Res*. 2013;57(3):523-535.

139. Erdmann GR, Wahba Khalil SK. Quantitative analysis of phenyl-acetic acid in*Proteus Mirabilis*cultures by high performance liquid chromatography. *J Liq Chromatogr*. 1985;8(8):1507-1517.

140. Olthof MR, Hollman PCH, Buijsman MNCP, van Amelsvoort JMM, Katan MB. Chlorogenic acid, quercetin-3-rutinoside and black tea phenols are extensively metabolized in humans. *J Nutr*. 2003;133(6):1806-1814.

141. Nemet I, Saha PP, Gupta N, et al. A Cardiovascular Disease-Linked Gut Microbial Metabolite Acts via Adrenergic Receptors. *Cell*. 2020;180(5):862-877.e22.

142. Doessegger L, Schmitt G, Lenz B, et al. Increased levels of urinary phenylacetylglycine associated with mitochondrial toxicity in a model of drug-induced phospholipidosis. *Ther Adv Drug Saf*. 2013;4(3):101-114.

143. Dodd D, Spitzer MH, Van Treuren W, et al. A gut bacterial pathway metabolizes aromatic amino acids into nine circulating metabolites. *Nature*. 2017;551(7682):648-652.

144. Yu F, Li X, Feng X, et al. Phenylacetylglutamine, a Novel Biomarker in Acute Ischemic Stroke. *Front Cardiovasc Med*. 2021;8:798765.

145. Zong X, Fan Q, Yang Q, Pan R, Zhuang L, Tao R. Phenylacetylglutamine as a risk factor and prognostic indicator of heart failure. *ESC Heart Fail*. 2022;9(4):2645-2653.

146. Liu Y, Liu S, Zhao Z, Song X, Qu H, Liu H. Phenylacetylglutamine is associated with the degree of coronary atherosclerotic severity assessed by coronary computed tomographic angiography in patients with suspected coronary artery disease. *Atherosclerosis*. 2021;333:75-82.

147. Wei H, Wu J, Wang H, et al. Increased circulating phenylacetylglutamine concentration elevates the predictive value of cardiovascular event risk in heart failure patients. *J Intern Med*. 2023;294(4):515-530.

148. Romano KA, Nemet I, Prasad Saha P, et al. Gut Microbiota-Generated Phenylacetylglutamine and Heart Failure. *Circ Heart Fail*. 2023;16(1):e009972.

149. Kühn S, Düzel S, Colzato L, et al. Food for thought: association between dietary tyrosine and cognitive performance in younger and older adults. *Psychol Res*. 2019;83(6):1097-1106.

150. Wikoff WR, Anfora AT, Liu J, et al. Metabolomics analysis reveals large effects of gut microflora on mammalian blood metabolites. *Proc Natl Acad Sci U S A*. 2009;106(10):3698-3703.

151. Selmer T, Andrei PI. p-Hydroxyphenylacetate decarboxylase from Clostridium difficile. A novel glycyl radical enzyme catalysing the formation of p-cresol. *Eur J Biochem*. 2001;268(5):1363-1372.

152. Nemet I, Funabashi M, Li XS, et al. Microbe-derived uremic solutes enhance thrombosis potential in the host. *MBio*. Published online December 19, 2023. doi:10.1128/mbio.01331-23

153. Bone E, Tamm A, Hill M. The production of urinary phenols by gut bacteria and their possible role in the causation of large bowel cancer. *Am J Clin Nutr*. 1976;29(12):1448-1454.

154. Dawson LF, Donahue EH, Cartman ST, et al. The analysis of para-cresol production and tolerance in Clostridium difficile 027 and 012 strains. *BMC Microbiol*. 2011;11:86.

155. Harrison MA, Kaur H, Wren BW, Dawson LF. Production of -cresol by Decarboxylation of -HPA by All Five Lineages of Provides a Growth Advantage. *Front Cell Infect Microbiol*. 2021;11:757599.

156. Bergé-Lefranc D, Chaspoul F, Calaf R, Charpiot P, Brunet P, Gallice P. Binding of p-cresylsulfate and p-cresol to human serum albumin studied by microcalorimetry. *J Phys Chem B*. 2010;114(4):1661-1665.

157. Ramakrishna BS, Roberts-Thomson IC, Pannall PR, Roediger WE. Impaired sulphation of phenol by the colonic mucosa in quiescent and active ulcerative colitis. *Gut*. 1991;32(1):46-49.

158. de Bruin A. *Biochemical Toxicology of Environmental Agents*. Elsevier Science & Technology; 1976.

159. Meijers BKI, De Loor H, Bammens B, Verbeke K, Vanrenterghem Y, Evenepoel P. p-Cresyl Sulfate and Indoxyl Sulfate in Hemodialysis Patients. *Clin J Am Soc Nephrol*. 2009;4(12):1932.

160. Itoh Y, Ezawa A, Kikuchi K, Tsuruta Y, Niwa T. Protein-bound uremic toxins in hemodialysis patients measured by liquid chromatography/tandem mass spectrometry and their effects on endothelial ROS production. *Anal Bioanal Chem*. 2012;403(7):1841-1850.

161. Gryp T, Vanholder R, Vaneechoutte M, Glorieux G. p-Cresyl Sulfate. *Toxins* . 2017;9(2). doi:10.3390/toxins9020052

162. Bogiatzi C, Gloor G, Allen-Vercoe E, et al. Metabolic products of the intestinal microbiome and extremes of atherosclerosis. *Atherosclerosis*. 2018;273:91-97.

163. Schepers E, Meert N, Glorieux G, Goeman J, Van der Eycken J, Vanholder R. P-cresylsulphate, the main in vivo metabolite of p-cresol, activates leucocyte free radical production. *Nephrol Dial Transplant*. 2007;22(2):592-596.

164. Pletinck A, Glorieux G, Schepers E, et al. Protein-bound uremic toxins stimulate crosstalk between leukocytes and vessel wall. *J Am Soc Nephrol*. 2013;24(12):1981-1994.

165. Gross P, Massy ZA, Henaut L, et al. Para-cresyl sulfate acutely impairs vascular reactivity and induces vascular remodeling. *J Cell Physiol*. 2015;230(12):2927-2935.

166. Wang CH, Cheng ML, Liu MH, et al. Increased p-cresyl sulfate level is independently associated with poor outcomes in patients with heart failure. *Heart Vessels*. 2016;31(7):1100-1108.

167. Meijers BKI, Claes K, Bammens B, et al. p-Cresol and cardiovascular risk in mild-to-moderate kidney disease. *Clin J Am Soc Nephrol*. 2010;5(7):1182-1189.

168. Bammens B, Evenepoel P, Keuleers H, Verbeke K, Vanrenterghem Y. Free serum concentrations of the protein-bound retention solute p-cresol predict mortality in hemodialysis patients. *Kidney Int*. 2006;69(6):1081-1087.

169. Liabeuf S, Barreto DV, Barreto FC, et al. Free p-cresylsulphate is a predictor of mortality in patients at different stages of chronic kidney disease. *Nephrol Dial Transplant*. 2010;25(4):1183-1191.

170. Patel KP, Luo FJG, Plummer NS, Hostetter TH, Meyer TW. The production of p-cresol sulfate and indoxyl sulfate in vegetarians versus omnivores. *Clin J Am Soc Nephrol*. 2012;7(6):982-988.

171. Shifting from a Conventional Diet to an Uncooked Vegan Diet Reversibly Alters Fecal Hydrolytic Activities in Humans. *J Nutr*. 1992;122(4):924-930.

172. Lunn J, Buttriss JL. Carbohydrates and dietary fibre. *Nutr Bull*. 2007;32(1):21-64.

173. Morrison DJ, Preston T. Formation of short chain fatty acids by the gut microbiota and their impact on human metabolism. *Gut Microbes*. 2016;7(3):189-200.

174. Makki K, Deehan EC, Walter J, Bäckhed F. The Impact of Dietary Fiber on Gut Microbiota in Host Health and Disease. *Cell Host & Microbe*. 2018;23(6):705-715. doi:10.1016/j.chom.2018.05.012

175. Russell WR, Gratz SW, Duncan SH, et al. High-protein, reduced-carbohydrate weight-loss diets promote metabolite profiles likely to be detrimental to colonic health. *Am J Clin Nutr*. 2011;93(5):1062-1072.

176. Duncan SH, Belenguer A, Holtrop G, Johnstone AM, Flint HJ, Lobley GE. Reduced dietary intake of carbohydrates by obese subjects results in decreased concentrations of butyrate and butyrate-producing bacteria in feces. *Appl Environ Microbiol*. 2007;73(4):1073-1078.

177. Cummings JH, Pomare EW, Branch WJ, Naylor CP, Macfarlane GT. Short chain fatty acids in human large intestine, portal, hepatic and venous blood. *Gut*. 1987;28(10):1221-1227.

178. Louis P, Hold GL, Flint HJ. The gut microbiota, bacterial metabolites and colorectal cancer. *Nature Reviews Microbiology*. 2014;12(10):661-672. doi:10.1038/nrmicro3344

179. Hernández, Hernández, Canfora, Jocken, Blaak. The Short-Chain Fatty Acid Acetate in Body Weight Control and Insulin Sensitivity. *Nutrients*. 2019;11(8):1943. doi:10.3390/nu11081943

180. Perry RJ, Peng L, Barry NA, et al. Acetate mediates a microbiome–brain–β-cell axis to promote metabolic syndrome. *Nature*. 2016;534(7606):213-217. doi:10.1038/nature18309

181. Koh A, De Vadder F, Kovatcheva-Datchary P, Bäckhed F. From Dietary Fiber to Host Physiology: Short-Chain Fatty Acids as Key Bacterial Metabolites. *Cell*. 2016;165(6):1332-1345.

182. Reichardt N, Duncan SH, Young P, et al. Phylogenetic distribution of three pathways for propionate production within the human gut microbiota. *ISME J*. 2014;8(6):1323-1335.

183. Derrien M, Vaughan EE, Plugge CM, de Vos WM. Akkermansia muciniphila gen. nov., sp. nov., a human intestinal mucin-degrading bacterium. *Int J Syst Evol Microbiol*. 2004;54(5):1469-1476.

184. Ottman N, Davids M, Suarez-Diez M, et al. Genome-Scale Model and Omics Analysis of Metabolic Capacities of Reveal a Preferential Mucin-Degrading Lifestyle. *Appl Environ Microbiol*. 2017;83(18). doi:10.1128/AEM.01014-17

185. Louis P, Flint HJ. Formation of propionate and butyrate by the human colonic microbiota. *Environ Microbiol*. 2017;19(1):29-41.

186. Byrne CS, Chambers ES, Morrison DJ, Frost G. The role of short chain fatty acids in appetite regulation and energy homeostasis. *International Journal of Obesity*. 2015;39(9):1331-1338. doi:10.1038/ijo.2015.84

187. Albenberg L, Esipova TV, Judge CP, et al. Correlation between intraluminal oxygen gradient and radial partitioning of intestinal microbiota. *Gastroenterology*. 2014;147(5):1055-1063.e8.

188. Kelly CJ, Zheng L, Campbell EL, et al. Crosstalk between Microbiota-Derived Short-Chain Fatty Acids and Intestinal Epithelial HIF Augments Tissue Barrier Function. *Cell Host Microbe*. 2015;17(5):662-671.

189. Martin-Gallausiaux C, Marinelli L, Blottière HM, Larraufie P, Lapaque N. SCFA: mechanisms and functional importance in the gut. *Proc Nutr Soc*. 2021;80(1):37-49.

190. Chang PV, Hao L, Offermanns S, Medzhitov R. The microbial metabolite butyrate regulates intestinal macrophage function via histone deacetylase inhibition. *Proceedings of the National Academy of Sciences*. 2014;111(6):2247-2252. doi:10.1073/pnas.1322269111

191. Arpaia N, Campbell C, Fan X, et al. Metabolites produced by commensal bacteria promote peripheral regulatory T-cell generation. *Nature*. 2013;504(7480):451-455.

192. Beisner J, Filipe Rosa L, Kaden-Volynets V, Stolzer I, Günther C, Bischoff SC. Prebiotic Inulin and Sodium Butyrate Attenuate Obesity-Induced Intestinal Barrier Dysfunction by Induction of Antimicrobial Peptides. *Front Immunol*. 2021;12:678360.

193. Wang Y, Xu Q, Meng M, Chang G, Ma N, Shen X. Butyrate Protects against γ-d-Glutamyl--diaminopimelic Acid-Induced Inflammatory Response and Tight Junction Disruption through Histone Deacetylase 3 Inhibition in Bovine Mammary Epithelial Cells. *J Agric Food Chem*. 2023;71(40):14638-14648.

194. Yan H, Ajuwon KM. Butyrate modifies intestinal barrier function in IPEC-J2 cells through a selective upregulation of tight junction proteins and activation of the Akt signaling pathway. *PLoS One*. 2017;12(6):e0179586.

195. Anderson JW, Baird P, Davis RH, et al. Health benefits of dietary fiber. *Nutr Rev*. 2009;67(4):188-205.

196. Li M, van Esch BCAM, Henricks PAJ, Folkerts G, Garssen J. The Anti-inflammatory Effects of Short Chain Fatty Acids on Lipopolysaccharide- or Tumor Necrosis Factor α-Stimulated Endothelial Cells via Activation of GPR41/43 and Inhibition of HDACs. *Front Pharmacol*. 2018;9:373720.

197. Tayyeb JZ, Popeijus HE, Mensink RP, Konings MCJM, Mokhtar FBA, Plat J. Short-Chain Fatty Acids (Except Hexanoic Acid) Lower NF-kB Transactivation, Which Rescues Inflammation-Induced Decreased Apolipoprotein A-I Transcription in HepG2 Cells. *Int J Mol Sci*. 2020;21(14). doi:10.3390/ijms21145088

198. Aguilar EC, Leonel AJ, Teixeira LG, et al. Butyrate impairs atherogenesis by reducing plaque inflammation and vulnerability and decreasing NFκB activation. *Nutr Metab Cardiovasc Dis*. 2014;24(6):606-613.

199. Kasahara K, Krautkramer KA, Org E, et al. Interactions between Roseburia intestinalis and diet modulate atherogenesis in a murine model. *Nature Microbiology*. 2018;3(12):1461-1471.

200. Vijay A, Astbury S, Panayiotis L, et al. Dietary Interventions Reduce Traditional and Novel Cardiovascular Risk Markers by Altering the Gut Microbiome and Their Metabolites. *Front Cardiovasc Med*. 2021;8:691564.

201. Queenan KM, Stewart ML, Smith KN, Thomas W, Fulcher RG, Slavin JL. Concentrated oat beta-glucan, a fermentable fiber, lowers serum cholesterol in hypercholesterolemic adults in a randomized controlled trial. *Nutr J*. 2007;6:6.

202. Xu D, Feng M, Chu Y, et al. The Prebiotic Effects of Oats on Blood Lipids, Gut Microbiota, and Short-Chain Fatty Acids in Mildly Hypercholesterolemic Subjects Compared With Rice: A Randomized, Controlled Trial. *Front Immunol*. 2021;12:787797.

203. Natarajan N, Hori D, Flavahan S, et al. Microbial short chain fatty acid metabolites lower blood pressure via endothelial G protein-coupled receptor 41. *Physiol Genomics*. 2016;48(11):826-834.

204. Pluznick JL, Protzko RJ, Gevorgyan H, et al. Olfactory receptor responding to gut microbiota-derived signals plays a role in renin secretion and blood pressure regulation. *Proc Natl Acad Sci U S A*. 2013;110(11):4410-4415.

205. Yang T, Santisteban MM, Rodriguez V, et al. Gut Dysbiosis Is Linked to Hypertension. *Hypertension*. Published online 2015. doi:10.1161/HYPERTENSIONAHA.115.05315

206. Kamo T, Akazawa H, Suda W, et al. Dysbiosis and compositional alterations with aging in the gut microbiota of patients with heart failure. *PLoS One*. 2017;12(3):e0174099.

207. Li J, Zhao F, Wang Y, et al. Gut microbiota dysbiosis contributes to the development of hypertension. *Microbiome*. 2017;5(1):14.

208. de la Cuesta-Zuluaga J, Mueller NT, Álvarez-Quintero R, et al. Higher Fecal Short-Chain Fatty Acid Levels Are Associated with Gut Microbiome Dysbiosis, Obesity, Hypertension and Cardiometabolic Disease Risk Factors. *Nutrients*. 2018;11(1). doi:10.3390/nu11010051

209. Roshanravan N, Mahdavi R, Alizadeh E, et al. Effect of Butyrate and Inulin Supplementation on Glycemic Status, Lipid Profile and Glucagon-Like Peptide 1 Level in Patients with Type 2 Diabetes: A Randomized Double-Blind, Placebo-Controlled Trial. *Horm Metab Res*. 2017;49(11):886-891.

210. Tilves C, Yeh HC, Maruthur N, et al. Increases in Circulating and Fecal Butyrate are Associated With Reduced Blood Pressure and Hypertension: Results From the SPIRIT Trial. *J Am Heart Assoc*. 2022;11(13):e024763.

211. Chen L, He FJ, Dong Y, et al. Modest Sodium Reduction Increases Circulating Short-Chain Fatty Acids in Untreated Hypertensives: A Randomized, Double-Blind, Placebo-Controlled Trial. *Hypertension*. 2020;76(1):73-79.

CHAPTER 2: CLINICAL IMPROVEMENT OF ENDOTHELIAL FUNCTION FROM BLUEBERRY SUPPLEMENTATION IN POST-MENOPAUSAL FEMALES DOES NOT TRANSFER VASCULAR PHENOTYPE TO MICE VIA THE GUT MICROBIOTA

I. SUMMARY

Cardiovascular disease (CVD) is a significant cause of morbidity and the leading cause of death across the globe.[1] As biological females age, they may face an increased likelihood of experiencing cardiovascular comorbidities, particularly after menopause.[2] However, it has recently been suggested that plant compounds (ie. phytochemicals) in darkly pigmented fruit may offer protection against CVD progression.[3] Thus, our previous clinical trial found that daily consumption of highbush blueberry powder improved brachial artery endothelial-mediated dilation in a responder cohort of post-menopausal participants with elevated or stage I hypertension.[4] To explore gut microbiome-derived metabolites in mediating responses to this blueberry intervention, we conducted a fecal microbiota transplant from our human participants into germ-free mice. We hypothesized that vascular phenotypes from the donors would be transferred to the recipient mice. Transplants were comprised of pooled fecal material from the responder cohort before blueberry intervention (Pre-Blueberry) and after twelve weeks of blueberry powder consumption (Post-Blueberry). All animals were provided an irradiated, purified maintenance diet void of blueberries to target the microbiome's impact on vascular phenotype. Results showed no differences in endothelial-mediated dilation (Pre-Blueberry: 372.2±20.6, Post-Blueberry: 417.9±15.6 AUC; p=0.6778), pulse wave velocity (Pre-Blueberry: 437.8±15.3, Post-Blueberry: 438.3±17.1 cm/s; p=0.0890), or intrinsic stiffness (Pre-Blueberry: 2350±256.6, Post-Blueberry: 2126±269.6 kPa; p=0.6000). These results suggest that microbiome composition alone may not be sufficient to recreate vascular phenotypes in this model; rather, the observed outcomes may be more reliant on blueberry-microbiome interactions. Although there were varied responses to blueberry intervention within the human population, which may have masked the outcomes in mice receiving pooled microbiome

samples, this research indicates that future studies should focus on exploring the impact of individual microbiomes on vascular phenotypes.

II. INTRODUCTION

Cardiovascular disease (CVD) is a global health concern and the leading cause of fatalities worldwide, with the risk of CVD increasing with age.[5] However, the pathophysiology of CVD differs between biological males and females, with endogenous estrogen production playing a crucial role. Estrogen has been shown to lower the risk for CVD in pre-menopausal females compared to age-matched males.[6] However, these cardioprotective effects of estrogen disappear after menopause, when the concentrations of this hormone class plummets.[6] An independent risk factor for CVD is endothelial dysfunction, characterized by the limited ability of the blood vessels to dilate under appropriate stimulus,[7] in which postmenopausal females are at increased risk.[8] However, studies suggest that dietary interventions rich in plant polyphenols may aid in lowering the risk for endothelial dysfunction in this demographic.[9] Therefore, clinical interventions that leverage polyphenols for their effect on endothelial health are a potential therapeutic approach to reduce overall CVD progression in postmenopausal females.

Polyphenols are a diverse group of plant-derived compounds produced by plants as a natural defensive mechanism against biological threats like ultraviolet radiation, microorganisms, or animals,[3] and contribute to the perceived color, taste, smell, astringency, and bitterness of many fruits and vegetables. Several epidemiological studies have observed that diets prolific in fruit and vegetable intake reduce CVD-associated conditions.[10–13] More specifically, distinct polyphenol-rich food sources, such as blueberries, may improve cardiovascular outcomes. The Nurses Health study, a large-scale epidemiological trial, followed 93,600 adult females and scrutinized the connection between diet and myocardial infarction incidence as an ancillary endpoint.[14] Results indicated an inverse relationship between the combined intake of blueberry and strawberries >3 servings/week and myocardial infarction incidence over eighteen years of tracking.[14] In a clinical trial, acute blueberry polyphenol intake increased flow-mediated dilation (FMD) of blood vessels in healthy adult males, indicating that

blueberries may positively impact endothelial function.[15] Moreover, a 45-gram daily intake of blueberry powder in obese males and females with metabolic syndrome improved endothelial function, independent of blood pressure, after a six-week intervention.[16]

Despite these promising results, previous research on the effects of regular blueberry consumption in the post-menopausal female population has been limited.[16,17] To bridge this gap, we conducted a clinical trial where estrogen-deficient post-menopausal females with elevated blood pressure or stage I hypertension were recruited to consume 22 grams of highbush blueberry powder (equivalent to 1 cup of fresh blueberries) daily for twelve weeks. Although the blueberry treatment did not significantly impact blood pressure, there was an improvement in FMD of the brachial artery, indicating improved endothelial function.[4] An unexpected finding was that the blueberry treatment participants were stratified into responders (>+1% increase in FMD) and non-responders (<+1% increase in FMD) based on interindividual differences in the magnitude and direction of FMD. In the responder group, there was a significant positive correlation ($p=0.047$) between the sum of total circulating polyphenol metabolites from baseline to twelve weeks, while the non-responders exhibited a significantly negative correlation ($p=0.042$). Furthermore, the polyphenol metabolites screened in the plasma of the participants were not of parent compound polyphenol origin nor glycosylated storage forms of polyphenols, but from microbially transformed polyphenol metabolites after modification from the gut microbiome. These results led us to hypothesize that the improvements in endothelial function observed in the responders were not solely due to the consumption of blueberries, but via modulation from the gut microbiome.

The gut microbiome plays a crucial role in human health. Our lab,[18–20] and others[21–23] have reported that gut microbiota impacts endothelial function in both mouse and clinical settings. As such, dietary interventions that interact with the gut microbiome can impact endothelial function, as seen with our previous blueberry intervention.[4] However, it is unclear if the gut microbiome's structure and function enhance the endothelial outcomes in post-

menopausal females who responded to blueberry treatment, versus those who did not. This discrepancy highlights the impact of interindividual variability that complicates clinical outcomes. To study this interaction, the present research implemented a well-established fecal transplant model. We transferred the pooled gut microbiota from the post-menopausal responder cohort to germ-free mice both before and after a twelve-week blueberry intervention. We hypothesized that the humanized mice with the transplanted microbiome before the blueberry intervention would result in endothelial dysfunction, and that a blueberry-conditioned microbiome would reduce this vascular impairment.

III. MATERIALS AND METHODS

Human Fecal Microbiota Characterization. Fecal DNA from human stool was extracted using the FastDNA Kit (No. 6540600, MP Biomedicals, Irvine, CA), following the manufacturer's protocol. Construction of the 16s rRNA sequencing libraries followed the Earth Microbiome Protocol utilizing the 515F-806R primer set containing a unique 12-bp error-correcting barcode on the forward primer.[24] Amplicons were generated using the Bio-Rad CFX96 thermal cycler with the following cycling conditions: 94°C for three min and then thirty-five cycles of 94°C for forty-five sec, 50°C for sixty sec, and 72°C for ninety sec, followed by 72°C for ten min. To ensure accuracy and eliminate false positive results, negative DNA extraction controls and no template PCR controls were included with each run. Amplicons were purified using AmPure beads and pooled in equimolar ratios. The pooled library was then quantified and sequenced on an Illumina MiSeq at the Next-Generation Sequencing Facility at the University of Colorado, Boulder.

Experimental Design: Male C57BL/6J mice were bred and maintained in a germ-free facility at the University of Nebraska Gnotobiotic Mouse Facility, co-housed 3-5 per cage in a temperature and humidity-controlled environment on a 12:12 hr light-dark cycle. Germ-free isolators were routinely tested for sterility by 16s rRNA gene PCR analysis of feces. Mice were given *ad libitum* access to autoclaved water and an irradiated standard diet (No. D22110403 with growing rodent AIN-93G vitamin and mineral mix, Research Diets, New Brunswick, NJ) consisting of 40% protein, 64% carbohydrate, 16% fat calories. All animal procedures were reviewed and approved by the University of Nebraska and Colorado State University Institutional Animal Care and Use Committees.

At the age of seven weeks, germ-free mice (N=15/cohort) were colonized with an inoculum prepared from pooled fecal material post-menopausal human donors (N=4-5/cohort) both before and after the donors consumed twenty-two grams of highbush blueberry powder for twelve weeks. The inoculum was stored in reduced phosphate-buffered saline in a 1:1.5 w/v

ratio. Each mouse was inoculated twice by oral gavage forty-eight hours apart with 100µl of pooled donor fecal matter at each gavage under sterile conditions and kept in positive pressure cage racks for two weeks to allow stabilization of microbial colonization before transfer to Colorado State University. For eight weeks, the animals continued on an irradiated diet in which body weight and food intake were monitored weekly until termination.

Animal termination and tissue collection: The experimental rodents were weighed, and feces were collected and flash-frozen before termination. The mice were then anesthetized using isoflurane and euthanized by exsanguination via cardiac puncture. The liver, spleen, cecum, and adipose tissue (subcutaneous, epididymal, and mesenteric depots) were removed, weighed, and flash-frozen, and stored at -80°C. Colon length was then recorded before flash-freezing. The thoracic aorta was cleaned of per-ventricular adipose tissue and either trimmed into 2mm segments for force myography measurements or stored in neutral buffered formalin (No. 5701, Epredia, Kalamazoo, MI). Second-order mesenteric arteries from the intestines were excised then placed in 37°C physiological saline solution (PSS: 0.288g NaH_2PO_4, No. S5011, Sigma-Aldrich, St. Louis, MO; 1.802g glucose, No. G7021; Sigma-Aldrich; 0.44g sodium pyruvate, No. P2256, Sigma-Aldrich; 20.0g bovine serum albumin, No. BP1600; Fisher Bioreagents, Pittsburgh, PA; 16.94g NaCl, No. A123130, Alfa Aesar, Ward Hill, PA; 1.9g KCl, No. P4504; Sigma-Aldrich; 0.58g $CaCl_2H_4O_2$, No. C7902; Sigma-Aldrich; 0.58g $MgSO_4{\cdot}7H_2O$, No. M2773, Sigma-Aldrich, 0.139g MOPS sodium salt, no. M9024; Sigma-Aldrich, and 0.015g EDTA, No. E478, Fisher Bioreagents; per 2 liters double deionized H2O at pH 7.4) and cannulated for endothelial function experiments.

Quantitative Polymerase Chain Reaction (qPCR): Cecal contents of the mice were collected at termination, and DNA was extracted using the SsoAdvanced Universal SYBR Green Supermix DNA Purification Kit (No. 1725274, Bio-Rad, Hercules, CA) before quantitative PCR verified microbial load. Reactions were optimized for the 16s rRNA gene using universal bacterial primers (forward 5=-AAACTCAAAKGAATTGACGG-3=, reverse 5=-

CTCACRRCACGAGCTGA-3=). The conditions used for cycling on the Bio-Rad CFX96 thermal cycler are as stated: 95°C for three min and then forty cycles of 95°C for fifteen sec, 61°C for fifteen sec, 72°C for ten sec, and 85°C for five sec followed by florescence detection.

Cecal Short-Chain Fatty Acids (SCFAs): Short-chain fatty acids (SCFAs) from frozen cecal contents were weighed and extracted using acidified water (pH 2.5). Following homogenization and sonication, samples were centrifuged twice at 20,0000 rcf for fifteen min to remove particulate matter. The collected supernatant was analyzed on a Gas Chromatograph with Flame Ionization Detection (GC-FID; Agilent 6890 Plus GC Series, Agilent 7683 Injector Series, GC Column: TG-WAXMS A 30 m × 0.25 mm × 0.25 μm). SCFAs were quantified by comparing peak areas to standard curves of commercial standards of acetic acid, propionic acid, and butyric acid (No. AX0073, No. 944251, No. 19215; Millipore Sigma, Burlington, MA).

Measurement of Endothelial Function: Endothelial function was evaluated using a pressure myography technique, as previously described.[25] The procedure involved removing mesenteric adipose tissue from second-order mesenteric arteries and placing two candidate arteries in separate pressure myograph chambers (No. 130DC, Danish Myo Technology, Ann Arbor, MI) containing physiologic saline solution (PSS) at 37°C. The arteries were then cannulated onto glass micropipettes and secured with suture. Arteries were equilibrated, refreshing the PSS at twenty min, twenty min, and five min for a total of forty-five min, then measured for the passive diameter of the internal lumen using MyoView 3.0.7 software. Following this measurement, the arteries were constricted with increasing doses of phenylephrine (PE) in three min intervals (PE: 10^{-9} to 10^{-5}M) and subsequently dilated with the endothelium-dependent dilator acetylcholine (ACh) at two min intervals (ACh: 10^{-9} to 10^{-4}M). To restore equilibrium, the arteries were rinsed with fresh PSS twice between ten min intervals. After preconstriction of the arteries with PE (10^{-5}M) for 5 min, a dose-response curve was established with the endothelium-independent dilator sodium nitroprusside (SNP) at two min intervals (SNP: 10^{-10} to 10^{-4}M). The percent dilation was calculated for each dose of ACh or SNP

relative to the PE-induced preconstriction at each time point using the following formula: percent dilation (%) = (increase in luminal diameter to ACh/SNP)/ [maximum decrease in luminal diameter to PE (10^{-5}M) preconstriction]x100. Finally, the area under the dose-response curve (AUC; trapezoid method) was calculated for each response.

Arterial Stiffness: Aortic pulse wave velocity (aPWV) was measured at twelve weeks post-colonization using a Doppler flow velocity system (Mouse Doppler acquisition system, Indus Instruments, Webster, TX) per methods described by our lab.[20,26] Briefly, mice were placed supine on a board with electrocardiogram electrodes and anesthetized using 2% isoflurane and oxygen at a flow rate of 2L/min. A target heart rate of ~450 beats/min was maintained by adapting isoflurane concentration during measurements while Doppler probes were placed on the transverse aortic arch and abdominal aorta. Distance between the probes was calculated with precision calipers and five consecutive two sec readings were taken to ascertain the R-wave of the ECG and the base of the Doppler signer per each probe. aPWV (in cm/s) was calculated by the formula: aPWV=(distance between the two probes)/($\Delta time_{abdominal}$ - $\Delta time_{transverse}$). Mechanical stiffness was determined via a wire myograph chamber (No. DMT620M, Danish Myo Technology, Ann Arbor, MI) from the methods previously described.[27] Briefly, 2-mm segments of the thoracic aorta were attached to pins in the chamber in duplicates and stretched incrementally by ~10% every three min until shearing of the vessel occurred. A 20μm segment of the thoracic aorta was used for measuring diameter and wall thickness after preservation in neutral buffered formalin (No. 5701, Fisher Bioreagents, Pittsburgh, PA) on Visiopharm 2023.01 software (Broomfield, CO).

Statistics: Data expressed as means ± SEM with the assumption of normality. Statistical analyses were carried out using a paired t-test for human Pre-Blueberry and Post-Blueberry groups or an unpaired t-test for mouse Pre-Blueberry and Post-Blueberry groups. Missing values and outliers were excluded from the comparisons. A mixed effects model with the

Geisser-Greenhouse correction upon the assumption of non-sphericity was used for comparisons trending over time. A p-value of ≤0.05 was considered statistically significant.

Microbiome statistical method is as follows. Paired-end sequence reads were demultiplexed using rev-comp-barcodes error correction to obtain adequate quality in the open-source bioinformatics tool Qiime2 (version Qiime2-2023.9).[28–30] Filtered 16s rRNA reads were assessed using a PHRED quality score of 25. Following this, forward reads were truncated at 250, and negative reads truncated at 231 base pairs. A feature table with amplicon sequence variants (ASVs), denoised statistics, and a sequencing table was produced using the DADA2 method.[30,31] The ASVs were taxonomically classified on the 'SILVA 138 99% OTUs from the 515F/806R region of sequences' Naïve Bayes classifier.[32,33] To refine the dataset, reads that were assigned to chloroplasts and mitochondria were filtered out as they were not deemed to be part of the microbiome. The resulting feature tables, taxonomy, and metadata were imported into MicrobiomeAnalyst marker data profiling for secondary workflow.[34] To process the data, a low count was applied at a cutoff of 10% using standard deviation as the variance filter. Additionally, data normalization was performed based on total sum scaling. Relative abundance between phyla was assessed via a two-way ANOVA between groups. Alpha diversity was calculated for each sample using Shannon's diversity index at the genus taxonomic level using the nonparametric Mann-Whitney U-test. Beta diversity was calculated using the PCoA ordination method with Bray-Curtis distance methods calculated at the genus taxonomic level and analyzed with pairwise PERMANOVA statistics. Linear discriminant analysis effect size (LEfSe) was calculated at a genus level with a p-value cutoff at 0.05 for original data and log LDA score of 2.0. A p-value of ≤0.05 was considered statistically significant, while a p-value =0.05 before false-discovery rate correction was regarded as trending toward statistical significance.

IV. RESULTS

The premise of the current study was to evaluate the vascular phenotype of humanized mice after microbial inoculation from post-menopausal females with elevated or Stage I hypertension after a dietary blueberry intervention. General subject characteristics of the donors are shown in Table 1.1. The microbial donor cohort was selected based on an FMD response of >1% from pre to post-treatment after ingesting 22 grams of blueberry powder for twelve weeks (Pre-Blueberry: $4.7x10^{-6}\pm2.2x10^{-5}$, Post-Blueberry: $1.7x10^{-4}\pm4.3x10^{-5}$ FMD/SRauc; Table 1.1).

Table 1.1 *General Characteristics of Participants*

	PRE-BLUEBERRY (N=5)	POST-BLUEBERRY (N=5)
Age (y)	60.6±0.5	60.6±0.5
Height (m)	1.6±0.01	1.6±0.01
Weight (kg)	75.6±9.0	75.4±9.0
BMI ($kg{\cdot}m^{-2}$)	28.1±3.1	28.1±3.2
SBP (mmHg)	140.4±5.0	141.1±5.4
DBP (mmHg)	81.5±2.5	83.2±3.5
FMD/SRauc	$4.7x10^{-6}\pm2.2x10^{-5}$[a]	$1.7x10^{-4}\pm4.3x10^{-5}$[b]
PWV (m/s)	7.7±0.8	7.6±0.6

Values are mean±SEM. Abbreviations: *BMI*, body mass index, *SBP*, systolic blood pressure, *DBP*, diastolic blood pressure, *FMD/SRauc*, flow-mediated dilation normalized to shear rate area under the curve, *PWV*, pulse wave velocity. Statistical analysis was performed using a paired Student's t-test. [a,b] $P<0.05$, data with different superscripted letters differ significantly.

Prior to inoculating the mice, an analysis was conducted on the microbial communities obtained from human donors both before and after the implementation of the blueberry intervention. The primary aim was to ascertain the potential impact of the blueberry intervention on the human gut microbiome and to authenticate the microbial signatures present

in the donor inocula prior to their transfer to the mice. Relative abundance between the donors was not statistically significant, yet there was a shift in the phyla percentages from Pre to Post-Blueberry treatment (Fig. 1.1a). The *Bacteriodota* (Pre-Blueberry: 17.2±0.05, Post-Blueberry: 20.7±0.08 %; Fig. 1.1a) and *Bacillota* (Pre-Blueberry: 65.0±0.15, Post-Blueberry: 74.2±0.08 %; Fig. 1a) relative abundance in the Post-Blueberry cohort increased with a subsequent decrease in *Verrucomicrobiota* (Pre-Blueberry: 16.0±0.2, Post-Blueberry: 4.1±0.02 %; Fig. 1.1a) *Actinomycetota* (Pre-Blueberry: 0.68±0.01, Post-Blueberry: 0.35±0.01 %; Fig. 1.1a), and *Pseudomonadota* (Pre-Blueberry: 1.0±0.01, Post-Blueberry: 0.5±0.01 %; Fig. 1.1a). Shannon's diversity index for alpha diversity richness and evenness at the genus level did not show significant changes within cohorts (Pre-Blueberry: 2.5±0.2, Post-Blueberry: 2.9±0.2; p=0.4206 Fig. 1.1b). Bray-Curtis distances were used to assess dissimilarity across the donor cohorts. The results between cohorts showed clustering by treatment with trending statistical difference between the Pre-Blueberry and Post-Blueberry treatments before Benjamini-Hochberg false discovery rate statistic (PCoA; PERMANOVA F-Value=0.04; p=0.05, FDR Adjusted W-statistic=0.9, Fig. 1.1c). In particular, the Post-Blueberry samples clustered more tightly together than the Pre-Blueberry samples indicating that taxa dispersion become less after blueberry intervention. After linear discriminant analysis effect size (LEfSe) statistics to determine amplicon sequence variant differences between the Pre to Post-Blueberry treatment, there was a significant increase in the *Colidextribacter* (Pre-Blueberry: 15799, Post-Blueberry: 71641; $p<0.05$, FDR Adjusted W-Statistic=0.9, LDA score=-4.45, Fig. 1.1d), and *Monoglobus* genera (Pre-Blueberry: 24051, Post-Blueberry: 142870; $p<0.05$, FDR Adjusted W-Statistic=0.9, LDA score=-4.77, Fig. 1.1d) in the Post-Blueberry group, which have both been implicated in polyphenol degradation.[35,36] In contrast, the Pre-Blueberry group exhibited higher *Escherichia Shigella* (Pre-Blueberry: 46479, Post-Blueberry: 2367; $p<0.05$, FDR Adjusted W-Statistic=0.9, LDA score=4.34, Fig. 1.1d), a known pathobiont implicated in HTN.[37]

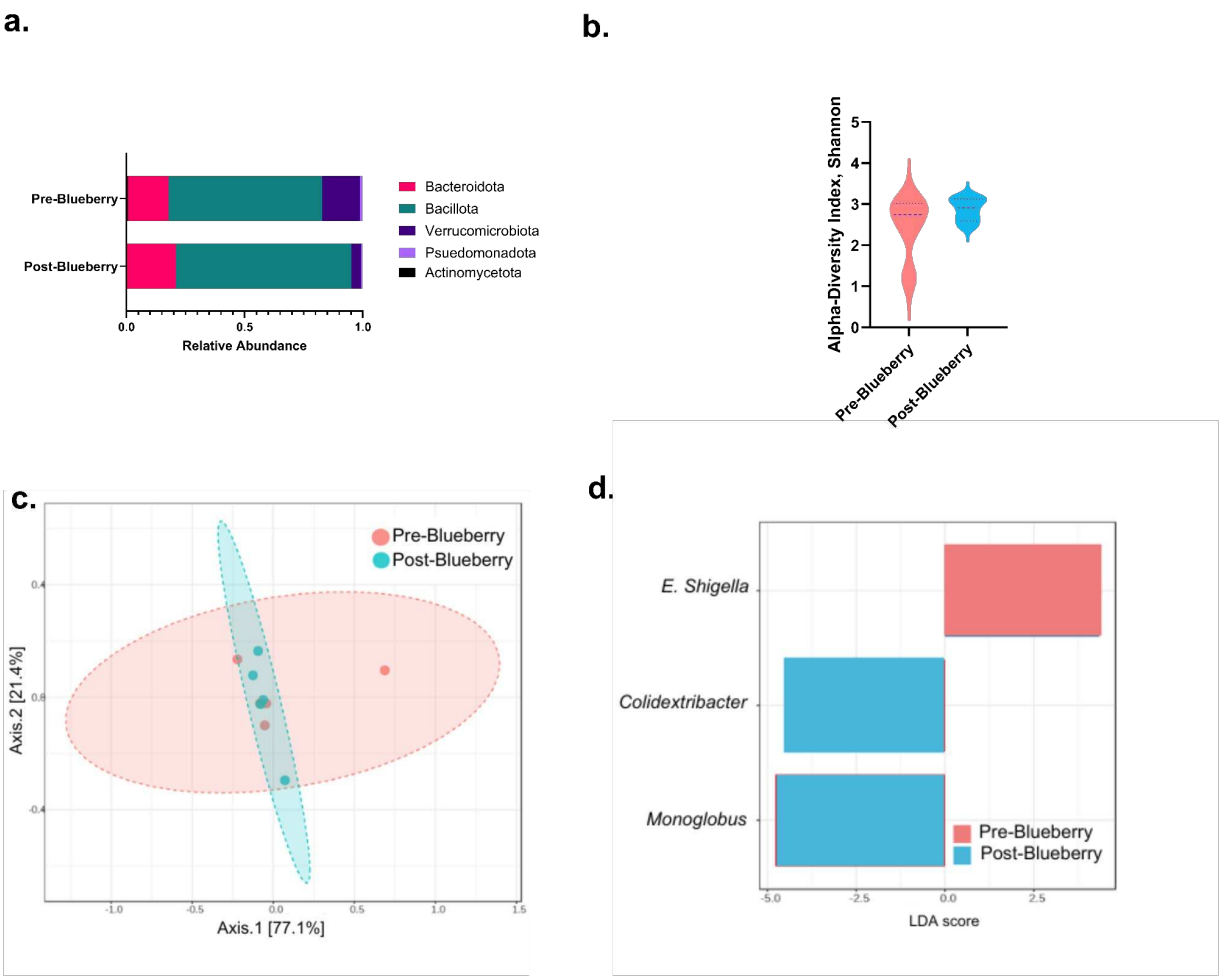

Fig. 1.1 Blueberry treatment in post-menopausal females shows trending differences in beta diversity. **a.** Relative abundance of major bacterial phyla **b.** Shannon's alpha diversity index **c**. Principle coordinate analysis (PCoA) of beta diversity at the phyla taxonomic level **d.** *Intestimonas* presence across cohorts **e.** *Colidextribacter* presence between Pre and Post Blueberry cohorts. Relative ASV abundance was analyzed using a two-way ANOVA. The Shannon's alpha diversity was calculated using the Mann-Whitney test, and the results were displayed through violin plots that indicate the minimum and maximum values, as well as the 25th-75th percentile range. PCoA is represented using the Bray-Curtis dissimilarity index at phyla level with pairwise PERMANOVA and Benjamini-Hochberg false discovery rate. Ellipses show the 95% confidence interval for each cohort. Bacterial genera presence using LefSe analysis of Kruskal-Wallis Test followed by linear discriminant analysis to evaluate differentially abundant genera.

Male C57/BL6 mice were chosen for this study over ovariectomized female mice to avoid unnecessary stress and increased risk of stress and infection, thereby affecting the physiology of the mice. After mice had been colonized with their respective donor inoculum (Pre-Blueberry or Post-Blueberry) at seven weeks of age, they were kept on a purified maintenance diet with an

appropriate nutritional composition to support the growth and development of young mouse pups. Mice were kept on their diet for eight weeks before termination to allow proper establishment of the donor microbiome and for maturity into adulthood. Weekly body weight and food intake were measured to assess the impact of colonization on feeding behavior, with tissue weights taken at termination. Mice displayed similar weights at baseline (p=0.7252). Average body weight (Pre-Blueberry: 29.8±0.5, Post-Blueberry: 29.4±0.5 g; p=0.0.5629, Fig. 1.2a) nor food intake (Pre-Blueberry: 16.7±0.6, Post-Blueberry: 17.1±1.3 g; p=0.8177, Fig. 1.2b) were significantly different between cohorts. The general characteristics of tissue weights between cohorts post-termination are delineated in Table 1.2. Overall, no statistically significant differences were noted in liver, spleen, adipose tissue, cecum weights, or colon length.

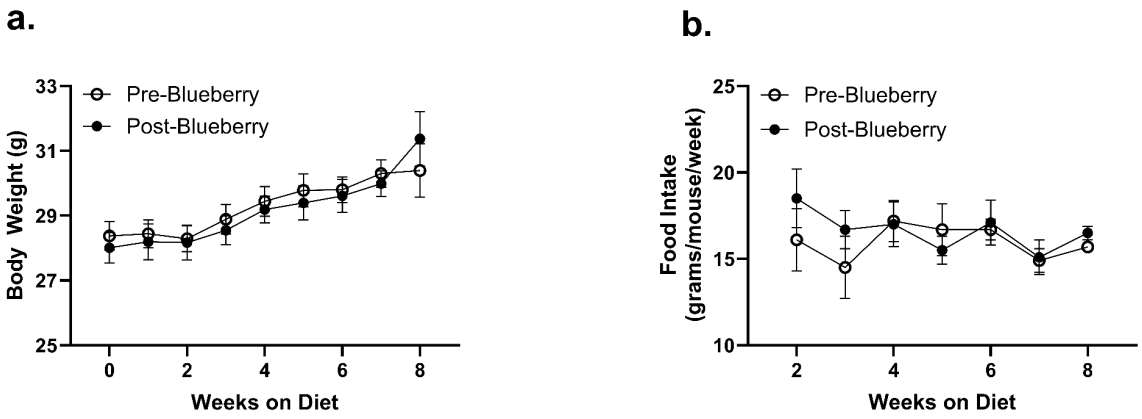

Fig. 1.2 Body weight and food intake do not vary based on donor inoculum. **a.** Body weight after inoculation **b.** Weekly food weight intake after inoculation. Statistical analysis was performed using a mixed-effects analysis with Geisser-Greenhouse correction upon the assumption of non-sphericity. Data expressed as mean±SEM; *n*=10-15/group.

Table 1.2. *General Characteristics of Mouse Tissue Weights & Colon Length*

	PRE-BLUEBERRY (N=15)	POST-BLUEBERRY (N=11)
Liver wt (mg)	1256.1±56.7	1243.6±39.2
Spleen wt (mg)	84.2±4.4	77.3±2.4
Epi Adipose wt (mg)	654.3±77.0	671.6±63.3
SQ Adipose wt (mg)	299.9±32.2	303.4±28.8
MAT (mg)	330.3±38.2	369.9±30.6
Cecum wt, whole (mg)	495.9±31.3[a]	517.9±34.7[a]
Colon length (cm)	5.2±0.1[a]	5.1±0.3[a]

Values are mean±SEM. *Epi* epididymal, *SQ* subcutaneous, *MAT* Mesenteric adipose tissue. Statistical analysis was performed using an unpaired Student's t-test. Data expressed as mean±SEM; *n*=11-15/group.

Next, we explored cecal microbial content related to the impact of blueberry conditioning on microbial metabolite production and its potential contribution to vascular response as endothelial function was improved in human donors after blueberry intervention. No significant differences existed in microbial load after quantitative polymerase chain reaction (PCR) of cecal contents (Pre-Blueberry: 20.02±0.2, Post-Blueberry:20.0±0.4 log(gene copy/µl); p=0.9355, Fig. 1.3a). We controlled for diet by keeping all mice on a standardized purified food before and after donor inoculation, then measured acetate, propionate, and butyrate as representative markers of short-chain fatty acids (SCFAs) concentration in the cecum after termination. No significant variations existed for acetate (Pre-Blueberry: 555.5±40.0, Post-Blueberry: 546.0.2±33.4 mM/gram; p=0.8679, Fig. 1.3b), propionate (Pre-Blueberry: 29.9±1.4, Post-Blueberry: 28.1±1.2; mM/gram; p=0.3752, Fig. 1.3c), or butyrate (Pre-Blueberry: 18.8±1.2, Post-Blueberry: 20.3±1.0; mM/gram; p=0.3834, Fig. 1.3d).

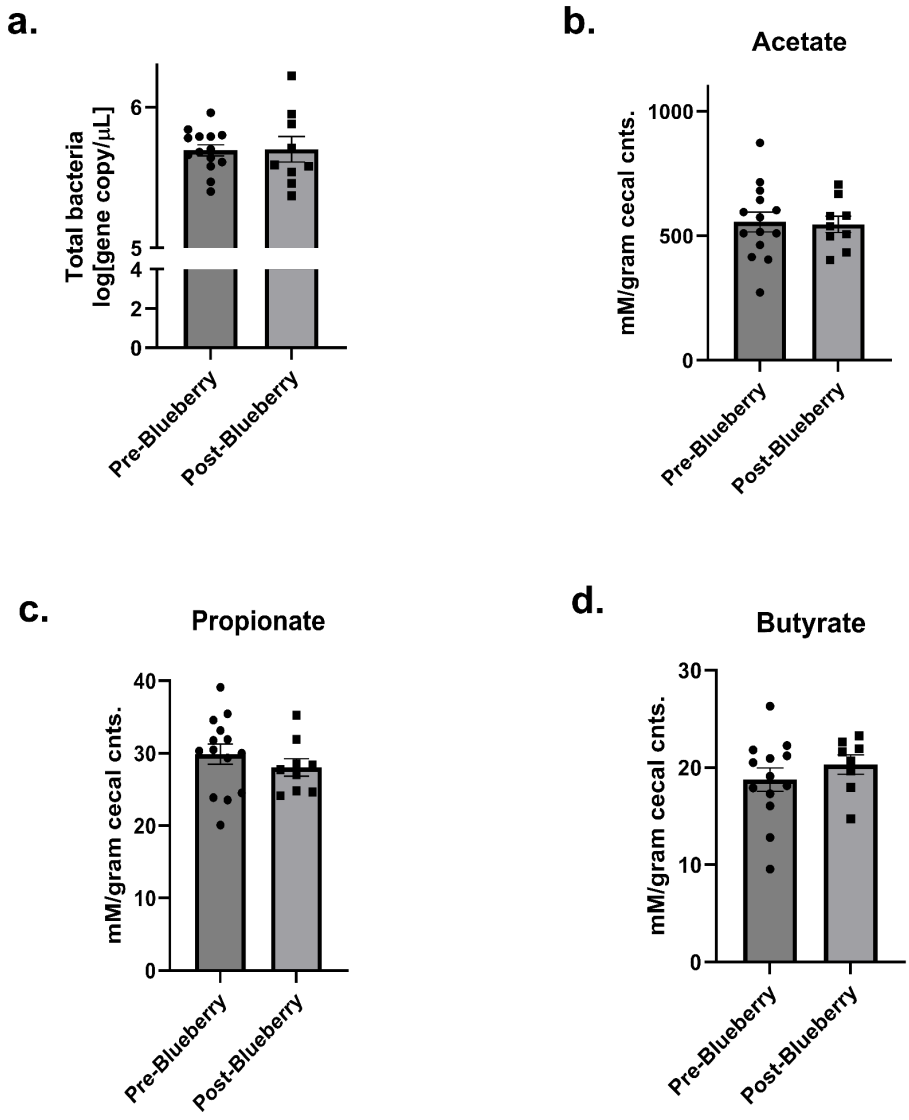

Fig. 1.3 Donor microbiome transplant does not impact cecal SCFA production. **a.** Total bacterial DNA per µl of cecal contents **b.** Acetate **c.** Propionate **d.** Butyrate. Statistical analysis was performed using an unpaired Student's t-test Data expressed as mean±SEM; *n*=8-13/group.

The vascular phenotype transfer in the mice was assessed through measurements of endothelial function and arterial stiffness. These measurements were selected due to their strong predictive value for future cardiovascular events.[38] Additionally, we investigated whether colonization from blueberry-conditioned microbiome impacted vascular function post-inoculation. Pressure myography of second-order mesenteric arteries was performed at termination to assess endothelial-dependent and independent response to pharmacological

vasodilators. There were no significant differences in passive luminal diameter (Pre-Blueberry: 173.7±5.3, Post-Blueberry: 179.1±5.6 μM; p=0.5117, Supp. 1a) or phenylephrine-induced preconstriction of isolated mesenteric arteries (Pre-Blueberry: 58.7±1.8 Post-Blueberry: 61.9±2.2 %; p=0.2633, Fig. 1.4a) before the addition of acetylcholine (ACh). Response and sensitivity to ACh endothelial-dependent dilation (EDD) were similar between all cohorts regardless of donor inoculum, with maximal average dilation of approximately 90% (Fig. 1.4b). No significant changes were seen in area under the curve (AUC: Pre-Blueberry: 372.2±20.6, Post-Blueberry: 417.9±15.6 AUC; p=0.2029, Fig. 1.4c). Although there were trending differences in endothelial-independent dilation (EID) between Pre-Blueberry and Post-Blueberry mice for the first two additions of sodium nitroprusside (SNP) (-10SNP: p=0.0666, -9SNP: p=0.0926, Fig. 1.4d), there were no changes in overall maximal dilation between cohorts (Pre-Blueberry: 97.8±1.8, Post-Blueberry: 97.5±1.5 %; p<0.05, Fig. 1.4d) nor AUC (Pre-Blueberry: 408.8±70.4, Post-Blueberry: 494.4±85.6 AUC; p=0.2392, Supp. 1b).

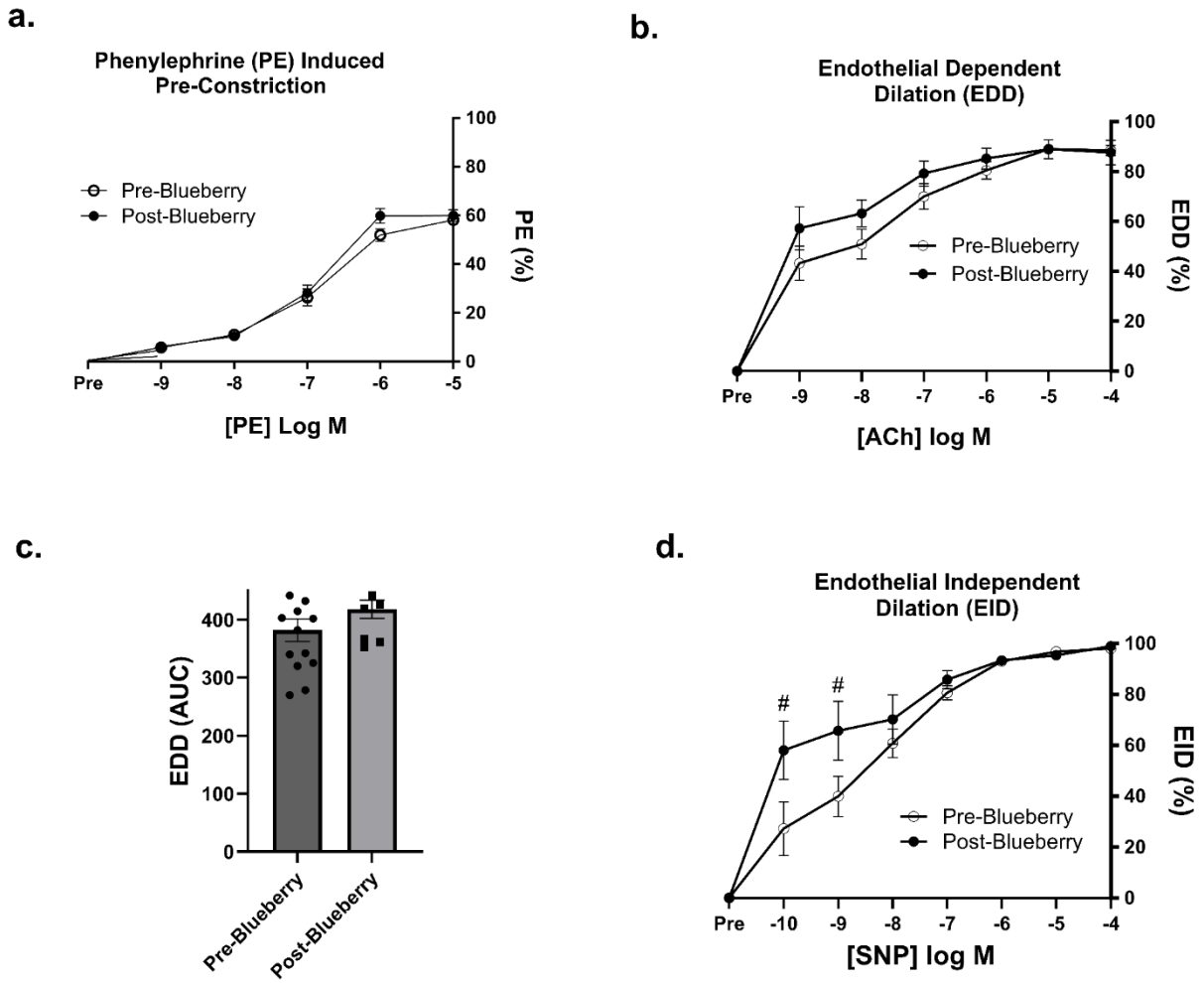

Fig. 1.4 Donor microbiome transplant does not impact endothelial function **a.** Phenylephrine (PE) induced preconstriction of maximal lumen diameter **b.** Endothelial-dependent dilation (EDD) in response to acetylcholine (ACh) **c.** Area under the curve of EDD **d.** Endothelial-independent dilation (EID) in response to sodium nitroprusside (SNP). Statistical analysis was performed using an unpaired Student's t-test for EDD area under the curve or mixed-effects analysis with Geisser-Greenhouse correction upon the assumption of non-sphericity (remaining outcomes). Data expressed as mean±SEM; *n*=8-15/group; #P=0.06-0.9.

In a separate analysis, arterial stiffness as measured by pulse wave velocity did not differ between cohorts at twelve weeks after inoculation (Pre-Blueberry: 437.8±15.3, Post-Blueberry: 438.3±17.1 cm/s; p=0.9817, Fig. 1.5a), nor did intrinsic stiffness of the thoracic aorta vary between groups at termination (Pre-Blueberry: 2350±256.6, Post-Blueberry: 2126±269.6 kPa; p=0.6000, Fig. 1.5b).

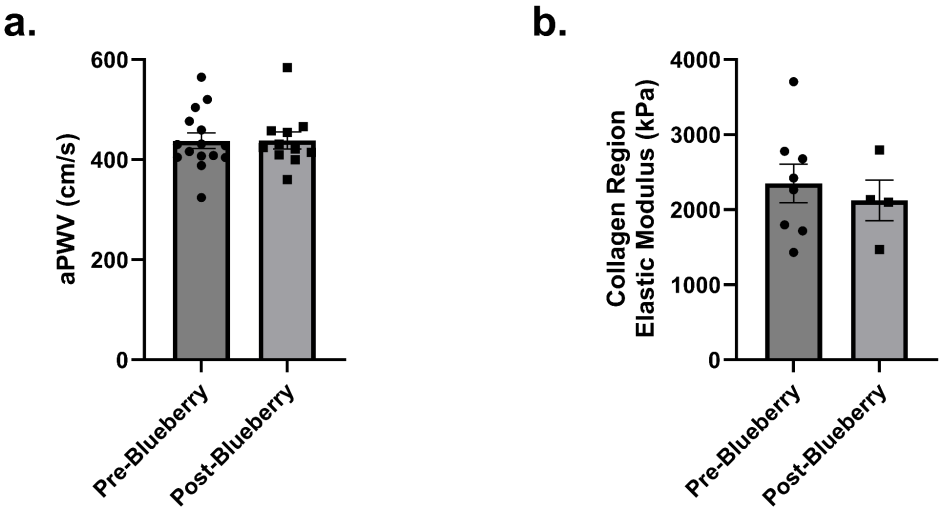

Fig. 1.5 Donor microbiome transplant does not impact arterial stiffness. **a.** arterial pulse wave velocity **b.** Intrinsic stiffness of thoracic aorta. Statistical analysis was performed using an unpaired Student's t-test. Data expressed as mean±SEM; *n*=11-15/group (aPWV), *n*=4-8/group (collagen region elastic modulus).

V. DISCUSSION

Given that nutrition has a significant impact on the gut microbiome, interventions that modify the diet present a promising opportunity to change the course of disease development. Innumerable studies,[21–23] including our own[18–20,25,26], have consistently demonstrated strong associations between the gut microbiome and vascular function. However, confounders such as genetics, lifestyle, dietary choices, and environment heavily influence clinical outcomes in humans, and a more controlled model is apt to tease out the impact of gut microbiome-targeted treatments. Transplantation of a human microbiome to germ-free mice is one of the most commonly used models to establish specific mechanistic relationships between the gut microbiome and disease, that cannot be efficiently evaluated in humans.[39,40] Therefore, the aim of this study was to establish if a hypertensive microbiome from post-menopausal females, either with or without blueberry conditioning, would confer vascular phenotype in naive germ-free mice. We hypothesized that if the gut microbiome aided in improved endothelial function after blueberry treatment in humans, similar effects would be observed in recipient mice.

The primary outcome of the present study runs contrary to our initial hypothesis. Specifically, our findings indicate that the gut microbiome of post-menopausal women with elevated or stage I hypertension does not impart a discernible vascular phenotype in mice. Neither mouse cohort demonstrated endothelial dysfunction, nor was there a significant alteration in arterial stiffness measured by pulse wave velocity and force myography. However, EID differed for the first two doses of SNP in mesenteric arteries, indicating that a blueberry-conditioned microbiome may have a vascular impact outside endothelial signaling of vasodilation. Food intake and body weight were consistent across cohorts throughout the course of the study, and tissue weights were respectively similar. Analysis of beta diversity in the donor microbiome indicated that after the blueberry treatment, post-menopausal females showed a higher degree of similarity compared to before intervention. In addition, *E. Shigella* was more present before intervention and *Monoglobus* and *Colidextribacter* genera were found to be significantly more abundant in the donors after blueberry treatment. Collectively, our data suggests that a hypertensive microbiome, either with or without blueberry conditioning, is not sufficient to confer vascular phenotype in mice, but distinct microbial signatures exist in the human donors after blueberry treatment that may have impacted vasodilation in the mice.

The fecal transplant failed to induce vascular dysfunction in mice, irrespective of donor status as endothelial dysfunction or arterial stiffness were not observed in either group. The lack of vascular phenotype transfer is in contradiction to previous studies. For example, Li. et al. transplanted elevated and hypertensive human microbiomes to mice and found that the blood pressure of the mice was reflective of their donor.[23] In a mouse-to-mouse fecal transplant, obese mice receiving donor inoculum from healthy mice supplemented with the polyphenol resveratrol exhibited a reduction in systolic blood pressure both with living and sterile fecal filtrates,[22] which was further corroborated by Greenburg et al., who confirmed that endothelial dysfunction could be induced or remediated by a fecal transplant between obese and lean mice.[21] Albeit there was no statistical difference in endothelial-dependent dilation, we noted that mice

with the blueberry-conditioned microbiome were more sensitive to the first two doses of SNP in endothelial-independent dilation. Although many polyphenols may induce endothelial nitric oxide release in mediating vascular dilation,[41] others have found that certain polyphenols impact the underlying smooth muscle. High polyphenol persimmon juice and leaf powder incubated with healthy rat mesenteric artery rings in a force-displacement transducer induced vasodilation after phenylephrine preconstriction.[42] Yet, the addition of the endothelial nitric oxide synthase inhibitor NG-nitro-L-arginine methyl ester (L-NAME) with carboxy-PTIO did not impact dilation, whereas non-selective potassium channel inhibitors did.[42] The researchers believed the mechanism of action from persimmon treatment may have been related to hyperpolarization of the vascular smooth muscle instead of directly impacting the endothelium. In another experiment involving pressure myography of rat mesenteric arteries bathed in the turmeric polyphenol curcumin, the researchers observed endothelial-dependent and independent vasodilation mechanisms.[43] Curmin dilated intact and endothelium-denuded arteries and was not affected by L-NAME or the soluble guanylyl cyclase inhibitor ODQ.[43] Additionally, curcumin induced dilation via inhibition of calcium from intracellular storage and induction of voltage-dependent potassium channels.[43]

Besides the potent antioxidant and anti-inflammatory actions of regular polyphenol intake, the processing of polyphenols by the gut microbiome into secondary metabolites has been implicated as a factor in the cardioprotective effect of polyphenols.[44] Data from our previous human study strongly suggested that the gut microbiome not only increased total circulating plasma metabolites but that these metabolites were from polyphenol modification by the gut microbiome after blueberry treatment.[4] While this study was unable to analyze bacterial taxa in the mice, there were differences in beta diversity in the human donors from before and after blueberry intervention. Bray-Curtis dissimilarity analysis indicated the microbiome samples evaluated after blueberry treatment clustered more tightly together in comparison to the baseline microbiome. This change in beta diversity has been corroborated by others who

have seen stratified differences in the microbiome of ovariectomized rats based on 0%, 2.5/5%, and 10/15% dietary blueberry inclusion.[45] Our beta diversity change may have been correlated to blueberry polyphenols and fiber as these compounds are prebiotic fuel sources for gut microbiota. We found higher polyphenol-degrading *Monoglobus*[35] and *Colidextribacter* bacteria[36] in the post-menopausal female microbiomes after blueberry treatment with a decrease in the pathobiont *E. Shigella*. As polyphenols can act as prebiotic fuel sources in the formation of SCFAs.[46] we specifically analyzed acetate, propionate, and butyrate production in the cecal contents of the recipient mice. However, we did not find a significant difference in the concentration of cecal SCFAs between groups, indicating a more subtle interplay of microbial blueberry polyphenol metabolism outside the scope of SCFA production.

The present study has several strengths. To ensure a representative microbial community and eliminate cage effects over time, all mice started in a germ-free environment and were gavaged with inoculum twice.[47] Throughout the study, the same diet was implemented to control for variations in dietary substrate available to the microbiome. We opted for a germ-free mouse model with inoculation at seven weeks of age over specific pathogen-free or antibiotic-treated mice for the following strengths: A germ-free mouse model is the gold standard for fecal transplantation. Inoculation early in life allows proper development of the immune system and gastrointestinal tract[47], which can be altered in adult germ-free mice. Additionally, there is no pre-established microbiome with which the inoculum engraftment can compete. However, there are also limitations to the current study that should be addressed. While the donors had validated elevations in blood pressure, a hypertensive microbial composition may not have been significant enough to drive vascular dysfunction in the donor mice. Also, while there was an improvement in the endothelial function in the human responders from the initial clinical trial, this dysfunction was not completely reversed. If normotensive individuals were included in the initial trial, a baseline for vascular alterations in the recipient mice could have been stratified by a normotensive post-menopausal donor cohort.

Regarding the fecal transplant, there is no standardized method for handling fecal samples, and we opted to freeze stool samples to halt microbial metabolism. The viability of microbiota after freezing can significantly decrease and also favor specific taxa that survive temperature gradients.[40] However, albeit using fresh stool or freezing in a maltodextrin-trehalose preservation medium[48], we cannot discredit the fact that anaerobic microbiota dominates the gut, and even when processing stool in strictly anaerobic conditions, 50% viability can be lost[49]. Moreover, all mice received a unified, pooled donor microbiome transplant to limit the interindividual microbiome composition from select participants. However, this choice may have blunted the microbial-mediated vascular phenotype transfer due to competing microbiota in the mixed samples. Lastly, we hypothesized that a blueberry-conditioned microbiome could alter vascular pathology in recipient mice under a standardized diet. However, there was no continuation of a targeted dose of blueberries in the diets of the mice, which may have been needed to validate vascular alterations between cohorts. The addition of blueberries to the mouse diets was outside the scope of our hypothesis but may be an avenue for future research to assess microbiome and vascular response.

VI. CONCLUSIONS

In conclusion, this study investigated a gut microbiota transplant from post-menopausal females with elevated or Stage I hypertension after blueberry treatment on vascular pathology in germ-free mice. Although the study did not yield similar results to previous research that linked fecal transplants to cardiovascular phenotype in germ-free mice, it did reveal subtle endothelium-independent vasodilation changes and microbiome alterations. These findings suggest that the therapeutic potential of a highbush blueberry powder-conditioned microbiome on vascular may not be solely due to changes in microbial signatures but the interaction of the microbiome and blueberries in conjunction. To further explore alternative mechanisms of action for the observed improvements in vascular health, future studies may focus on examining the

functional capacity of microbial-mediated polyphenol degradation as a mechanistic means for endothelial health.

REFERENCES

1. Wang MC, Lloyd-Jones DM. Cardiovascular Risk Assessment in Hypertensive Patients. *American Journal of Hypertension*. 2021;34(6):569-577. doi:10.1093/ajh/hpab021

2. Song JJ, Ma Z, Wang J, Chen LX, Zhong JC. Gender Differences in Hypertension. *J Cardiovasc Transl Res*. 2020;13(1):47-54.

3. Del Rio D, Rodriguez-Mateos A, Spencer JPE, Tognolini M, Borges G, Crozier A. Dietary (poly)phenolics in human health: structures, bioavailability, and evidence of protective effects against chronic diseases. *Antioxid Redox Signal*. 2013;18(14):1818-1892.

4. Woolf EK, Terwoord JD, Litwin NS, et al. Daily blueberry consumption for 12 weeks improves endothelial function in postmenopausal women with above-normal blood pressure through reductions in oxidative stress: a randomized controlled trial. *Food Funct*. 2023;14(6):2621-2641.

5. Benjamin EJ, Muntner P, Alonso A, et al. Heart Disease and Stroke Statistics-2019 Update: A Report From the American Heart Association. *Circulation*. 2019;139(10):e56-e528.

6. Yang XP, Reckelhoff JF. Estrogen, hormonal replacement therapy and cardiovascular disease. *Curr Opin Nephrol Hypertens*. 2011;20(2):133-138.

7. Rossi R, Nuzzo A, Origliani G, Modena MG. Prognostic role of flow-mediated dilation and cardiac risk factors in post-menopausal women. *J Am Coll Cardiol*. 2008;51(10):997-1002.

8. Mehta JL, McSweeney J. *Gender Differences in the Pathogenesis and Management of Heart Disease*. Springer; 2018.

9. Andriantsitohaina R, Auger C, Chataigneau T, et al. Molecular mechanisms of the cardiovascular protective effects of polyphenols. *Br J Nutr*. 2012;108(9):1532-1549.

10. Dauchet L, Amouyel P, Hercberg S, Dallongeville J. Fruit and vegetable consumption and risk of coronary heart disease: a meta-analysis of cohort studies. *J Nutr*. 2006;136(10):2588-2593.

11. Rienks J, Barbaresko J, Nöthlings U. Association of Polyphenol Biomarkers with Cardiovascular Disease and Mortality Risk: A Systematic Review and Meta-Analysis of Observational Studies. *Nutrients*. 2017;9(4). doi:10.3390/nu9040415

12. Behl T, Bungau S, Kumar K, et al. Pleotropic Effects of Polyphenols in Cardiovascular System. *Biomed Pharmacother*. 2020;130:110714.

13. Zurbau A, Au-Yeung F, Blanco Mejia S, et al. Relation of Different Fruit and Vegetable Sources With Incident Cardiovascular Outcomes: A Systematic Review and Meta-Analysis of Prospective Cohort Studies. *J Am Heart Assoc*. 2020;9(19):e017728.

14. Cassidy A, Mukamal KJ, Liu L, Franz M, Eliassen AH, Rimm EB. High anthocyanin intake is associated with a reduced risk of myocardial infarction in young and middle-aged

women. *Circulation*. 2013;127(2):188-196.

15. Rodriguez-Mateos A, Rendeiro C, Bergillos-Meca T, et al. Intake and time dependence of blueberry flavonoid-induced improvements in vascular function: a randomized, controlled, double-blind, crossover intervention study with mechanistic insights into biological activity. *Am J Clin Nutr*. 2013;98(5):1179-1191.

16. Stull AJ, Cash KC, Champagne CM, et al. Blueberries improve endothelial function, but not blood pressure, in adults with metabolic syndrome: a randomized, double-blind, placebo-controlled clinical trial. *Nutrients*. 2015;7(6):4107-4123.

17. Johnson SA, Figueroa A, Navaei N, et al. Daily blueberry consumption improves blood pressure and arterial stiffness in postmenopausal women with pre- and stage 1-hypertension: a randomized, double-blind, placebo-controlled clinical trial. *J Acad Nutr Diet*. 2015;115(3):369-377.

18. Trikha SRJ, Lee DM, Ecton KE, et al. Transplantation of an obesity-associated human gut microbiota to mice induces vascular dysfunction and glucose intolerance. *Gut Microbes*. 2021;13(1):1940791.

19. Trotter RE, Vazquez AR, Grubb DS, et al. DE111 intake may improve blood lipids and endothelial function in healthy adults. *Benef Microbes*. 2020;11(7):621-630.

20. Battson ML, Lee DM, Jarrell DK, et al. Suppression of gut dysbiosis reverses Western diet-induced vascular dysfunction. *Am J Physiol Endocrinol Metab*. 2018;314(5):E468-E477.

21. Greenberg NT, VanDongen NS, Gioscia-Ryan RA, et al. Vascular Endothelial Dysfunction Induced by a Western-Style Diet Can Be Transferred via Fecal Microbiota Transplant in Mice. *The FASEB Journal*. 2020;34(S1):1-1.

22. Kim TT, Parajuli N, Sung MM, et al. Fecal transplant from resveratrol-fed donors improves glycaemia and cardiovascular features of the metabolic syndrome in mice. *Am J Physiol Endocrinol Metab*. 2018;315(4):E511-E519.

23. Li J, Zhao F, Wang Y, et al. Gut microbiota dysbiosis contributes to the development of hypertension. *Microbiome*. 2017;5(1):14.

24. 16S Illumina Amplicon Protocol : earthmicrobiome. Accessed June 18, 2024. https://earthmicrobiome.org/protocols-and-standards/16s/

25. Lee DM, Battson ML, Jarrell DK, et al. SGLT2 inhibition via dapagliflozin improves generalized vascular dysfunction and alters the gut microbiota in type 2 diabetic mice. *Cardiovasc Diabetol*. 2018;17(1):62.

26. Battson ML, Lee DM, Li Puma LC, et al. Gut microbiota regulates cardiac ischemic tolerance and aortic stiffness in obesity. *Am J Physiol Heart Circ Physiol*. 2019;317(6):H1210-H1220.

27. Sindler AL, Cox-York K, Reese L, Bryan NS, Seals DR, Gentile CL. Oral nitrite therapy improves vascular function in diabetic mice. *Diab Vasc Dis Res*. 2015;12(3):221-224.

28. Hamady M, Knight R. Microbial community profiling for human microbiome projects: Tools, techniques, and challenges. *Genome Res*. 2009;19(7):1141-1152.

29. Hamady M, Walker JJ, Harris JK, Gold NJ, Knight R. Error-correcting barcoded primers for pyrosequencing hundreds of samples in multiplex. *Nat Methods*. 2008;5(3):235-237.

30. Bolyen E, Rideout JR, Dillon MR, et al. Reproducible, interactive, scalable and extensible microbiome data science using QIIME 2. *Nat Biotechnol*. 2019;37(8):852-857.

31. Callahan BJ, McMurdie PJ, Rosen MJ, Han AW, Johnson AJA, Holmes SP. DADA2: High-resolution sample inference from Illumina amplicon data. *Nat Methods*. 2016;13(7):581-583.

32. Robeson MS, O'Rourke DR, Kaehler BD, et al. RESCRIPt: Reproducible sequence taxonomy reference database management for the masses. *bioRxiv*. Published online October 5, 2020:2020.10.05.326504. doi:10.1101/2020.10.05.326504

33. Bokulich NA, Kaehler BD, Rideout JR, et al. Optimizing taxonomic classification of marker-gene amplicon sequences with QIIME 2's q2-feature-classifier plugin. *Microbiome*. 2018;6(1):1-17.

34. Chong J, Liu P, Zhou G, Xia J. Using MicrobiomeAnalyst for comprehensive statistical, functional, and meta-analysis of microbiome data. *Nature Protocols*. 2020;15(3):799-821. doi:10.1038/s41596-019-0264-1

35. Goris T, Cuadrat RRC, Braune A. Flavonoid-Modifying Capabilities of the Human Gut Microbiome—An In Silico Study. *Nutrients*. 2021;13(8):2688.

36. Li X, Wei T, Li J, et al. Tyrosol Ameliorates the Symptoms of Obesity, Promotes Adipose Thermogenesis, and Modulates the Composition of Gut Microbiota in HFD Fed Mice. *Mol Nutr Food Res*. 2022;66(15):e2101015.

37. Naik SS, Ramphall S, Rijal S, et al. Association of Gut Microbial Dysbiosis and Hypertension: A Systematic Review. *Cureus*. 2022;14(10):e29927.

38. Tanaka A, Tomiyama H, Maruhashi T, et al. Physiological Diagnostic Criteria for Vascular Failure. *Hypertension*. Published online November 2018. doi:10.1161/HYPERTENSIONAHA.118.11554

39. Turnbaugh PJ, Ridaura VK, Faith JJ, Rey FE, Knight R, Gordon JI. The effect of diet on the human gut microbiome: a metagenomic analysis in humanized gnotobiotic mice. *Sci Transl Med*. 2009;1(6):6ra14.

40. Park JC, Im SH. Of men in mice: the development and application of a humanized gnotobiotic mouse model for microbiome therapeutics. *Exp Mol Med*. 2020;52(9):1383-1396.

41. Schini-Kerth VB, Auger C, Etienne-Selloum N, Chataigneau T. Polyphenol-induced endothelium-dependent relaxations role of NO and EDHF. *Adv Pharmacol*. 2010;60:133-175.

42. Kudo R, Yuui K, Kasuda S. Endothelium-Independent Relaxation of Vascular Smooth Muscle Induced by Persimmon-Derived Polyphenol Phytocomplex in Rats. *Nutrients*. 2021;14(1). doi:10.3390/nu14010089

43. Zhang H, Liu H, Chen Y, Zhang Y. The Curcumin-Induced Vasorelaxation in Rat Superior Mesenteric Arteries. *Ann Vasc Surg*. 2018;48:233-240.

44. Bianchi F, Cappella A, Gagliano N, Sfondrini L, Stacchiotti A. Polyphenols-Gut-Heart: An Impactful Relationship to Improve Cardiovascular Diseases. *Antioxidants (Basel)*. 2022;11(9). doi:10.3390/antiox11091700

45. Weaver CM, Ferruzzi MG, Maiz M, et al. Crop, Host, and Gut Microbiome Variation Influence Precision Nutrition: An Example of Blueberries. *Antioxidants (Basel)*. 2023;12(5). doi:10.3390/antiox12051136

46. Kawabata K, Yoshioka Y, Terao J. Role of Intestinal Microbiota in the Bioavailability and Physiological Functions of Dietary Polyphenols. *Molecules*. 2019;24(2). doi:10.3390/molecules24020370

47. Wrzosek L, Ciocan D, Borentain P, et al. Transplantation of human microbiota into conventional mice durably reshapes the gut microbiota. *Sci Rep*. 2018;8(1):6854.

48. Bokoliya SC, Dorsett Y, Panier H, Zhou Y. Procedures for Fecal Microbiota Transplantation in Murine Microbiome Studies. *Front Cell Infect Microbiol*. 2021;11:711055.

49. Papanicolas LE, Choo JM, Wang Y, et al. Bacterial viability in faecal transplants: Which bacteria survive? *EBioMedicine*. 2019;41:509-516.

CHAPTER 3: THE GUT MICROBIOME REGULATES POLYPHENOL BIOAVAILABILITY IN POST-MENOPAUSAL FEMALES WITH IMPROVED ENDOTHELIAL FUNCTION AFTER BLUEBERRY TREATMENT

I. SUMMARY

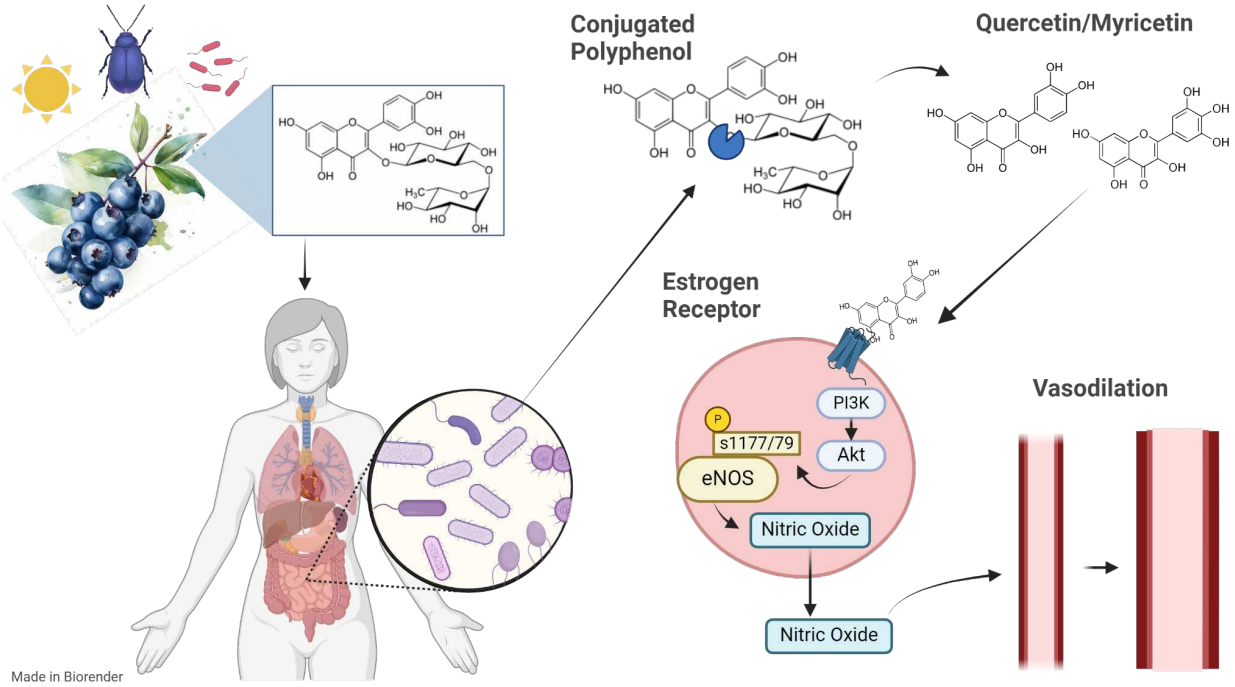

Fig 2.05. Proposed mechanism of microbial liberation of quercetin and myricetin from blueberries and the effect on endothelial-mediated dilation via estrogen receptors.

Cardiovascular disease (CVD) is a major contributor to illness and mortality worldwide, with biological females experiencing an increased risk of developing cardiovascular complications and hypertension following menopause.[1,2] Yet, epidemiological data indicate that a diet rich in plant-based food offers protection against the advancement of CVD which is partially attributed to polyphenol-rich food sources.[3] Blueberries, in particular, are a rich source of polyphenols and have been researched for their cardioprotective effects.[4] In our previous clinical trial, we found that daily twelve-week consumption of highbush blueberry powder improved arterial endothelial function through flow-mediated dilation measurements in post-menopausal females with elevated blood pressure or stage I hypertension. However, there was a degree of interindividual variability in the size and magnitude of endothelial response, which enabled us

to divide the cohort into responders (n=7) and non-responders (n=8). Although there were subtle differences in baseline characteristics, we also observed differences in circulating polyphenol-specific metabolites throughout the duration of the study. Based on our observations, we formulated a hypothesis that at the individual level, the gut microbiome varies in its capacity to metabolize polyphenols mediating levels of exposure to the bioactive metabolites of blueberries. Thus, we found responders to have a lower observed ASV alpha diversity index (responder: 55.75±3.9, non-responder: 75.5±1.5; $p<0.005$) and a significantly higher presence of polyphenol-degrading *Agathobacter, Monoglobus,* and *Dialister* ($p<0.005$) in the responders. Metagenomic profiling of the presence/absence of features showed no significant differences in polyphenol degradation or glucosidase pathways. However, the responders had higher circulating secondary polyphenolic metabolites, myricetin ($p<0.05$) and quercetin ($p=0.09$), that act as antioxidants and signaling molecules for blood vessel dilation at the vascular endothelium. Both *Phascolarctobacterium faecium* and *Alistipes shahii* were present in both the responders and non-responders. However, only *P. facium* and *A. shahii* in the responders had significantly higher quercetin-2,3 dioxygenase (QueD) genes responsible for processing quercetin and myricetin (*P. faecium*: log2FC=1.3, $p=0.0530$, *A. stipes*: log2FC=1.5; $p=0.0652$). In summary, this study suggests that gut microbiome may play a vital role in the variable endothelial response to highbush blueberry consumption in post-menopausal females with elevated blood pressure due to variations in gut microbiome polyphenol processing (**Fig. 2.05)**.

II. INTRODUCTION

Cardiovascular disease (CVD) is a grave global health concern, accounting for the highest number of deaths worldwide.[5] The risk of developing CVD increases with age, and it varies between biological males and females.[2] Females generally have a lower overall risk of CVD than age-matched males until they reach menopause.[2] A preclinical risk factor for CVD is related to a condition called endothelial dysfunction, characterized by blood vessels that are unable to fully dilate.[6] Endothelial dysfunction has been linked not only to vascular aging but to a lower concentration of estrogen in post-menopausal females.[1] Among its many functions, estrogen binds to estrogen receptors alpha (ERα) and beta (ERβ) on the vascular endothelium, inducing the release of nitric oxide (NO), to dilate blood vessels.[7] During menopause, estrogen levels in the body decrease, which can lead to a reduction in ER expression.[8,9] This, in turn, can cause a decrease in NO release associated with ER signaling, suggesting a modulatory role of estrogens on the endothelium.[8] However, studies in ovariectomized rodents suggest that estrogen supplementation can increase endothelial ER expression to restore NO signaling.[9,10] Furthermore, certain compounds consumed from plants in the diet have estrogenic properties that bind to ERα and ERβ, suggesting that diet may be a means to reduce endothelial dysfunction in postmenopausal females.[11]

Epidemiological data indicates that a diet rich in plant-based food offers protection against the advancement of CVD.[3,12,13] This is partially attributed to the presence of phytochemicals, particularly polyphenols, from fruits and vegetables in the diet. Polyphenols are classified into four main groups - flavonoids, phenolic acids, lignans, and stilbenes - based on the number of phenol rings and their functional groups. Plants contain various concentrations and types of polyphenols, but foods high in flavonoids and phenolic acids have been studied for their antioxidant properties in mitigating CVD.[3,13,14] Blueberries, are an incredibly rich source of phenolic acids and flavonoids[15] with approximately 300 milligrams per 100 grams of fresh fruit,[16] and have been researched for their cardioprotective effects. For example, a six-week

intervention in obese males and females with metabolic syndrome who consumed 45 grams of blueberry powder daily experienced a notable improvement in endothelial function, regardless of blood pressure.[17] Similar results were observed in another study involving the same demographic, where a decrease in blood pressure was observed after an eight-week intervention involving 50 grams of freeze-dried blueberry powder.[18] Additionally, the consumption of blueberries on an acute basis has been found to enhance flow-mediated dilation (FMD) of blood vessels in healthy adult males, indicating a positive impact of blueberries on endothelial function.[19] However, the implications of blueberry intervention on endothelial function in postmenopausal females have been relatively limited[17,20] and thus the basis for our initial clinical trial. Post-menopausal females who had elevated blood pressure or stage I hypertension consumed 22 grams of highbush blueberry powder daily for a period of twelve weeks. While the blueberry treatment did not show significant results in terms of reducing blood pressure, an increase in FMD, as a proxy for improvement in endothelial function was observed.[21]

Despite the overall benefits of blueberry consumption, there were individuals who were responders (with a >+1% FMD increase) or non-responders (with a <+1% FMD increase). The responders showed a greater improvement than the non-responders, with a notable difference of +4.26% versus -1.25% ($p<0.001$). Although the cause for this inter-individuality in response is unknown,[17,22,23] we noted higher baseline estradiol concentrations ($p=0.002$), lower ending plasma nitrate ($p=0.028$), lower baseline FMD ($p=0.031$), higher intercellular adhesion molecule-1 ($p=0.010$), and higher phosphorylated endothelial nitric oxide synthase (eNOS) in responders ($p=0.019$).[24] Interestingly, total polyphenol-specific metabolites increased at weeks four and twelve ($p=0.047$) along with alterations in specific secondary metabolites over time.[24] Our analysis of the metabolites present in the plasma of the participants revealed that they were not glycosylated storage forms of polyphenols, but rather polyphenol secondary metabolites that had been modified by the gut microbiome. As a result, we hypothesized that gut microbiome differences may account for a portion of the variability in response.

The gut microbiome is a consortium of bacteria, fungi, archaea, virus, and the metabolites they produce that reside in the gastrointestinal tract.[25] Among its many functions, the gut microbiome plays an integral role in the degradation of plant polyphenols to allow their secondary metabolites to be accessed by the host to exert their pleiotropic effects.[26,27] Glycosylated polyphenol parent compounds are rarely found in circulation due to low bioavailability and require biotransformation by the gut microbiome and intestinal enzymes before entering the bloodstream.[28] The diverse range of polyphenol-metabolizing enzymes present in microbial species can collectively result in the production of different secondary metabolites depending on the taxa present. Therefore, variation in the gut microbiome might explain different levels of exposure to the bioactive polyphenols that modulate endothelial-mediated dilation.

With the continuous improvement of microbial detection techniques, we have made significant strides in defining the structure and function of the gut microbiome through complementary methods such as 16srRNA and metagenomic sequencing. With these advancements, we have recognized that the gut microbiota fulfills critical needs in digestion that systematically affect host metabolism in health, and in CVD. However, the metabolic pathways and end metabolites interacting with endothelial-mediated dilation in post-menopausal females remain unclear. To explore the microbial contribution to the interindividual response to a dietary blueberry intervention in this demographic, we utilized a multifaceted approach that studied the connections between polyphenols, the gut microbiome, and circulating polyphenol metabolites. The objective was to identify the polyphenol degradation features of the gut microbiome and their relationship to circulating metabolites that may play a crucial role in inducing vasodilation, and promotion of a healthy endothelial response. We hypothesized differences in gut microbiome polyphenol decomposition pathways would lead to the liberation of vasoactive metabolites driving endothelial-mediated dilation in the responder group of our blueberry intervention.

III. METHODS

16s rRNA Fecal Microbiota Characterization: Fecal DNA was collected from stool samples and extracted using the FastDNA Kit (No. 6540600; MP Biomedicals, Irvine, CA) as per the manufacturer's instructions for preparation and 16s sequencing libraries. The Earth Microbiome Protocol was used for Quantitative PCR, which utilized the 515F-806R primer set containing a unique 12-bp error-correcting barcode on the forward primer for amplification of the V4 16S rRNA region. Thermal cycling conditions using the Bio-Rad CFX96 thermal cycler involved thirty-five cycles at 94°C for forty-five seconds, 50°C for sixty seconds, and 72°C for ninety seconds, followed by 72°C for ten minutes. Negative DNA extraction controls and no template PCR controls were included in the 96-well plates to eliminate false positive results and ensure accuracy. The extracted amplicons were purified using AmPure beads and pooled in equimolar ratios before quantification and sequencing on an Illumina MiSeq at the Next-Generation Sequencing Facility at Colorado State University.

Metagenomic Sequence and Assembly: A total amount of 1ug DNA per sample was used as input material in sample preparations. Sequencing libraries were generated using the NEBNext® Ultra™ DNA Library Prep kit (No. NEB E7645, New England Biolabs, Ipswich, MA) for Illumina following the manufacturer's recommendations. Index codes were added to attribute sequences to each sample. DNA was fragmented via sonication to a size of 350bp and DNA fragments were end-polished, A-tailed, and ligated with the full-length adaptor for Illumina sequencing with further PCR amplification. Lastly, PCR products were purified using the AMPure XP system (Beckman Coulter, Chaska, MN), and libraries were analyzed for size distribution by the Agilent 2100 Bioanalyzer (No. G2939BA, Agilent, Santa Clara, CA) and quantified using real-time PCR. The clustering of the index-coded samples was performed on a cBot Cluster Generation System (No. SY-301-2002, Illumina, San Diego, CA) according to the manufacturer's instructions. After cluster generation, the library preparations were sequenced on an Illumina HiSeq platform (No. SY-401-1001, Illumina, San Diego, CA) and paired-end

reads were generated. The original data obtained from the high throughput sequencing platforms were transformed into sequenced reads by base calling. Raw data were recorded in Fastq files containing sequenced reads and corresponding sequencing quality information. Fastq files ran through quality control, removing reads containing adapters, reads containing N>10%, and reads containing a Qscore ≤5. Taxonomy assigned to metagenomic assemblies using MetaPhlAn4.[29] A gene-centric approach using DRAM2[30,31] with CAMPER[31] software was used to filter out contigs <2500bp and subsequently call genes using Prodigal (v2.6.3).[32] CD-Hit-EST (v4.8.1)[33] was used to cluster genes at 95% identity with an alignment coverage of 80% for the shorter sequence. A bowtie (v2.4.5) database was built using the clustered genes. Each set of quality controls was then mapped back to the clustered gene database. CoverM (v0.7.0)[34] was then used to normalize gene counts which aligned at ≥97% identification, ≥3x depth, and ≥75% coverage. The coverM normalized gene counts were then input Maaslin2 (v1.7.3)[35] in R software to determine multivariable associations between phenotypes, then subsampled at fifteen million reads. Enzymes were mined from DRAM and CAMPER raw outputs and cross-referenced with GenomeNet database for validation against bacterial taxa.[36]

Circulating Polyphenol Metabolites: Targeted plasma polyphenol metabolomics was performed per micro-elution solid phase extraction (μ-SPE) combined with ultra-high-performance liquid chromatography triple-quadrupole time-of-flight mass spectrometry (UHPLC-Qq TOF MS) in methods previously described.[37] Polyphenolic metabolites were extracted from stored plasma samples of the study participants after thawing in an ice bath. Undiluted plasma samples were acidified with 4% phosphoric acid (v:v 1:1) and centrifuged at 15,000rcf for fifteen minutes at 4°C and spiked with 50nM of a taxifolin internal standard. 600 μL of the prepared plasma samples were first loaded into an μ-SPE Oasis HLB plate (No. 186005837, Waters, Eschborn, Germany), washed with 200μL water and 0.2% acetic acid, before eluting with 60μL methanol and sealed with a polyolefin film to prevent evaporation. 5 μL of the eluded samples were injected through a Raptor Biphenyl column 2.1 x 50 mm, 1.8μm

(No. 9309252, Restek, Bellefonte, USA) with a compatible Raptor Biphenyl Guard Cartridges 5 x 2.1 mm (No. 9309U0252, Restek, Bellefonte, USA) on a triple quadrupole mass spectrometer (No. LCMS-8060, SHIMADZU, Kyoto, Japan) in negative mode. During the run, a maintained flow rate at 0.5 mL/min, with the mobile gradient phase consisting of 0.1% formic acid (solvent A) and acetonitrile with 0.1% formic acid (solvent B) lasting fourteen minutes, at a temperature of 30°C. The elution profile began at 1% solvent B, increasing to 10% after five minutes, then 25% at eight minutes, and to 99% at nine minutes. The percentage of solvent B was held constant for one minute. The gradient was then reverted to 1% solvent B for two min to equilibrate the column. To identify the metabolites, retention times were compared with authentic polyphenol standards in corresponding multiple reaction monitoring transitions. The quantity of metabolites was measured by using calibration curves made from standard mixes through the SHIMADZU LabSolutions™ LCMS Software.

Statistics: Data expressed as means ± SEM without the assumption of normality. Missing values and outliers were excluded from the comparisons and triplicate measures in each group were required for calculations. A p-value of ≤0.05 was considered statistically significant, while a p-value=0.051-0.09 before false-discovery rate correction was regarded as trending toward statistical significance.

Microbiome statistical method for 16s rRNA data is as follows. Paired-end sequence reads were demultiplexed using rev-comp-barcodes error correction and assessed for quality in the open-source bioinformatics tool Qiime2 (version Qiime2-2023.9).[38–40] Next, 16s rRNA reads were filtered and assessed using a PHRED quality score of 25. Forward reads were then truncated at 250, and negative reads truncated at 242 base pairs resulting in a feature table with amplicon sequence variants (ASVs), denoised statistics, and a sequencing table using the DADA2 method.[40,41] The ASVs were taxonomically classified on the 'SILVA 138 99% OTUs from the 515F/806R region of sequences' Naïve Bayes classifier[42,43] before filtering out reads assigned to chloroplasts and mitochondria as they were not considered part of the bacterial gut

microbiome. Microbiome Analyst marker data profiled for secondary workflow was used from the resulting feature tables, taxonomy, and metadata.[44] A 10% low count cutoff of 10% was applied using standard deviation as the variance filter and data normalization was performed based on total sum scaling. Relative abundance for dominant phyla calculated using a two-way ANOVA with Sidak's multiple comparison's test. Alpha diversity was calculated for each sample using observed and Shannon's diversity index at the genus taxonomic level using the non-parametric unpaired t-test, with a Mann-Whitney post hoc test when a significant main effect was observed. Beta diversity was calculated using the PCoA ordination method with Bray-Curtis distance methods calculated at the genus taxonomic level and analyzed with PERMDISP multivariate statistics. Empirical analysis of digital gene expression in R (EDGER) univariate analysis was performed at a genus level for comparison between groups assuming read counts followed a negative binomial distribution, where the mean of the count is less than the variance.[45,46]

Microbiome statistical method for metagenomic polyphenol metabolism pathways as follows. Resulting DRAM, relative abundance and presence/absence datasets, and CAMPER pathway analysis were independently analyzed in the MetaboAnalyst 6.0 workflow.[47,48] Data was auto-scaled and normalized to the median value before univariate, chemometric, and cluster analyses. Meta-analysis was performed at the pathway level. The percentage of response variance was predicted using orthogonal partial least squares (OPLS) by R2X (and respectively R2Y) percentage of predictor variance explained by the full model, and Q2 as a cross-validation of predictive performance using two (DRAM), four (carbohydrate/glycoside), and two (CAMPER) permutations respectively. Heatmaps were produced using Euclidean distance measure with the Ward clustering algorithm on normalized data for the direct parent compounds of detected serum plasma metabolites with hierarchical clustering based on abundance. Fold change (FC) was calculated to compare the ratios of group means using non-responders as the control, only features with FC>2.0, or log2FC>0.5 were considered further.

Statistical analysis for metabolomic volcano plot used a non-parametric unpaired two-tailed Student's t-test against log2FC of the respective metabolites. Metabolite-metabolite interaction network associations were extracted from the search tool for interactions of chemicals (STITCH) tool so that only highly confident interactions are exhibited for chemical structure and molecular activities. Kyoto Encyclopedia of Genes and Genomes (KEGG) global metabolic network used to visually explore fold change integration from joint plasma metabolomics and bacterial metagenomic data.

IV. RESULTS

We first investigated the relative abundance of the gut microbiota along with alpha and beta diversity between blueberry intervention responders and non-responders. Analysis of 16s rRNA sequencing demonstrated that there were no discernible variations in the relative abundance of the six most prevalent gut bacterial phyla ($p=0.9891$, Fig. 2.1a). However, we did observe a lower number of observed amplicon sequence variants (ASVs) at the genus level in the responders (responder: 55.75±3.9, non-responder: 75.5±1.5; $p<0.005$, Fig. 2.1b), which was also reflected as a trending reducing in Shannon's diversity index (responder: 2.70±0.14, non-responder: 3.03±0.1; $p=0.0667$, Fig. 2.1c). Bray-Curtis beta diversity distances using pairwise PERMANOVA multivariate permutation test was used to assess dissimilarity between groups and ordination plots showed clustering by outcome attained genus level significance (PCoA: PERMANOVA F-Value=1.79; $p=0.0570$, Fig. 2.1d). Yet, PERMDISP analysis for evaluating dispersion and location between groups was insignificant (PCoA: PERMDISP F-Value=0.44; $p=0.5236$, Fig. 2.1d). Heat tree analysis indicated that responders had higher abundance of *Negativicutes* with lower abundance of *Prevotella, Bifidobacterium, Lachnospiriaceae, Peptostreptococcales, and Oscillospiraceae* than non-responders (Supp. Figure 1a). EDGER single-factor analysis showed higher *Agathobacter, Monoglobus,* and *Dialister* in responders(*Agathobacter*: log2FC=3.7; $p<0.005$, *Monoglobus*: log2FC=3.5; $p<0.005$, *Dialister*:

log2FC=6.1; p,0.0005; Supp. Figure 2 a,b,c), all with established links to deglycosylation or degradation of polyphenols to short-chain fatty acids (SCFAs).[49]

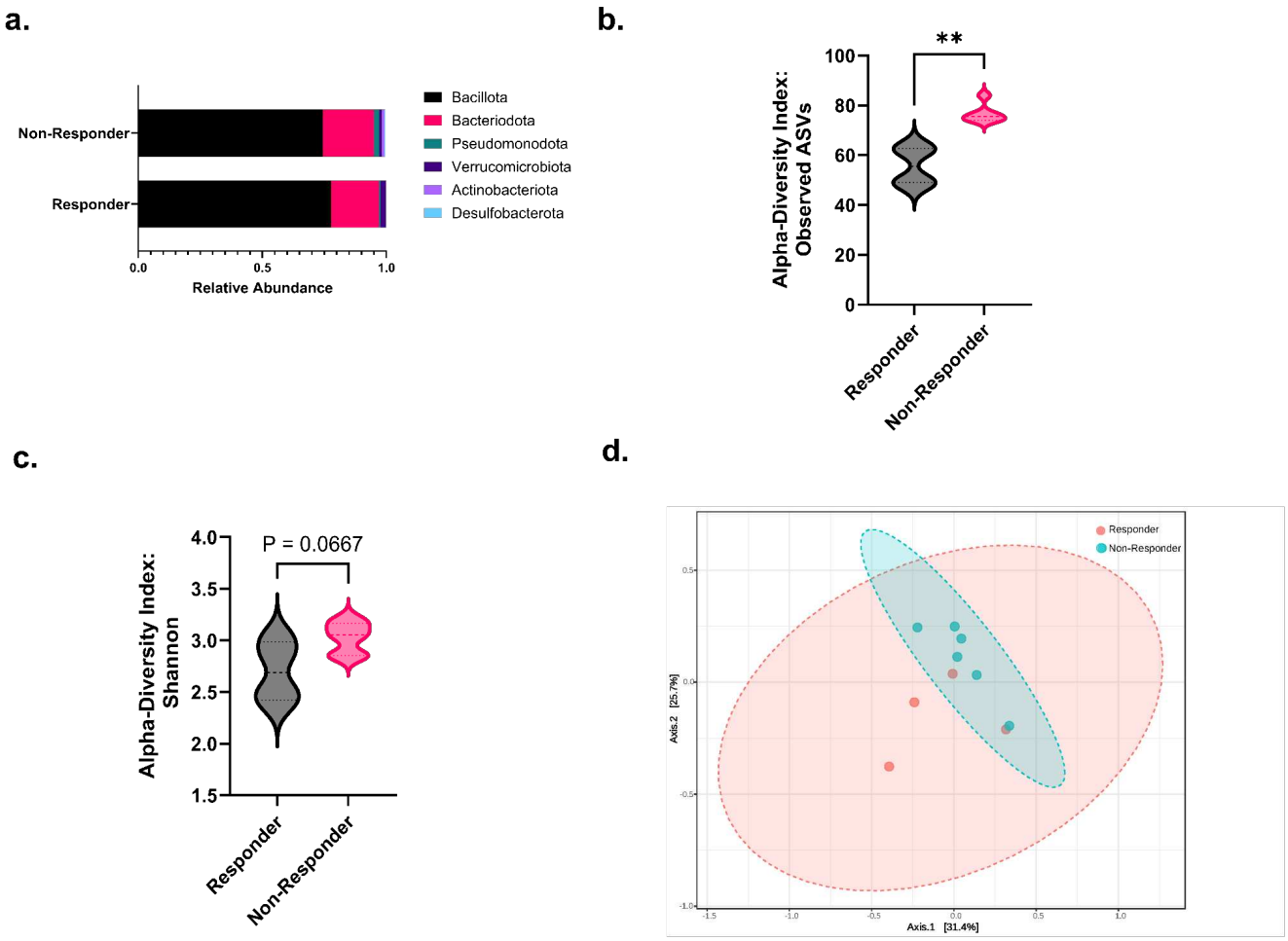

Fig 2.1. Bacterial alpha diversity differs between responders and non-responders. **a.** Relative abundance of primary bacterial phyla **b.** Observed ASV alpha diversity at the genus level **c.** Shannon's alpha diversity at the genus level **d**. Principle coordinate analysis (PCoA) of beta diversity at the genus taxonomic level. Microbiome graphs derived from 16s rRNA sequences. Taxa barplot was analyzed using two-way full effects ANOVA with Sidak's multiple comparisons test. Alpha diversity graphs were calculated using the non-parametric Mann-Whitney test after FDR correction, and the results were displayed through violin plots indicating the minimum and maximum values, as well as the 25th-75th percentile range. PCoA is represented using the Bray-Curtis dissimilarity index using PERMDISP multivariate analysis with the Benjamini-Hochberg false discovery rate. Ellipses show the 95% confidence interval for each cohort. *n*=4-6/group; **p<0.005.

To evaluate circulating blueberry polyphenol metabolites in the participants' plasma, we employed a targeted metabolomics panel using ultra-high-performance liquid chromatography triple-quadrupole time-of-flight mass spectrometry (UHPLC-Qq TOF MS). There were no significant changes in total polyphenol metabolites between groups. (Responder: $1.8x10^5 \pm 9.5x10^4$, Non-Responder: $2.0x10^5 \pm 3.8x10^4$ uM; p=0.5358, Fig. 2.2a), or in the absolute or relative abundance of circulating polyphenol metabolite classes (p=0.9999, Fig. 2.2b). Furthermore, there were no changes in CAMPER polyphenol metabolism (R2X=0.28, R2Y=0.15, Q2=-0.14 last orthogonal component; Fig. 2.2c) and CAZy glucosidase metabolism pathways (R2X=0.31, R2Y=0.20, Q2=-0.42 last orthogonal component; Fig. 2.2d) from gut microbial metagenomic sequencing.

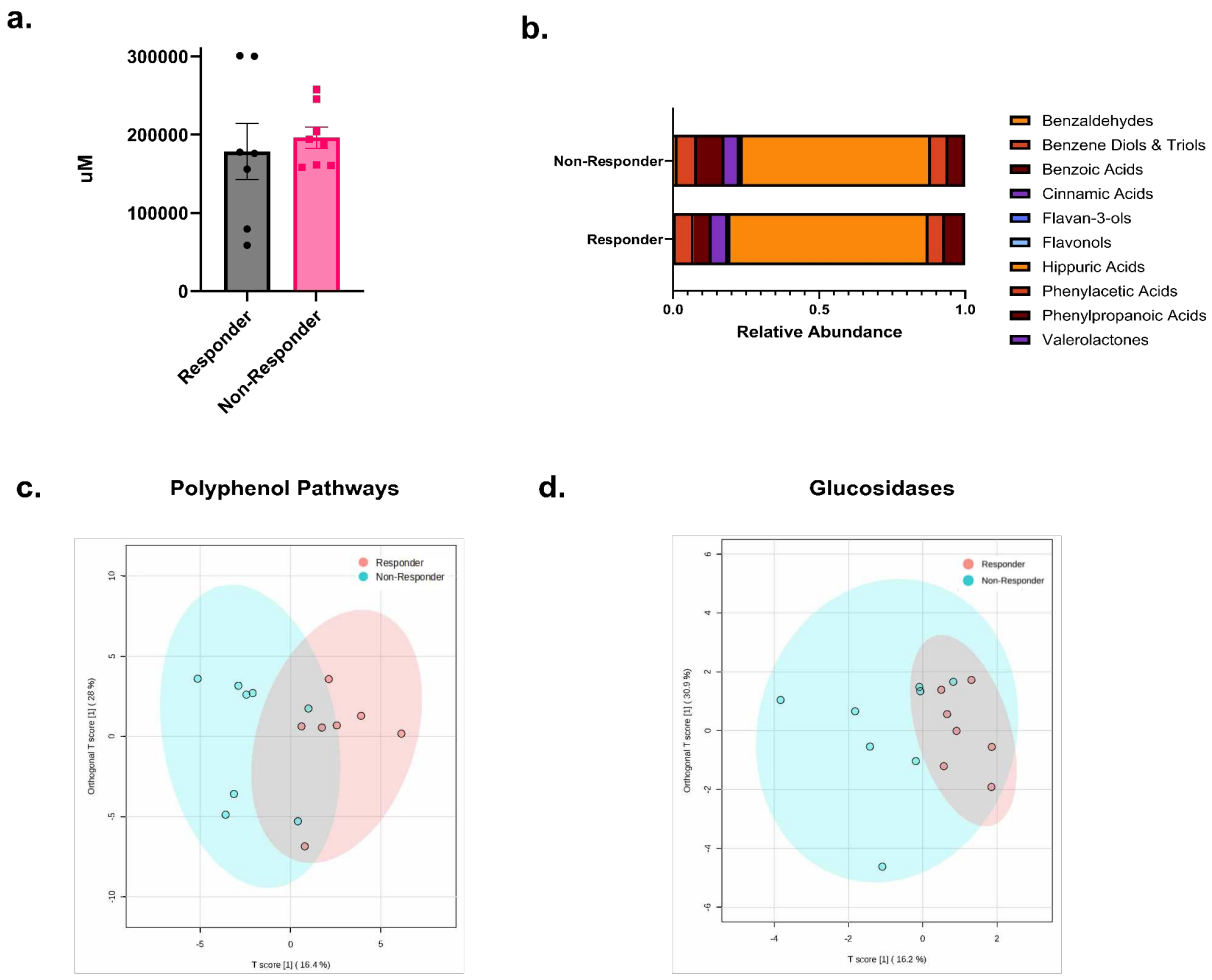

Fig 2.2. Plasma polyphenol metabolites do not differ between responders and non-responders **a.** Total detected plasma polyphenol metabolites **b.** Relative abundance of plasma polyphenols **c.** Orthogonal partial least squares (OPLS) of polyphenol degradation pathways **d.** OPLS model of glucosidase pathways. Metabolite abundance analyzed using a non-parametric unpaired two-tailed Student's t-test, with a Mann-Whitney post hoc test. Taxa barplot analyzed using two-way full effects ANOVA with Sidak's multiple comparisons test. OPLS score plot of each model in the plane of the first predictive (t-score 1) and the last orthogonal (orthogonal t-score 1) components for two and four permutated orthogonal components respectively. Ellipses show the 95% confidence interval for each cohort. *n*=7-8/group.

As global alterations in polyphenol degrading and glycoside processing profiles did not differ between groups, we next evaluated individual metabolites and their direct parent compounds. Metabolomic analysis of the direct parent class of plasma metabolites revealed that responders had a higher abundance of circulating flavonols (ie. class of flavonoids) than non-responders (Responder: 165.5±915.7, Non-Responder: 110.8±35.4 uM; $p<0.05$, Fig. 2.3 a & b). Importantly, we discovered two specific flavonols, quercetin, and a similar flavonol myricetin, to be trending higher in responders (Quercetin: log2FC=1.3, $p=0.09$, Myricetin: log2FC=1.1; $p<0.05$, Fig. 2.3c).

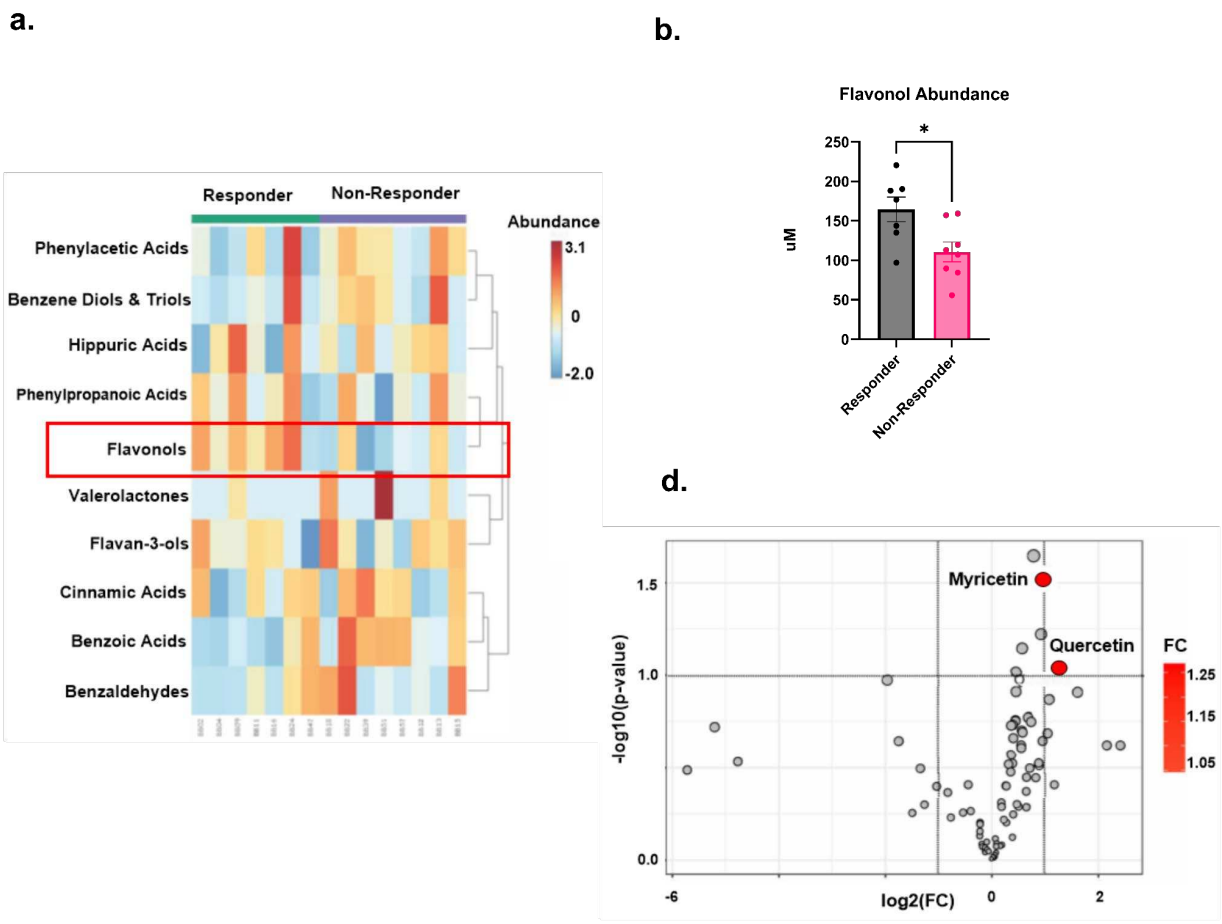

Fig 2.3. Myricetin and quercetin flavonols are higher in responders **a.** Heatmap of polyphenol direct parent compounds in plasma samples **b.** Absolute flavonol abundance **c.** Volcano plot of significant plasma metabolites in responders. Heatmap produced using Euclidean distance measure with Ward clustering algorithm on normalized data for the direct parent compounds of detected serum plasma metabolites with hierarchical clustering based on abundance. Flavonol abundance analyzed using a non-parametric unpaired two-tailed Student's t-test, with a Mann-Whitney post hoc test. Statistical analysis for the volcano plot was performed using a non-parametric unpaired two-tailed Student's t-test against FC=log2(Y). *n*=7-8/group.

Myricetin and quercetin share a similar structure, with myricetin possessing an additional hydroxyl group at the 5' position of the aromatic B-ring (Pink dot=upregulated FC, Fig. 2.4a). Highbush blueberries contain copious amounts of both of these flavonoids stored in their glycosidic forms (Quercetin Glycoside: 1.5-9.0, Myricetin Glycoside: 1.0-12.2 mg/100g fruit weight) and must be extracted to be in their most active form.[50] While the abundance of myricetin and quercetin were elevated in the responders, we also examined secondary

metabolites that may have contributed to observed cardiovascular outcomes. Phenylacetic acid (PAA), is an intermediary hub metabolite from the degradation of compounds containing phenyl groups, such as myricetin and quercetin or aromatic amino acids and can be anti or proinflammatory depending on its modifications (Supp. Figure 3a). We analyzed circulating PAA and its hepatically modified metabolites to determine if there was a divergence between responders and non-responders in gut microbiome processing of phenyl-containing compounds. We did not find significant deviations in PAA, 3-hydroxyphenylacetic acid (3-HPAA), 3',4'-dihydroxyphenylacetic acid-4'sulfate (DHPA), or homovanillic acid (HVA) between groups ($p=0.4129$, Fig. 2.4b). Additionally, PAA was below the limit of detection in the plasma of two of the responders and one of the non-responders (Fig. 2.4b). We also found that microbial tyrosine and phenylalanine metabolic pathways were downregulated in the responders (Phenylalanine: $p<0.0001$, Tyrosine: $p<0.05$, Fig. 2.4c), suggesting that the contribution of these pathways to the circulating PAA pool is limited.

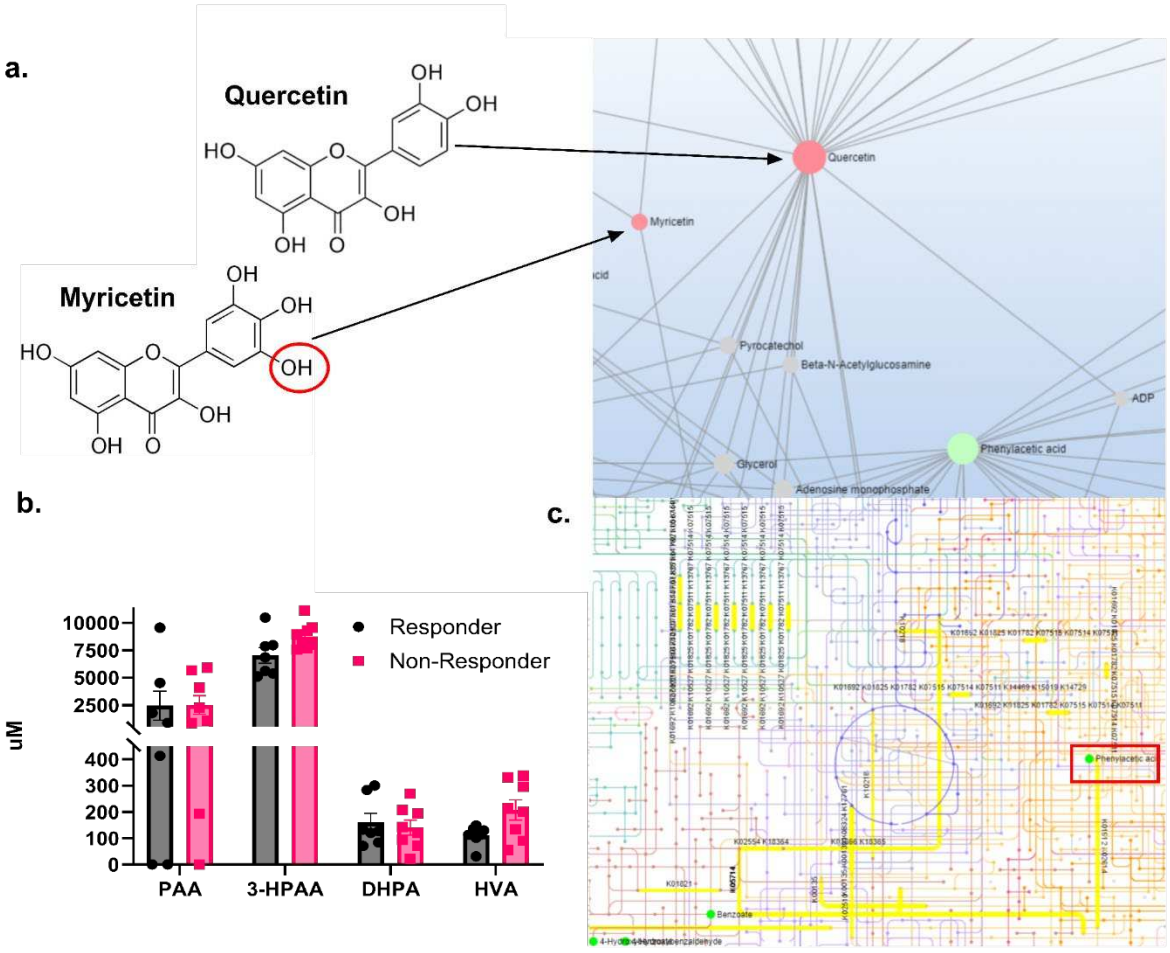

Fig 2.4. PAA is not a significant driver of myricetin and quercetin degradation **a.** Quercetin, myricetin, and phenylacetic acid interaction network (pink dots exhibit higher FC, whereas green dot is a lower FC in responders) **b.** Circulating phenylacetic acid metabolites **c.** Phenylacetic acid metabolic map. Metabolic maps FC=log(Y), >2.0 for fold change significance for comparing metabolites against metabolic pathways using STITCH tool for highly confident interactions with KEGG annotations. PAA metabolites assessed using a two-way full effects ANOVA with Sidak's multiple comparisons test. *n*=7-8/group.

The rise in myricetin and quercetin levels, coupled with the minimal contribution of PAA in the bloodstream of responders, led us to investigate whether there were differences in microbial polyphenol degradation pathways between the groups. In a presence/absence analysis, we found two relevant KEGG ortholog (KOs) identifiers. Quercetin-2,3-dioxygenase (QueD/PIR, [E.C. 1.13.11.24], K06911) and gallate decarboxylase (LpdC, [E.C. 4.1.1.59], K22958), were more present in responders (log2FC=>1.0; p<0.05, Fig. 2.5a). Additionally, 1,2-epoxy phenylacetyl-CoA isomerase (PaaG, [E.C. 5.3.3.18], KO15866), as part of the gene

complex that initiates PAA biotransformation into SCFAs[51] in the gut was present, but not significantly higher in responders (log2FC=1.1; p=0.2893, Fig. 2.5a).

We then identified two bacteria in our metagenomic data that contained one to three of these polyphenol degradation genes in the responders. Out of fifty-eight bacteria detected with the QueD gene, *Phascolactobacterium faecium (P. faecium)* and *Alistipes shahii (A. shahii)* both contained trending higher abundance of this quercetin and myricetin degrading enzyme[52] in the responders (*P. faecium*: log2FC=1.3, p=0.0530, *A. stipes*: log2FC=1.5; p=0.0652, Fig. 2.5b), but was not present in non-responders. Additionally, the *P. faecium* species also contained LpdC and PaaG genes, though not statistically significant (LpdC: log2FC=1.4, p=0.1028, PaaG: log2FC=0.4, p=0.2590). Interestingly, both *A. shahii* and *P. faecium* commensals presence were not significantly different between responders and non-responders (*A. Shahii*, p=0.3153, *P. faecium*, p=0.3026, Fig. 2.5 c & d).

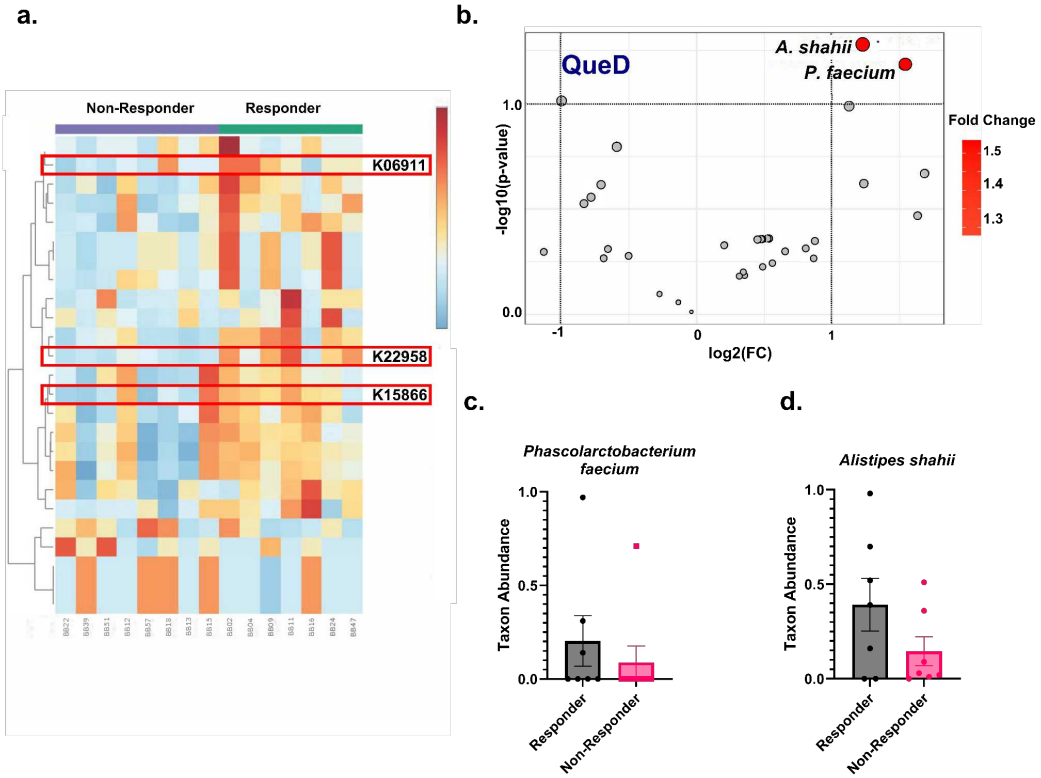

Fig 2.5. *P. faecium* and *A. stipes* metabolize quercetin and myricetin. **a.** Heatmap of microbial genes that process quercetin and myricetin **b.** Volcano plot of bacteria containing the QueD/PIR gene in the responders **c.** *P. faecium* **d.** *A. shahii*. Statistical analysis for genes in heatmap and bacteria in volcano plot was performed using a non-parametric unpaired two-tailed Student's t-test against FC=log2(Y). MetaPhlAn taxonomic profiles of computed absolute taxon abundances and compared using a non-parametric unpaired two-tailed Student's t-test, with a Mann-Whitney post hoc test. *n*=7-8/group.

V. DISCUSSION

This study demonstrates that post-menopausal females who responded to blueberry treatment had higher plasma concentrations of quercetin and myricetin. This observation was accompanied by decreased microbial alpha diversity and significantly higher *Agathobacter, Monoglobus,* and *Dialister* polyphenol-degrading bacteria in the responders. However, these changes in the gut microbiome were independent of detected microbial polyphenol degradation pathways, or glucosidase profiles. An in-depth analysis revealed that the presence of QueD, LpdC, and PaaG polyphenol-degrading genes in *P. faecium* or *A. stipes* in the responders may be a subtle factor in flavonol digestion. Additionally, the responders had a higher generalized concentration of flavonols, without significant changes in circulating anti or proinflammatory PAA metabolites. This result establishes that quercetin and myricetin were not completely metabolized into other derivatives, and instead remained intact, enabling them to enter circulation and contact the vascular endothelium.

The results of our study revealed that post-menopausal females who exhibited improved FMD after a blueberry intervention had elevated circulating secondary polyphenol metabolites myricetin and quercetin. Both of these metabolites are highly prevalent in blueberries and are deemed to be cardioprotective via their indirect action as antioxidants.[53–56] For example, supplementation of quercetin and myricetin containing grape powder in pre and post-menopausal females reduced markers for endothelial inflammation, with favorable alterations in lipoprotein profiles.[57] Others have also found that quercetin can decrease malondialdehyde as a proxy for LDL oxidation, specifically in post-menopausal females.[58] Albeit these are generalized cardiovascular mechanisms, quercetin and myricetin also have direct effects on the

vascular endothelium. Studies conducted on rodent models have demonstrated that myricetin and quercetin induce arterial endothelial-mediated relaxation.[59,60] Furthermore, these polyphenol metabolites stimulate the expression of eNOS, which leads to the release of nitric oxide, as observed in endothelial cell culture models.[55,61] Clinical research exploring the impact of quercetin and myricetin on endothelial function in post-menopausal females is limited. However, a study conducted by Dower et al. shed light on the potential benefits of quercetin supplementation on endothelial function in (pre)hypertensive males and females aged forty to eighty years old. In this randomized, placebo-controlled, crossover study, participants ingested quercetin capsules for four weeks. The results showed a significant decrease in soluble endothelial selectin, and pro-inflammatory interleukin-1β levels,[62] however endothelial receptor interaction was not explored. Of the endothelial receptors quercetin and myricetin bind to, ERα and ERβ are of primary interest. After menopause, ER expression on the endothelium significantly decreases which contributes to endothelial dysfunction.[8] Quercetin and myricetin bind to ERα and ERβ,[63] located in multiple tissues including the vascular endothelium, and coupling to ERs stimulates eNOS to produce nitric oxide to relax the smooth muscle in the dilation of blood vessels.[64] As estrogen is the primary metabolite that binds to ERs, it can be inferred that both myricetin and quercetin act as phytoestrogens and are capable of stimulating ERs in an estrogen-depleted, post-menopausal state. Moreover, this idea supports our earlier observation of blueberry treatment stimulating eNOS as the expression of phosphorylated eNOS in the responders was increased ($p=0.019$),[24] which has been correlated with endothelial ERα abundance.[8]

The amount of quercetin and myricetin ingested was consistent between the groups, yet these secondary polyphenol metabolites were more present in the bloodstream of the responders. This suggests differential polyphenol processing and liberation that we hypothesized to be mediated by the gut microbiome. Although these conjugated polyphenols in blueberries can be absorbed intact,[65] parent polyphenolic compounds have extremely low

bioavailability, and thus low bioactivity[66]. Most quercetin and myricetin in plants are bound to glycone residues (ie. saccharide moiety) as quercetin-3-*O*-galactoside and myricetin-3-*O*-arabinoside.[67] Cleavage of the glycosidic bond in the gut liberates quercetin and myricetin from its side group, which increases bioavailability.[66] Absorption and time to reach maximal systemic concentration is generally between one and nine hours based on food source and composition of the gut microbiome.[68] Interestingly, there seems to be a difference in polyphenolic modification based on gender and age. Researchers have observed that premenopausal females hydrolyze the flavonoid rutin (quercetin 3-rutinoside) into quercetin more efficiently than males, resulting in higher circulating quercetin.[69] Furthermore, there are indications that microbiota composition may be more similar between postmenopausal females and males than premenopausal and postmenopausal females,[70] where microbial-mediating polyphenol processing may differ after menopause. Certain genera of bacteria possess *β*-glucosidase enzymes that are capable of *O*-deglycosylation, such as the *Agathobacter* and *Monoglobus,*[49] which we found to be more abundant in responders. Specifically, others have found that *Monoglobus* produces rhamnosidase in liberation of quercetin[49] and *Agathobacter* species can cleave carbon glucosides that human glucosidases do not have access to[71]. However, not all members of these genera produce glucosidases, and a limitation of our experiment was insufficient sequencing depth to fully assemble the metagenome and accurately infer differences in enzymatic pathways associated with specific taxa. In addition to microbes with *β*-glucosidase activity, we identified bacteria with links to polyphenol processing after the removal of the glycone residue. *Dialister* genera, which was more present in the responders, has been documented to contain the phloretin hydrolase (PHY) gene involved in flavonoid reduction to SCFAs.[49] Furthermore, we found two bacteria with direct myricetin and quercetin processing genes. *Phascolarctobacterium* and *Alistipes* are commensal bacteria in the human gastrointestinal tract that feed on dietary fiber[72] through *β*-glucosidase action.[73,74] Van den Abbeele et al. demonstrated further processing capabilities of *P. faecium* by showing this bacteria metabolizes

carrot pectin down to SCFAs.[75] Their observation indicates that *P. faecium* possesses additional genetic traits to facilitate the degradation of plant matter in a prebiotic fashion beyond glucosidase activity. After cross-referencing our metagenomic data with the KEGG database, we discovered the presence of QueD, LpdC, and PaaG polyphenol degradation enzymes. *P. faecium*, contained all three genes. Additionally, *A. shahii* also possessed the quercetin dioxygenase enzyme, QueD, which is capable of breaking down flavonol compounds like kaempferol, in addition to quercetin[76] into other metabolites such as SCFAs. This indicates that QueD may also metabolize myricetin due to its structural similarity to quercetin. Although others have studied QueD activity in the metabolism of *Bacillus subtilis* and *Aspergillus spp.*,[76] to our knowledge this is the first study to demonstrate that the established presence of *P. faecium* correlates with blueberry polyphenol metabolism. However, even though these post-glucosidase enzymatic genes were higher in the responders, intact myricetin and quercetin were also significant in this group. This discrepancy is unclear but may be due to subtle differences in the gut microbiome. Neither *P. faecium* nor *A. stipes* differed in abundance between responders and non-responders, but the detection of QueD did, suggesting that functional rather than taxonomic differences are more important in understanding microbial metabolism.

Outside of the gut microbiome's capacity to metabolize polyphenols, numerous transformations can occur to change the fate of a single metabolite. It is unclear how microbial genes contribute to the removal of quercetin and myricetin from circulation through SCFA processing. However, our observations did not reveal any differences in plasma PAA or its derivatives, and a targeted fecal metabolomic profile may have been a complementary analysis. PAA is generated from aromatic compounds, such as myricetin and quercetin, or amino acids like phenylalanine and tyrosine, by the gut microbiome.[77] If PAA is not dissimilated in the gut, it can enter the bloodstream for further modification. Previous studies have indicated the PAA metabolites DHPA and 3-HPAA, can significantly impact the cardiovascular system by improving endothelial function[78] and lowering blood pressure[79] respectively in rodent models.

However, PAA itself and other hepatically modified derivatives such as phenylacetylglutamine (PAGln) and paracresol sulfate (PCS) are considered uremic toxins and can trigger vascular inflammation[80–82] in the development of CVD.[83,84] As there were no significant variations in serum PAA metabolites between responders and non-responders, and phenylalanine and tyrosine pathways were downregulated in our results, quercetin and myricetin were not appreciably contributing to the PAA pool, allowing them to subsist in the bloodstream.

This study is noteworthy for its multi-pronged approach. We leveraged a combination of 16s rRNA and metagenomic sequencing, a well-curated polyphenol database, and a targeted polyphenol metabolomics panel to conduct a comprehensive multi-omic analysis. By investigating microbial polyphenol degradation pathways in relation to the secondary polyphenol metabolites, we were able to correlate microbial processing of polyphenols with interindividual differences in participants on the same treatment. This full-circle analysis allowed us to uncover important insights that may have been missed with a more limited approach. However, considering that we utilized a polyphenol metabolite panel, we were not able to capture other metabolites that may have been useful in deciphering the intricacies of blueberry polyphenol metabolism. Quantification of SCFAs and the endothelial inflammatory PAA-derivatives, PAGln and PCS measurements would have been helpful in determining if there was yet another distinction between responders and non-responders. Also, while we did not control for diet in our study, it is important to note that the participants were instructed to maintain their regular dietary habits throughout the study period. Therefore, any contribution of myricetin, quercetin, or other PAA sources in the diet would have been consistent throughout the study.

VI. CONCLUSIONS

Post-menopausal females who experienced an improvement in flow-mediated dilation after a blueberry intervention showed elevated levels of circulating myricetin and quercetin. Indeed, the results indicate that blueberry intervention may be beneficial in mitigating

cardiovascular disease risk in post-menopausal females by supporting the presence of beneficial polyphenol metabolizing bacterial genera, and the genes they carry for the metabolism of these compounds. Although the exact mechanisms underlying the observed effects of blueberry intervention on endothelial function remain unclear, the findings of this study contribute to the growing body of evidence supporting the cardioprotective effects of blueberries. It is essential that future studies undertake a comprehensive exploration of the association between *P. faecium* and *A. shahii* and their prospective metabotypes in the context of blueberry flavonoid processing. Such investigations could pave the way for a better understanding of the mechanisms underlying the biological effects of these flavonoids in post-menopausal females, and offer new insights into therapeutic strategies for CVD.

REFERENCES

1. Taddei S, Virdis A, Ghiadoni L, et al. Menopause Is Associated With Endothelial Dysfunction in Women. *Hypertension*. Published online October 1996. doi:10.1161/01.HYP.28.4.576

2. Yang XP, Reckelhoff JF. Estrogen, hormonal replacement therapy and cardiovascular disease. *Curr Opin Nephrol Hypertens*. 2011;20(2):133-138.

3. Rangel-Huerta OD, Pastor-Villaescusa B, Aguilera CM, Gil A. A Systematic Review of the Efficacy of Bioactive Compounds in Cardiovascular Disease: Phenolic Compounds. *Nutrients*. 2015;7(7):5177-5216.

4. Kocabas S, Sanlier N. The power of berries against cardiovascular diseases. *Nutr Rev*. Published online September 11, 2023. doi:10.1093/nutrit/nuad111

5. Wang MC, Lloyd-Jones DM. Cardiovascular Risk Assessment in Hypertensive Patients. *Am J Hypertens*. 2021;34(6):569-577.

6. Rossi R, Nuzzo A, Origliani G, Modena MG. Prognostic role of flow-mediated dilation and cardiac risk factors in post-menopausal women. *J Am Coll Cardiol*. 2008;51(10):997-1002.

7. Mendelsohn ME. Genomic and nongenomic effects of estrogen in the vasculature. *Am J Cardiol*. 2002;90(1A):3F - 6F.

8. Gavin KM, Seals DR, Silver AE, Moreau KL. Vascular endothelial estrogen receptor alpha is modulated by estrogen status and related to endothelial function and endothelial nitric oxide synthase in healthy women. *J Clin Endocrinol Metab*. 2009;94(9):3513-3520.

9. Pinna C, Cignarella A, Sanvito P, Pelosi V, Bolego C. Prolonged Ovarian Hormone Deprivation Impairs the Protective Vascular Actions of Estrogen Receptor αAgonists. *Hypertension*. Published online April 1, 2008. doi:10.1161/HYPERTENSIONAHA.107.106807

10. Guo X, Razandi M, Pedram A, Kassab G, Levin ER. Estrogen Induces Vascular Wall Dilation: MEDIATION THROUGH KINASE SIGNALING TO NITRIC OXIDE AND ESTROGEN RECEPTORS α AND β *. *J Biol Chem*. 2005;280(20):19704-19710.

11. Khalil RA. Estrogen, vascular estrogen receptor and hormone therapy in postmenopausal vascular disease. *Biochem Pharmacol*. 2013;86(12):1627-1642.

12.Speer H, D'Cunha NM, Botek M, et al. The Effects of Dietary Polyphenols on Circulating Cardiovascular Disease Biomarkers and Iron Status: A Systematic Review. *Nutr Metab Insights*. 2019;12:1178638819882739.

13.Dong Y, Wu X, Han L, et al. The Potential Roles of Dietary Anthocyanins in Inhibiting Vascular Endothelial Cell Senescence and Preventing Cardiovascular Diseases. *Nutrients*. 2022;14(14). doi:10.3390/nu14142836

14.Micek A, Raźny U, Paweł K. Association between health risk factors and dietary flavonoid intake in cohort studies. *Int J Food Sci Nutr*. 2021;72(8):1019-1034.

15.Michalska A, Łysiak G. Bioactive Compounds of Blueberries: Post-Harvest Factors Influencing the Nutritional Value of Products. *Int J Mol Sci*. 2015;16(8):18642-18663.

16.Moyer RA, Hummer KE, Finn CE, Frei B, Wrolstad RE. Anthocyanins, phenolics, and antioxidant capacity in diverse small fruits: vaccinium, rubus, and ribes. *J Agric Food Chem*. 2002;50(3):519-525.

17.Stull AJ, Cash KC, Champagne CM, et al. Blueberries improve endothelial function, but not blood pressure, in adults with metabolic syndrome: a randomized, double-blind, placebo-controlled clinical trial. *Nutrients*. 2015;7(6):4107-4123.

18. Basu A, Du M, Leyva MJ, et al. Blueberries decrease cardiovascular risk factors in obese men and women with metabolic syndrome. *J Nutr*. 2010;140(9):1582-1587.

19.Rodriguez-Mateos A, Rendeiro C, Bergillos-Meca T, et al. Intake and time dependence of blueberry flavonoid-induced improvements in vascular function: a randomized, controlled, double-blind, crossover intervention study with mechanistic insights into biological activity. *Am J Clin Nutr*. 2013;98(5):1179-1191.

20. Johnson SA, Figueroa A, Navaei N, et al. Daily blueberry consumption improves blood pressure and arterial stiffness in postmenopausal women with pre- and stage 1-hypertension: a randomized, double-blind, placebo-controlled clinical trial. *J Acad Nutr Diet*. 2015;115(3):369-377.

21.Woolf EK, Terwoord JD, Litwin NS, et al. Daily blueberry consumption for 12 weeks improves endothelial function in postmenopausal women with above-normal blood pressure through reductions in oxidative stress: a randomized controlled trial. *Food Funct*. 2023;14(6):2621-2641.

22. Riso P, Klimis-Zacas D, Del Bo' C, et al. Effect of a wild blueberry (Vaccinium angustifolium) drink intervention on markers of oxidative stress, inflammation and endothelial function in humans with cardiovascular risk factors. *Eur J Nutr*. 2013;52(3):949-961.

23. Wood E, Hein S, Mesnage R, et al. Wild blueberry (poly)phenols can improve vascular function and cognitive performance in healthy older individuals: a double-blind randomized controlled trial. *Am J Clin Nutr*. 2023;117(6):1306-1319.

24. Woolf, E. K. (2023). Cardiovascular-protective effects of blueberry consumption in postmenopausal women with above-normal blood pressure (Order No. 30523709). Available from Dissertations & Theses @ Colorado State University; ProQuest Dissertations & Theses Global. (2852408832). Retrieved from https://ezproxy2.library.colostate.edu/login?url=https://www.proquest.com/dissertations-theses/cardiovascular-protective-effects-blueberry/docview/2852408832/se-2

25. Berg G, Rybakova D, Fischer D, et al. Microbiome definition re-visited: old concepts and new challenges. *Microbiome*. 2020;8(1):103.

26. Saura-Calixto F, Pérez-Jiménez J, Touriño S, et al. Proanthocyanidin metabolites associated with dietary fibre from in vitro colonic fermentation and proanthocyanidin metabolites in human plasma. *Mol Nutr Food Res*. 2010;54(7):939-946.

27. Clifford MN. Diet-derived phenols in plasma and tissues and their implications for health. *Planta Med*. 2004;70(12):1103-1114.

28. Wan MLY, Co VA, El-Nezami H. Dietary polyphenol impact on gut health and microbiota. *Crit Rev Food Sci Nutr*. 2021;61(4):690-711.

29. Blanco-Míguez A, Beghini F, Cumbo F, et al. Extending and improving metagenomic taxonomic profiling with uncharacterized species using MetaPhlAn 4. *Nat Biotechnol*. 2023;41(11):1633-1644.

30. Shaffer M, Borton MA, McGivern BB, et al. DRAM for distilling microbial metabolism to automate the curation of microbiome function. *Nucleic Acids Res*. 2020;48(16):8883-8900.

31. McGivern BB, Tfaily MM, Borton MA, et al. Decrypting bacterial polyphenol metabolism in an anoxic wetland soil. *Nat Commun*. 2021;12(1):2466.

32. GitHub - hyattpd/Prodigal: Prodigal Gene Prediction Software. GitHub. Accessed March 1, 2024. https://github.com/hyattpd/Prodigal

33. GitHub - weizhongli/cdhit: Automatically exported from code.google.com/p/cdhit. GitHub. Accessed March 1, 2024. https://github.com/weizhongli/cdhit

34. GitHub - wwood/CoverM: Read coverage calculator for metagenomics. GitHub. Accessed March 1, 2024. https://github.com/wwood/CoverM

35. GitHub - biobakery/Maaslin2: MaAsLin2: Microbiome Multivariate Association with Linear Models. GitHub. Accessed March 1, 2024. https://github.com/biobakery/Maaslin2

36.GenomeNet. Accessed April 2, 2024. https://www.genome.jp/

37. Feliciano RP, Mecha E, Bronze MR, Rodriguez-Mateos A. Development and validation of a high-throughput micro solid-phase extraction method coupled with ultra-high-performance liquid chromatography-quadrupole time-of-flight mass spectrometry for rapid identification and quantification of phenolic metabolites in human plasma and urine. *J Chromatogr A*. 2016;1464:21-31.

38. Hamady M, Knight R. Microbial community profiling for human microbiome projects: Tools, techniques, and challenges. *Genome Res*. 2009;19(7):1141-1152.

39. Hamady M, Walker JJ, Harris JK, Gold NJ, Knight R. Error-correcting barcoded primers for pyrosequencing hundreds of samples in multiplex. *Nat Methods*. 2008;5(3):235-237.

40. Bolyen E, Rideout JR, Dillon MR, et al. Reproducible, interactive, scalable and extensible microbiome data science using QIIME 2. *Nat Biotechnol*. 2019;37(8):852-857.

41.Callahan BJ, McMurdie PJ, Rosen MJ, Han AW, Johnson AJA, Holmes SP. DADA2: High-resolution sample inference from Illumina amplicon data. *Nat Methods*. 2016;13(7):581-583.

42. Robeson MS, O'Rourke DR, Kaehler BD, et al. RESCRIPt: Reproducible sequence taxonomy reference database management for the masses. *bioRxiv*. Published online October 5, 2020:2020.10.05.326504. doi:10.1101/2020.10.05.326504

43. Bokulich NA, Kaehler BD, Rideout JR, et al. Optimizing taxonomic classification of marker-gene amplicon sequences with QIIME 2's q2-feature-classifier plugin. *Microbiome*. 2018;6(1):1-17.

44. Chong J, Liu P, Zhou G, Xia J. Using MicrobiomeAnalyst for comprehensive statistical, functional, and meta-analysis of microbiome data. *Nature Protocols*. 2020;15(3):799-821. doi:10.1038/s41596-019-0264-1

45. Nearing JT, Douglas GM, Hayes MG, et al. Microbiome differential abundance methods produce different results across 38 datasets. *Nat Commun*. 2022;13(1):1-16.

46. Robinson MD, McCarthy DJ, Smyth GK. edgeR: a Bioconductor package for differential expression analysis of digital gene expression data. *Bioinformatics*. 2010;26(1):139-140.

47. GitHub - xia-lab/MetaboAnalystR: R package for MetaboAnalyst. GitHub. Accessed March 12, 2024. https://github.com/xia-lab/MetaboAnalystR

48. Xia J, Psychogios N, Young N, Wishart DS. MetaboAnalyst: a web server for metabolomic data analysis and interpretation. *Nucleic Acids Res*. 2009;37(Web Server issue):W652-W660.

49. Goris T, Cuadrat RRC, Braune A. Flavonoid-Modifying Capabilities of the Human Gut Microbiome—An In Silico Study. *Nutrients*. 2021;13(8):2688.

50. Showing all polyphenols found in Highbush blueberry, raw - Phenol-Explorer. Accessed March 18, 2024. http://phenol-explorer.eu/contents/food/95

51.Ismail W, El-Said Mohamed M, Wanner BL, et al. Functional genomics by NMR spectroscopy. Phenylacetate catabolism in Escherichia coli. *Eur J Biochem*. 2003;270(14):3047-3054.

52. Steiner RA, Meyer-Klaucke W, Dijkstra BW. Functional analysis of the copper-dependent quercetin 2,3-dioxygenase. 2. X-ray absorption studies of native enzyme and anaerobic complexes with the substrates quercetin and myricetin. *Biochemistry*. 2002;41(25):7963-7968.

53. Dagher O, Mury P, Thorin-Trescases N, Noly PE, Thorin E, Carrier M. Therapeutic Potential of Quercetin to Alleviate Endothelial Dysfunction in Age-Related Cardiovascular Diseases. *Front Cardiovasc Med*. 2021;8:658400.

54. Guo J, Meng Y, Zhao Y, Hu Y, Ren D, Yang X. Myricetin derived from Hovenia dulcis Thunb. ameliorates vascular endothelial dysfunction and liver injury in high choline-fed mice. *Food Funct*. 2015;6(5):1620-1634.

55. Berköz M, Yıldırım M, Yalın S, İlhan M, Yunusoğlu O. Myricetin inhibits angiotensin converting enzyme and induces nitric oxide production in HUVEC cell line. *Gen Physiol Biophys*. 2020;39(3):249-258.

56. Bertin R, Chen Z, Marin R, et al. Activity of myricetin and other plant-derived polyhydroxyl compounds in human LDL and human vascular endothelial cells against oxidative stress. *Biomed Pharmacother*. 2016;82:472-478.

57. Zern TL, Wood RJ, Greene C, et al. Grape polyphenols exert a cardioprotective effect in pre- and postmenopausal women by lowering plasma lipids and reducing oxidative stress. *J Nutr*. 2005;135(8):1911-1917.

58. Arteaga E, Villaseca P, Rojas A, Marshall G, Bianchi M. Phytoestrogens possess a weak antioxidant activity on low density lipoprotein in contrast to the flavonoid quercetin in vitro in postmenopausal women. *Climacteric*. 2004;7(4):397-403.

59. Khoo NKH, White CR, Pozzo-Miller L, et al. Dietary flavonoid quercetin stimulates vasorelaxation in aortic vessels. *Free Radic Biol Med*. 2010;49(3):339-347.

60. Angelone T, Pasqua T, Di Majo D, et al. Distinct signalling mechanisms are involved in the dissimilar myocardial and coronary effects elicited by quercetin and myricetin, two red wine flavonols. *Nutr Metab Cardiovasc Dis*. 2011;21(5):362-371.

61. Li PG, Sun L, Han X, Ling S, Gan WT, Xu JW. Quercetin induces rapid eNOS phosphorylation and vasodilation by an Akt-independent and PKA-dependent mechanism. *Pharmacology*. 2012;89(3-4):220-228.

62. Dower JI, Geleijnse JM, Gijsbers L, Schalkwijk C, Kromhout D, Hollman PC. Supplementation of the Pure Flavonoids Epicatechin and Quercetin Affects Some Biomarkers of Endothelial Dysfunction and Inflammation in (Pre)Hypertensive Adults: A Randomized Double-Blind, Placebo-Controlled, Crossover Trial. *J Nutr*. 2015;145(7):1459-1463.

63. Estrogenic biological activity and underlying molecular mechanisms of green tea constituents. *Trends Food Sci Technol*. 2020;95:247-260.

64. Arias-Loza PA, Jazbutyte V, Pelzer T. Genetic and pharmacologic strategies to determine the function of estrogen receptor alpha and estrogen receptor beta in cardiovascular system. *Gend Med*. 2008;5 Suppl A:S34-S45.

65. Du QH, Peng C, Zhang H. Polydatin: a review of pharmacology and pharmacokinetics. *Pharm Biol*. 2013;51(11):1347-1354.

66. Pandey KB, Rizvi SI. Plant polyphenols as dietary antioxidants in human health and disease. *Oxid Med Cell Longev*. 2009;2(5):270-278.

67. Showing all polyphenols found in Highbush blueberry, raw - Phenol-Explorer. Accessed March 26, 2024. http://phenol-explorer.eu/contents/food/95

68. Dabeek WM, Marra MV. Dietary Quercetin and Kaempferol: Bioavailability and Potential Cardiovascular-Related Bioactivity in Humans. *Nutrients*. 2019;11(10). doi:10.3390/nu11102288

69. Erlund I, Kosonen T, Alfthan G, et al. Pharmacokinetics of quercetin from quercetin aglycone and rutin in healthy volunteers. *Eur J Clin Pharmacol*. 2000;56(8):545-553.

70. Santos-Marcos JA, Rangel-Zuñiga OA, Jimenez-Lucena R, et al. Influence of gender and menopausal status on gut microbiota. *Maturitas*. 2018;116:43-53.

71. Braune A, Blaut M. Bacterial species involved in the conversion of dietary flavonoids in the human gut. *Gut Microbes*. 2016;7(3):216-234.

72. Li F, Hullar MAJ, Schwarz Y, Lampe JW. Human gut bacterial communities are altered by addition of cruciferous vegetables to a controlled fruit- and vegetable-free diet. *J Nutr*. 2009;139(9):1685-1691.

73. Song Y, Könönen E, Rautio M, et al. Alistipes onderdonkii sp. nov. and Alistipes shahii sp. nov., of human origin. *Int J Syst Evol Microbiol*. 2006;56(Pt 8):1985-1990.

74. Parkar SG, Frost JKT, Rosendale D, et al. The sugar composition of the fibre in selected plant foods modulates weaning infants' gut microbiome composition and fermentation metabolites in vitro. *Sci Rep*. 2021;11(1):9292.

75. Van den Abbeele P, Duysburgh C, Cleenwerck I, Albers R, Marzorati M, Mercenier A. Consistent Prebiotic Effects of Carrot RG-I on the Gut Microbiota of Four Human Adult Donors in the SHIME Model despite Baseline Individual Variability. *Microorganisms*. 2021;9(10). doi:10.3390/microorganisms9102142

76. Tranchimand S, Ertel G, Gaydou V, Gaudin C, Tron T, Iacazio G. Biochemical and molecular characterization of a quercetinase from Penicillium olsonii. *Biochimie*. 2008;90(5):781-789.

77. Jiao M, He W, Ouyang Z, Shi Q, Wen Y. Progress in structural and functional study of the bacterial phenylacetic acid catabolic pathway, its role in pathogenicity and antibiotic resistance. *Front Microbiol*. 2022;13:964019.

78. Pourová J, Najmanová I, Vopršalová M, et al. Two flavonoid metabolites, 3,4-dihydroxyphenylacetic acid and 4-methylcatechol, relax arteries ex vivo and decrease blood pressure in vivo. *Vascul Pharmacol*. 2018;111:36-43.

79. Dias P, Pourová J, Vopršalová M, Nejmanová I, Mladěnka P. 3-Hydroxyphenylacetic Acid: A Blood Pressure-Reducing Flavonoid Metabolite. *Nutrients*. 2022;14(2). doi:10.3390/nu14020328

80. Morita M, Yano S, Yamaguchi T, Yamauchi M, Sugimoto T. Phenylacetic acid stimulates reactive oxygen species generation and tumor necrosis factor-α secretion in vascular endothelial cells. *Ther Apher Dial*. 2011;15(2):147-150.

81. Fu H, Kong B, Zhu J, Huang H, Shuai W. Phenylacetylglutamine increases the susceptibility of ventricular arrhythmias in heart failure mice by exacerbated activation of the TLR4/AKT/mTOR signaling pathway. *Int Immunopharmacol*. 2023;116:109795.

82. Meijers BKI, Van Kerckhoven S, Verbeke K, et al. The uremic retention solute p-cresyl sulfate and markers of endothelial damage. *Am J Kidney Dis*. 2009;54(5):891-901.

83. Nemet I, Li XS, Haghikia A, et al. Atlas of gut microbe-derived products from aromatic amino acids and risk of cardiovascular morbidity and mortality. *Eur Heart J*. 2023;44(32):3085-3096.

84. Nemet I, Saha PP, Gupta N, et al. A Cardiovascular Disease-Linked Gut Microbial Metabolite Acts via Adrenergic Receptors. *Cell*. 2020;180(5):862-877.e22.

CHAPTER 4: *BACILLUS SUBTILIS* DECA9 PARTIALLY REVERSES ENDOTHELIAL DYSFUNCTION IN HIGH FAT-DIET FED MICE[1]

I. SUMMARY

Imbalances in the gut microbiome have emerged as an important factor in endothelial dysfunction, a significant risk factor for cardiovascular disease. Thus, interventions targeting the microbiome may prove helpful in preventing or reversing this impairment. We previously reported that a spore-forming *Bacillus subtilis* probiotic improved endothelial function in a cohort of healthy, non-obese humans after a four-week intervention. Building on these promising results, the present study sought to investigate whether administering *Bacillus subtilis* could reverse endothelial dysfunction in mice with diet-induced obesity. Male C57BL/6J mice were fed a Western diet (WD; n=24) or standard diet (SD; n=24) for ten weeks to induce endothelial dysfunction, after which half of the animals in each group (n=12) were allocated to receive a *Bacillus subtilis* probiotic (hereafter, PB) formulated into the diets for an additional eight weeks. Outcomes included endothelial-dependent arterial dilation, body weight, microbiota profiles, and assessments of intestinal permeability and mucosal immunity markers. Furthermore, a cell culture model of gut barrier function was used to further assess the effects of PB on gut barrier integrity. Mesenteric endothelial-dependent arterial dilation was partially recovered in WD-fed mice after PB treatment, independent of changes in other cardiometabolic parameters. Endothelial function improvements in the WD-fed animals occurred despite a significant effect of diet on Shannon's alpha diversity of gut microbiota and without improvement in gut barrier function. *In vitro* trans-epithelial electrical resistance of the Caco-2 cell culture confirmed that neither PB-conditioned media nor fecal waters from *B. subtilis*-

[1] A modified version of this chapter is currently under peer review at *Beneficial Microbes* listed as: *Bacillus subtilis* DECA9 partially reverses endothelial dysfunction in high fat -diet fed mice, **B.D. Risk**, E.L. Graham, M. Zhang, Y.Wei[1], G. Stark, G. Brown, C. L. Gentile, T. L. Weir.

treated human stool resulted in gut barrier improvements, nor did they protect against inflammation-associated barrier disruptions. These data suggest that PB consumption partially reverses diet-induced endothelial dysfunction. Although the underlying mechanisms of this protection were not pinpointed, these results appear to be independent of PB-mediated improvements in cardiometabolic dysregulation markers and gut barrier function. Future studies should explore immune regulation or metabolite-mediated benefits as mechanisms of *B. subtilis* endothelial protection.

II. INTRODUCTION

Cardiovascular disease (CVD) accounts for nearly 30% of all worldwide deaths.[1] Chronic dysfunction of the innermost layer of cells lining the lumen of blood vessels, known as the vascular endothelium, increases the risk of adverse cardiovascular events and mortality[2–4] through mechanisms, including severely limiting the ability of blood vessels to dilate appropriately.[2,3] Numerous environmental and behavioral factors have been shown to influence endothelial function.[2,3] with a key contributor that interfaces with the diet and host metabolism being a consortium of microorganisms, known as a gut microbiome. Disturbances to the equilibrium of the gut microbiome through nutrient excess and increased body weight has been shown to contribute to degenerative diseases, including CVD.[5,6] Investigations from our lab[7–9] and others[10] have shown that obesity-related vascular dysfunction is due, at least in part, to alterations in the gut microbiome. For example, suppressing the obese microbiota via antibiotic administration improves endothelial dysfunction in diet-induced obese mice.[7] Furthermore, we have shown the vascular phenotype of lean and obese mice is transferable following gut microbiome transplantation.[8] These data suggest that therapeutic modalities to alter the gut microbiome's composition may improve endothelial dysfunction.

Probiotics are living microorganisms that have the potential to confer a health benefit to the host when administered at a therapeutic dose.[10] These clinically studied microorganisms are gaining popularity amongst the general public and garnering increased attention in the scientific community. However, maximizing the potential benefits of probiotics for human health and well-being requires an understanding of which bacterial species and strains interact with the host to impact targeted outcomes.

Bacillus subtilis (B. subtilis) is a Gram-positive, exopolysaccharide-producing bacterium predominantly found in soil, yet specific strains such as *B. subtilis* HU58 and HU78 occur naturally in the human gastrointestinal tract.[12] *B. subtilis* strains, such as DE111, may be particularly well suited as a probiotic due to their ability to form endospores, and survive

extreme conditions of the digestive system.[12,13] *B. subtilis* endospores remain intact upon ingestion and stay dormant until reaching the small intestine, where the pH and nutrient availability induce sporulation to a vegetative state.[12–14] The effects of *B. subtilis* DE111 supplementation in humans has recently been reviewed,[15] and include increasing bacterial alpha diversity in children,[16] regulating bowel movements,[17] and increasing T-regulatory immune cell populations after a lipopolysaccharide (LPS) challenge.[18] Notably, *B. subtilis* DE111 supplementation improved reactive hyperemia index (RHI) scores, an indicator of endothelial function, and plasma lipid profiles in healthy adults.[19] Based on these findings, we hypothesized that *B. subtilis* supplementation could reverse obesity-associated endothelial dysfunction. To test this hypothesis, we examined the effects of daily consumption of $1x10^9$ CFU/d of the animal-compliant variation of *B. subtilis* DE111 (ie. *B. subtilis* DECA9) in mice with diet-induced obesity and endothelial dysfunction. In addition, we implemented a well-established cell culture model of intestinal barrier function to further explore the underlying mechanisms of *B. subtilis*-host interactions.

III. METHODS

Animal Study

Experimental Design: Male C57BL/6J mice were obtained from the Jackson Laboratory (Bar Harbor, ME, USA) and acclimated for one week with *ad libitum* access to a standard diet (SD; No. D14042701, Research Diets, New Brunswick, NJ, USA) consisting of 4.5% fat (54.6% saturated, 29.8% monounsaturated, 7.7% polyunsaturated), 77.0% carbohydrate (0% sucrose), and 18.5% protein calories. Mice were co-housed two per cage in a temperature and humidity-controlled environment on a 12:12 hr light-dark cycle. All animal procedures were reviewed and approved by the Colorado State University Institutional Animal Care and Use Committee. Once acclimated, ARRIVE guidelines were followed[20] to randomly assign six-week-old mice to maintain a standard diet (SD; n=24) or a Western diet (WD; n=24) (No. D12079B, Research Diets, New Brunswick, NJ, USA) consisting of 23.0% fat (62.4% saturated, 30.7%

monounsaturated, 6.9% polyunsaturated), 55.0% carbohydrate (35% sucrose accounting for 70% carbohydrate), and 22.0% protein calories for eighteen weeks. Body weight and food intake were recorded weekly per ARRIVE guidelines.[20] For the final eight weeks of the diet intervention (i.e., during weeks ten-eighteen on diet), SD and WD mice were randomized to receive either non-supplemented food (SD; n=12, WD; n=12) or food formulated with $1x10^9$ CFU/d of *B. subtilis* DECA9 (PB) based on average dietary intake of 3 grams/d (SD+PB; n=12, WD+PB; n=12) (Deerland Probiotics and Enzymes, Kennesaw, GA, USA). This dose was chosen as this is the standard commercial dose that has been administered to humans.[19] The concentration and viability of *B. subtilis* endospores formulated into the rodent diets were confirmed by laboratory quality testing (Q Labs, Cincinnati, OH, USA) before the initiation of the experiment.

Animal termination and tissue collection: At termination, feces were collected and flash-frozen, body weights measured, then mice anesthetized with isoflurane and euthanized by exsanguination via cardiac puncture. Blood was collected in a 0.5 M EDTA-coated (No. 15575020, Invitrogen, Carlsbad, CA, USA) syringe. Based on the volume of blood collected, 2% EDTA was added, and plasma was obtained by centrifugation at 2,000 g for ten min at 4°C and immediately flash frozen. The liver, spleen, heart, and adipose tissue (subcutaneous, epididymal, and mesenteric depots) were then removed, weighed, and flash frozen. The GI tract was excised, and colon length was recorded before extracting colon contents and flash-freezing both tissue and feces. A 0.25cm section of ileum was obtained at the cecum juncture before freezing. Cecal contents and cecum were separated and weighed before flash-freezing and storing at -80°C. Second-order mesenteric arteries from the small intestine were excised and placed in 37°C physiological saline solution (PSS: 0.288g NaH_2PO_4, Sigma-Aldrich, St. Louis, MO, USA; 1.802g $C_6H_{12}O_6$, Sigma-Aldrich; 0.44g $C_3H_3NaO_3$, Sigma-Aldrich; 1.9g KCl, Sigma-Aldrich; 0.58g $CaCl_2H_4O_2$, Sigma-Aldrich; 0.58g $MgSO_4{\cdot}7H_2O$, Sigma-Aldrich; 0.139g MOPS sodium salt, Sigma-Aldrich; 16.94g NaCl, Alfa Aesar, Ward Hill, PA, USA; 20.0g bovine serum

albumin, Fisher Bioreagents, Pittsburgh, PA, USA; and 0.015g EDTA, Fisher Bioreagents; per 2 L ddH_2O at pH 7.4) and cannulated for endothelial function experiments.

Measurement of Endothelial Function: Endothelial function was determined via pressure myography, as previously described.[7,9] Briefly, two second-order mesenteric arteries were stripped of mesenteric adipose tissue and placed in separate pressure myograph chambers (No. 130DC, Danish Myo Technology, Ann Arbor, MI, USA) containing 37°C PSS. Arteries were cannulated onto glass micropipettes secured with suture and equilibrated for forty-five min, during which time the PSS was refreshed three times. Arteries were then measured for passive diameter of the internal lumen, then constricted with increasing doses of phenylephrine (PE) (No. P1626, Sigma-Aldrich, St. Louis, MO, USA) in three min intervals (PE: 10^{-9} to 10^{-5}M) followed immediately by a dose-response with the endothelium-dependent dilator acetylcholine (ACh) (No. A6625, Sigma-Aldrich, St. Louis, MO, USA) at two min intervals (ACh: 10^{-9} to 10^{-4}M). Arteries were then rinsed twice for ten min with fresh PSS and reconstructed with PE (10^{-5}M) for five min. A dose-response curve was then obtained with the endothelium-independent dilator sodium nitroprusside (SNP) (No. 228710, Sigma-Aldrich, St. Louis, MO, USA) at two min intervals (SNP: 10^{-10} to 10^{-4}M). Inner artery diameters were measured by MyoView 3.0.7 software (DMT) and used to calculate percent dilation for each dose of ACh or SNP relative to the PE-induced preconstriction at each time point: percent dilation (%) = (increase in luminal diameter to ACh/SNP)/ [maximum decrease in luminal diameter to PE (10^{-5}M) preconstriction]x100. Area under the dose-response curve (AUC; trapezoid method) was calculated for each response.

Liver and plasma triglycerides: Plasma and liver triglycerides were measured using a triglyceride colorimetric assay kit (No. 10010303, Cayman Chemical, Ann Arbor, MI, USA). For liver samples, ethanolic potassium hydroxide was used to digest the tissue before being diluted to a 1:5 ratio of liver extract to diluent. Plasma samples were diluted to a 1:2 ratio, and triglyceride concentrations were calculated based on the manufacturer's instructions.

Insulin: Plasma insulin was measured using an Ultra-Sensitive Mouse Insulin ELISA Kit (No. 90080, Crystal Chem, Elk Grove Village, IL, USA) following the manufacturer's instructions. The assay used a 1:19 plasma dilution and was quantified by fitting to a curve of standard concentrations.

Glucose tolerance test: At week ten and again one week before termination, all mice were transferred to new cages, and food was withheld for six hrs. Blood glucose was determined from tail-vein blood (AlphaTRAK 2 glucose meters; Abbott Laboratories, Chicago, IL, USA). After baseline glucose readings, mice received an intraperitoneal injection of 2 g/kg glucose from a 20% sterile stock solution, and blood glucose levels were measured at fifteen, thirty, sixty, ninety, and one-hundred twenty min post-injection.[7,21]

Intestinal permeability: One week before termination, all mice were fasted for twelve hrs in the dark cycle. An oral gavage of a solution containing 125 mg/ml fluorescein isothiocyanate-dextran (FiTC-dextran) (4,000 mol wt, No. 46944, Sigma-Aldrich, St. Louis, MO, USA) was administered in sterile 1x phosphate buffered saline (1xPBS), with a target dose of 600 mg/kg body weight of FiTC-dextran. After oral gavage, tail-vein blood samples were collected at four hrs to quantify plasma FITC-dextran concentration. The blood samples were centrifuged at 12,000 g for four min, and plasma was diluted in 1xPBS (pH 7.4) at a ratio of 1:4. The fluorescence was measured on a BioTek Synergy 2 Multi-Detection Microplate Reader (No. 18531, BioTek Instruments, Winooski, VT, USA) at 485/20 (excitation) and 528/20 (emission). The plasma concentrations were calculated using a standard curve of known FITC-dextran concentrations prepared in 1xPBS.

Secretory immunoglobulin A (sIgA) & Ileum intestinal alkaline phosphatase (IAP): Frozen ileal tissue was thawed, homogenized, diluted to 1:20,000 before enzyme-linked immunoassay of sIGA (No. AS-72146, Anaspec, Fremont, CA, USA) or IAP (No. M7584, Biotang, Lexington, MA, USA). Quantification for each assay was performed per the manufacturer’s

protocols and normalized to ng/ml per 5 ug of total protein as measured by the bicinchoninic acid assay (No. 23225, Thermo Fisher Scientific, Waltham, MA, USA).

LPS-binding protein (LBP): To estimate plasma lipopolysaccharide (LPS) activity, circulating levels of LBP were measured in stored plasma extracted from terminal measures. The plasma was augmented with 2% EDTA and stored at -80°C until ready for use. The Picokine ELISA kit (No. EK1274, Boster Biological Technology, Pleasanton, CA, USA) was utilized to measure LBP concentration, as per the manufacturer's instructions. Plasma was diluted 1:800 to diluent against the standard concentrations provided.

Quantitative Polymerase Chain Reaction (qPCR): Fecal contents of the mice were collected at termination, and DNA was extracted using the SsoAdvanced Universal SYBR Green Supermix DNA Purification Kit (No. 1725274, Bio-Rad, Hercules, CA, USA) before quantitative PCR verified microbial load. Reactions were optimized for the 16s rRNA gene using universal bacterial primers (forward 5=-AAACTCAAAKGAATTGACGG-3=, reverse 5=-CTCACRRCACGAGCTGA-3=). The conditions used for cycling on the Bio-Rad CFX96 thermal cycler are as stated: 95°C for three min and then forty cycles of 95°C for fifteen sec, 61°C for fifteen sec, 72°C for ten sec, and 85°C for five sec followed by florescence detection.

Microbiota characterization: Fecal DNA was extracted using the FastDNA Kit (No. 116540400; MP Biomedicals, Irvine, CA, USA), following the manufacturer's protocol. Amplification of the V4 16S rRNA region via PCR using the Earth Microbiome Protocol was completed utilizing the 515F-806R primer set containing a unique 12-bp error-correcting barcode included on the forward primer.[22] Cycling conditions using the Bio-Rad CFX96 thermal cycler were as follows: 94°C for three min and then thirty-five cycles of 94°C for forty-five sec, 50°C for sixty sec, and 72°C for ninety sec, followed by 72°C for ten min. Negative DNA extraction controls and no template PCR controls were included on 96-well plates. Amplicon libraries of the V4 region were then constructed by purifying amplicons using AmPure beads and quantifying and pooling equimolar ratios of each sample. The pooled library was quantified

and sequenced on an Illumina MiSeq at the Next-Generation Sequencing Facility at Colorado State University.

Cell Culture

Caco-2 Cell Preparation: A Caco-2 cell line from human colonic adenocarcinoma epithelial cells (No. HTB-37, American Type Culture Collection, Manassas, VA, USA) from passages two-seven were grown in Dulbecco's Modified Eagle Medium (DMEM) (No.15-027-CV, Corning, Glendale, AZ, USA) supplemented with 10% FBS (No. SH-30071, Cytiva, Marlborough, MA, USA), 0.5% penicillin-Streptomycin (No. SV30010, Cytiva, Marlborough, MA, USA), 1x MEM amino acids (No. 11130-051, Gibco, Billings, MT, USA), 1mM sodium pyruvate (No. 11360-070, Gibco, Billings, MT, USA) in a 75cm^2 flask and kept in a CO2 jacketed incubator at 37℃, 5% CO_2, 20% O_2. DMEM was changed every forty-eight hrs until cells reached 80% confluency after which they were treated with 0.25% trypsin (No. SH30041.01, Cytiva, Marlborough, MA, USA) and then seeded at a density of 1x$10^4$$cm^{-2}$ cells/well in 0.33cm^2 Transwell® inserts (No. 9320402, Sterlitech, Auburn, WA, USA). DMEM was changed every forty-eight hrs for the next four to six days until 80% confluency, then allowed to differentiate into a monolayer for precisely twenty-one days before experimentation.

Cell Culture Treatments: B. subtilis DECA9 from the manufacturer (Deerland Probiotics and Enzymes, Kennesaw, GA, USA)was cultured in Luria Bertani (LB) broth at 37°C for twenty-four to forty-eight hrs until a pellicle confirming the viability of the bacteria was formed. Cultures were checked for purity, and single colony isolates were subcultured in LB broth to an optical density of OD_{600}=0.2. The culture was then vortexed at 4969 g before being filtered through a 0.22µm mesh, vortexed at 20,800 g for ten min and sterile filtered an additional 3x until the optical density was the same as the background media. The resulting PB-conditioned media was stored at -80°C after confirming lack of bacterial growth.

Fecal waters were prepared from the frozen stool of humans both before and after supplementation with *B. subtilis* DE111 for four weeks (n=3). Briefly, thawed fecal material was diluted 1:1 (w/v) with sterile phosphate-buffered saline. To ensure homogeneity, the samples were briefly vortexed and subsequently centrifuged at 4,000 g at 4℃ for two hrs. The resulting supernatant was carefully filtered through a 0.22µm mesh and pooled according to timepoint (pre/post intervention). The samples were aliquoted into multiple centrifuge tubes and preserved at -80°C until further experimentation.

Transepithelial Electrical Resistance (TEER) Assays: Integrity of Caco-2 monolayers was determined using EVOM2 probes (No. EVOM2, World Precision Instruments, Sarasota, FL, USA). Values were determined in units of $\Omega \cdot cm^2$ and were adjusted for background and Transwell® membrane insert resistance. After removing the culture DMEM media, fresh media that contained 10% probiotic-conditioned media or 0.5% of the human fecal waters prepared from samples taken before or after probiotic supplementation were added to the apical compartment of Transwell® inserts, while fresh DMEM was added to the basolateral compartments. Cells were incubated for twenty-four hrs at 37℃, and TEER was measured again. In a few replicates, a pro-inflammatory cocktail containing 100 ng/ml tumor necrosis factor alpha (TNF-α: No.94948-59-1, Sigma Aldrich, St. Louis, IL, USA), 2ug/ml lipopolysaccharide from *E. coli* (LPS: No. 102979-140, Adipogen, San Diego, CA, USA), 100 ng/ml interferon gamma (IFN-ɣ: No. 10773-476, VWR, Radnor, PA, USA), and 50ng/ml interleukin-1 beta (IL-1β: No. 102491-634, BioVendor, Asheville, NC, USA) was introduced into the apical compartment along with the addition of 2ug/ml LPS to the basolateral compartment and additional TEER measurements were taken at forty-eight hrs.

Human Umbilical Vein Cell (HUVEC) Culture: HUVECs (No. C2519A, Lonza, Hayward, CA, USA) were kept in liquid nitrogen until ready for use. Only cells from passages two through seven were grown in Endothelial Cell Growth Basal Medium-2 (EBM-2) supplemented with a

single kit of Endothelial Singlequots (EGM-2) (No. CC-3162, Lonza, Hayward, CA, USA) in a 75cm^2 flask and kept in a CO2 jacketed incubator (No. SCO6AD, Sheldon Manufacturing, Cornelius, OR, USA) at 37°C, 5% CO_2, 20% O_2. EBM-2 and EGM-2 were changed every forty-eight hours until cells reached 80% confluency, in which they were trypsinized and then seeded at a density of 1x10^{4}cm^{-2} cells per 24 or 96-well tissue culture plate (No. 3526, Corning, Glendale, AZ, USA). Before experimentation, the culture medium of HUVEC cells was changed every forty-eight hrs, while allowing the cells to reach 100% confluency to ensure optimal growth and health.

In vitro Co-Culture System: Immediately after the final TEER was measured in Caco2 monolayers, 80% of the basolateral compartment media was mixed with 20% of fresh EBM-2/EGM-2 to replace confluent HUVEC cell media. The Transwell® membrane inserts with the treated Caco2 monolayers were transferred with 100% of the apical media to the HUVEC wells and incubated for four hrs. To image for nitric oxide (NO) and reactive oxygen species (ROS) production from the HUVEC endothelium, the media was removed via suction and washed three times with phenol red-free EBM (No. CC-3129, Lonza, Hayward, CA, USA) before staining with fluorophores. Either 5µM of CellROX Deep Red (No. C10422, Thermo Fisher Scientific, Waltham, MA, USA) or 5µM of DAF-FM (No. D23844, Thermo Fisher Scientific, Waltham, MA, USA) were suspended in phenol red-free EBM and EGM-2 and incubated with the HUVECs for thirty min at 37°C. Fluorophores were suctioned, and cells washed three times with phenol red-free EBM. A final quantity of 300µl phenol red-free EBM and EGM-2 were added to the 24-well plates, and the cells were maintained in standard conditions in a microencapsulated environment of an inverted fluorescent microscope (No. BZ-X700, Keyence, Itasca, IL, USA) for thirty min. 100µM of acetylcholine (No. 460-007-G010, Enzo Life Sciences, Farmingdale, NY, USA), which is the same maximal concentration used for pressure myography of murine secondary mesenteric arteries, was added as a stimulant for endothelial release of NO, five min prior to imaging. There was no stimulant added to cells stained for ROS production. Photos of

live fluorescence from each condition were taken at 10x with an eYFP 535/30 nm emission and 500/20 nm excitation cube for the DAF-FM stain or Cy5 700/75 nm emission and 620/60 nm excitation cube for CellROX Deep Red ROS stain and quantified using Keyence BZ-XAnalyzer software.

Plasma-Treated HUVECs: Blood from venous blood samples was collected from participants in ethylenediaminetetraacetic acid-coated tubes at baseline and after a forty-five day treatment of *Bacillus subtilis* DE111 within twenty-four hrs after their last dose of the probiotic. Baseline and post-treatment plasma from one representative sample was added at a 10% concentration of plasma to EBM-2/EGM-2 to HUVECs grown in a 96-well plate with methods previously described in this paper. After a four-hr incubation, the plasma and media was removed via suction and washed three times with phenol red-free EBM (No. CC-3129, Lonza, Hayward, CA, USA) before staining with fluorophores. Either 5μM of CellROX Deep Red (No. C10422, Thermo Fisher Scientific, Waltham, MA, USA) or 10ul of peroxynitrite sensor green (No. AB233468, Abcam, Eugene, OR, USA) were suspended in phenol red-free EBM and EGM-2 and incubated with the plasma-treated HUVECs for thirty min at 37°C. Fluorophores and media were suctioned, and cells washed three times with phenol red-free EBM. A final quantity of 100μl phenol red-free EBM and EGM-2 were added, and the cells were maintained in standard conditions in a microencapsulated environment of an inverted fluorescent microscope (No. BZ-X700, Keyence, Itasca, IL, USA) for thirty min. Cells were imaged at baseline, and again fifteen min after adding 50μM of menadione (No. 460-007-G010, Enzo Life Sciences, Farmingdale, NY, USA) as a positive control as a stimulant of peroxynitrite and general ROS release. Photos of live fluorescence were taken at 10x with eYFP 535/30nm emission and 500/20 nm excitation cube for peroxynitrite stainCy5 700/75 nm emission and 620/60 nm excitation cube for CellROX Deep Red ROS stain and quantified using Keyence BZ-XAnalyzer software.

Cell Viability: HUVEC cell counts and viability were determined by growing cells in a 96-well plate at 100% confluency. Each partitioned well was incubated for four hrs with vehicle control (media supplemented with 10% LB broth), probiotic supernatant, human fecal water, or human fecal water after forty-five days of PB treatment. Cells were washed with 1x phosphate buffered saline then 0.25% trypsin and 20ul 1x phosphate buffered saline, and incubated at 37℃ for one min to release the cells from the plate. 20ul of EBM-2/EGM-2 were added and cells from each treatment were pooled in a 0.5ml conical tube. The tube was gently hand vortexed, 25ul placed in a new 0.5ml tube, and 0.4% trypan blue solution (No. T-6246, Sigma St. Louis, MO, USA) added. The solution was hand vortexed again and 20ul of each sample added to the slide of the Nexcelom brightfield cell counter (Cellometer Auto T4, Nexcelom, Waltham, MA, USA) to detect viable cells.

Statistics: Data are expressed as means ± SEM and were evaluated for normality using Shapiro Wilkes tests. Before statistical analysis, missing values and outliers (ROUT method) were excluded from the data. Caco-2 cell culture changes in barrier integrity are expressed as TEER ($\Omega \cdot cm^2$) or change from baseline. Welch's unpaired t-test (GraphPad Prism Version 9.2.0, San Diego, CA, USA) was implemented to compare two groups. For comparisons between more than two groups or measured over time, statistical analyses were performed using a one-way ANOVA or two-way mixed effects model. When a significant main effect was observed, Tukey's *post hoc* test was performed to determine specific pairwise differences. A p-value of ≤ 0.05 was considered statistically significant.

Single-end sequence reads were demultiplexed using the open-source bioinformatics tool Qiime2 (version Qiime2-2022.2).[23–25] The filtered 16s rRNA forward reads were evaluated with a PHRED quality score set at thirty, then truncated at two hundred thirty-two base pairs. The DADA2 method was used to denoise and produce a feature table with amplicon sequence variants (ASVs), denoised statistics, and a sequencing table.[25,26] The ASVs were taxonomically classified on the 'SILVA 138 99% OTUs from the 515F/806R region of sequences' Naïve Bayes

classifier.[27,28] Reads assigned to chloroplasts and mitochondria were removed from the dataset. A phylogenetic tree was constructed using the sepp-refs-gg-13.8 pre-trained classifier and the fragment-insertion plugin in Qiime2 to be used in diversity analyses.[29] Resulting feature tables, taxonomy, metadata, and phylogeny files were imported into Microbiome Analyst marker data profiling for secondary workflow.[30] The low count and variance filters were set at 10% based on the interquartile range and data normalization using total sum scaling (TSS). Alpha diversity for each sample was represented by Shannon's diversity index at the genus level, and pairwise comparisons between the four groups were statistically analyzed using the nonparametric Mann-Whitney test with Benjamini-Hochberg false discovery rate expressed as 'W-statistic'. Beta diversity was visualized by PCoA ordination of Bray-Curtis distances calculated at the genus taxonomic level and analyzed with pairwise PERMANOVA and PERMDISP statistics. Multivariate analysis using MaAsLin2 multiple linear regression with linear adjustment was implemented to specifically evaluate WD and WD+PB mice using diet as the covariate. Linear discriminant analysis effect size (LefSe) was employed using Kruskal-Wallis to detect significant features with significant differential abundance followed by linear discriminant analysis (LDA) to evaluate effect size of differentially abundant features. Heat tree analysis using a non-parametric Wilcoxon Rank Sum test was used to identify taxonomic differences between pairs of experimental conditions.

IV. RESULTS

At baseline, mice displayed similar body weights (Figure 1a), but WD-fed mice gained significantly more weight than SD mice over 18 weeks, and PB intervention did not alter body weight (SD; 31.2±3.3, SD+PB; 30.2±2.1, WD; 47.4±3.3, WD+PB; 45.7±4.0 g; $p<0.0001$; Fig. 3.1a). Similarly, food intake was increased in both WD-fed groups, and not impacted by PB intervention (SD; 75.7±1.8, SD+PB; 73.80±1.0, WD; 91.38±1.7, WD+PB; 99.1±1.5 kcal/wk; $p<0.0001$; Fig. 3.1b). SD and WD mice that consumed PB approximately met the targeted probiotic dose of 3.0 $x10^9$ CFU/d, with an average daily intake of 2.8$x10^9$ CFU/d.

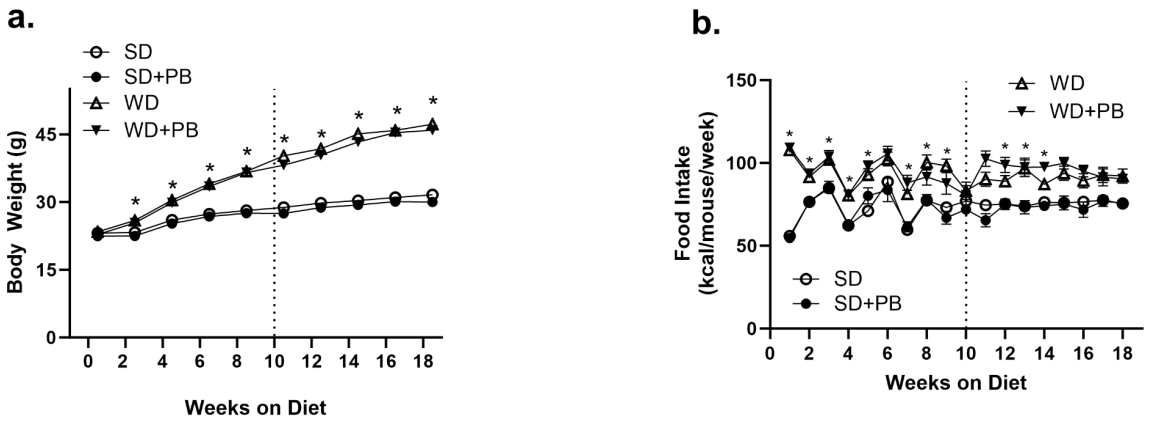

Fig. 3.1 Body weights but not food intake vary based on diet. **a.** Body weight of mice fed a standard diet (SD) or Western Diet (WD) with or without PB treatment for eighteen weeks **b.** Kilocalorie intake over the feeding and treatment period. Statistical analysis was performed using a mixed-effects analysis. When a significant main effect was observed, Tukey's post-hoc test was implemented to estimate pairwise comparisons. Data expressed as mean±SEM; n=12/group *p<0.05 WD vs. SD-fed mice.

Tissue weights of mice at termination are shown in Table 3.1. Compared to SD, mice fed the WD displayed significantly greater liver and adipose tissue mass and reduced cecum weight, which was unaltered by PB supplementation. Colon length and heart weight were not affected by diet or PB supplementation.

Table 3.1. *General Characteristics of Tissue Weights & Colon Length*

	SD	SD+PB	WD	WD + PB
Liver wt (mg)	1337.3±45.5[a]	1192.9±61.2[a]	3595.8±205.0[b]	3323.9±196.8[b]
Spleen wt (mg)	100.4±7.3[a]	97.7±10.8[a,b]	113.2±4.9[a]	130.9±9.4[a,c]
Heart wt (mg)	155.5±5.1[a]	146.0±4.9[a]	155.5±6.9[a]	159.5±6.9[a]
Epi Adipose wt (mg)	575.2±73.3[a]	614.3±66.8[a]	2120.6±115.9[b,c]	2083.0±78.5[c]
SQ Adipose wt (mg)	206.9±15.4[a]	283.6±28.3[a]	1197.2±84.9[b]	1079.6±79.0[b]
MAT (mg)	337.7±41.1[a]	356.7±39.7[a]	1073.7±101.4[b]	966.2±111.9[b]
Cecum wt (mg)	466.9±43.5[a]	367.4±38.6[a]	259.5±14.1[b]	281.9±23.4[b]
Colon length (cm)	5.5±0.2[a]	5.6±0.2[a]	5.6±0.2[a]	5.6±0.2[a]

Values are mean±SEM. *Epi* epididymal, *SQ* subcutaneous, *MAT* Mesenteric adipose tissue. Statistical analysis was performed using a one-way ANOVA with Tukey's *post hoc* test. [a,b,c] P<0.05, data with different superscript letters differ significantly.

Maximal endothelial-dependent dilation (EDD) was significantly impaired in WD-fed mice, and PB treatment partially reversed this dysfunction (Fig. 3.2 a & b). Specifically, maximal dilation in SD-fed mice was 86%, but was reduced to 62% in WD-fed animals. However, PB supplementation partially attenuated endothelial dysfunction in the WD cohort, demonstrating a maximal dilation was 79% after PB introduction. No differences were observed in passive luminal diameter (SD; 160.2±6.9, SD+PB; 164.5±9.0, WD; 165.0±4.4, WD+PB; 167.5±5.5 μm; p=0.68) or maximal phenylephrine-induced preconstriction (SD; 57.3±3.2, SD+PB; 59.5±2.2, WD; 59.5±2.2, WD+PB; 59.5±2.6 %; p=0.99, Fig. 3.2c). AUC for endothelial-independent dilation (EID), as measured by the addition of sodium nitroprusside (SNP), was not altered by diet or PB treatment (SD; 429.1±45.4, SD+PB; 444.6±53.2, WD; 488.6±16.8, WD+PB; 469.4±36.5 AUC; p=0.74, Fig. 3.2d).

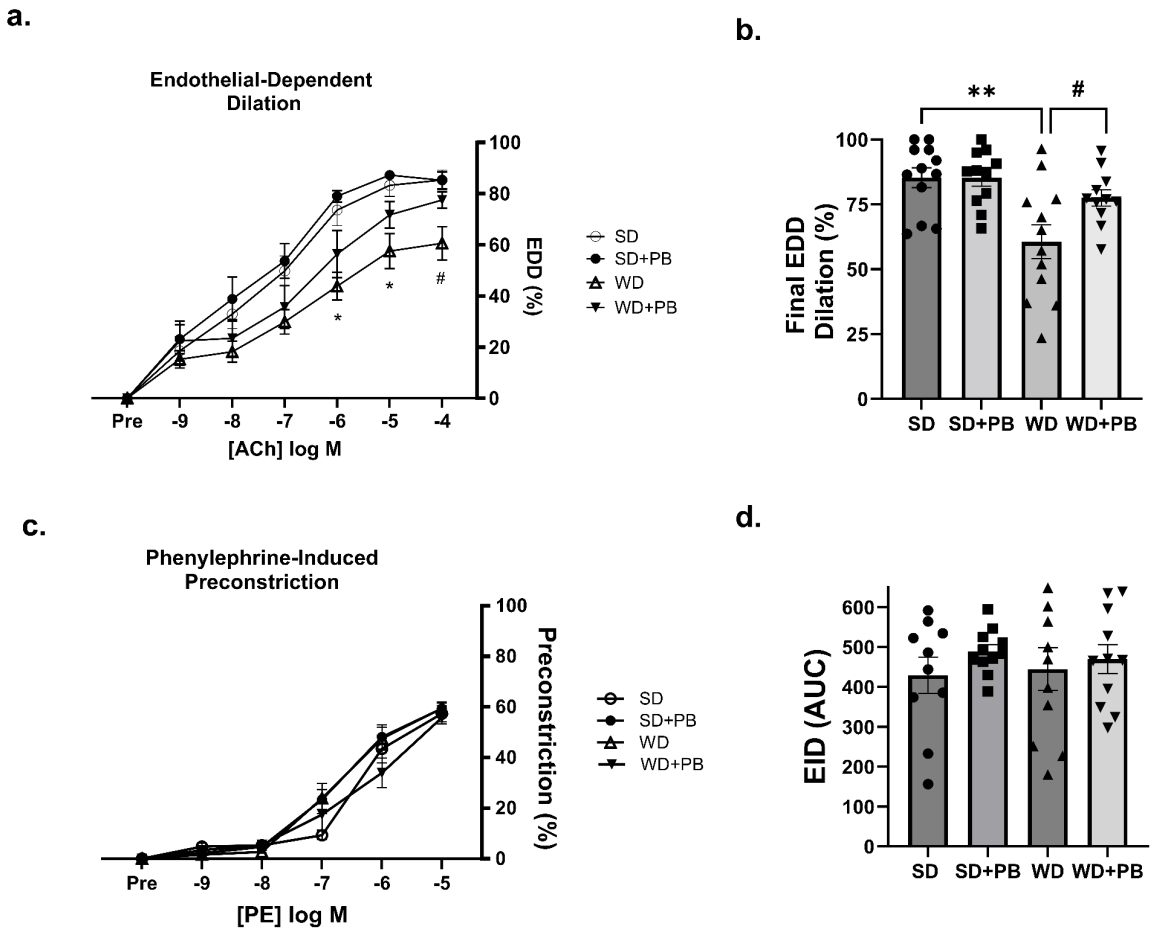

Fig. 3.2 Probiotic intervention partially reverses Western diet-induced endothelial dysfunction. **a.** Endothelial-dependent dilation (EDD) in response to acetylcholine (ACh) **b.** EDD percent dilation after final addition of ACh **c.** Phenylephrine (PE)-induced preconstriction curve **d.** Area under the curve of endothelial independent dilation (EID). Statistical analysis was performed using a mixed-effects analysis (EDD to ACh curve) or one-way ANOVA (remaining outcomes). When a significant main effect was observed, Tukey's post-hoc test was implemented to estimate pairwise comparisons. Data expressed as mean±SEM; *n*=11-12/group; *p<0.05 WD vs. SD, **p<0.005 WD vs. SD, #p=0.05 WD vs. WD+PB, data with different superscript letters are significantly different.

Liver triglyceride concentrations were significantly higher in the WD-fed mice than in SD-fed mice independent of PB supplementation (SD; 14±1.65 SD+PB; 17±2.5 WD; 110.1±9.8 WD+PB; 130.5±8.2 mg/g; p<0.0001; Fig. 3.3a), yet circulating plasma triglyceride levels were similar between all groups (SD; 83.9±4.9 SD+PB; 82±5.7 WD; 93.5±8.7 WD+PB; 86.3±6.9 mg/dl; p=0.64; Fig. 3.3b). Plasma insulin at termination was elevated in both WD cohorts (SD; 35.53±11.7, SD+PB; 50.04±2.2 WD; 110±14.1 WD+PB 102.3±7.9 ng/ml; p<0.0002; Fig. 3.3c).

Likewise, the WD mice exhibited significantly impaired glucose tolerance and PB treatment did not improve these values (Fig. 3.3 d & e).

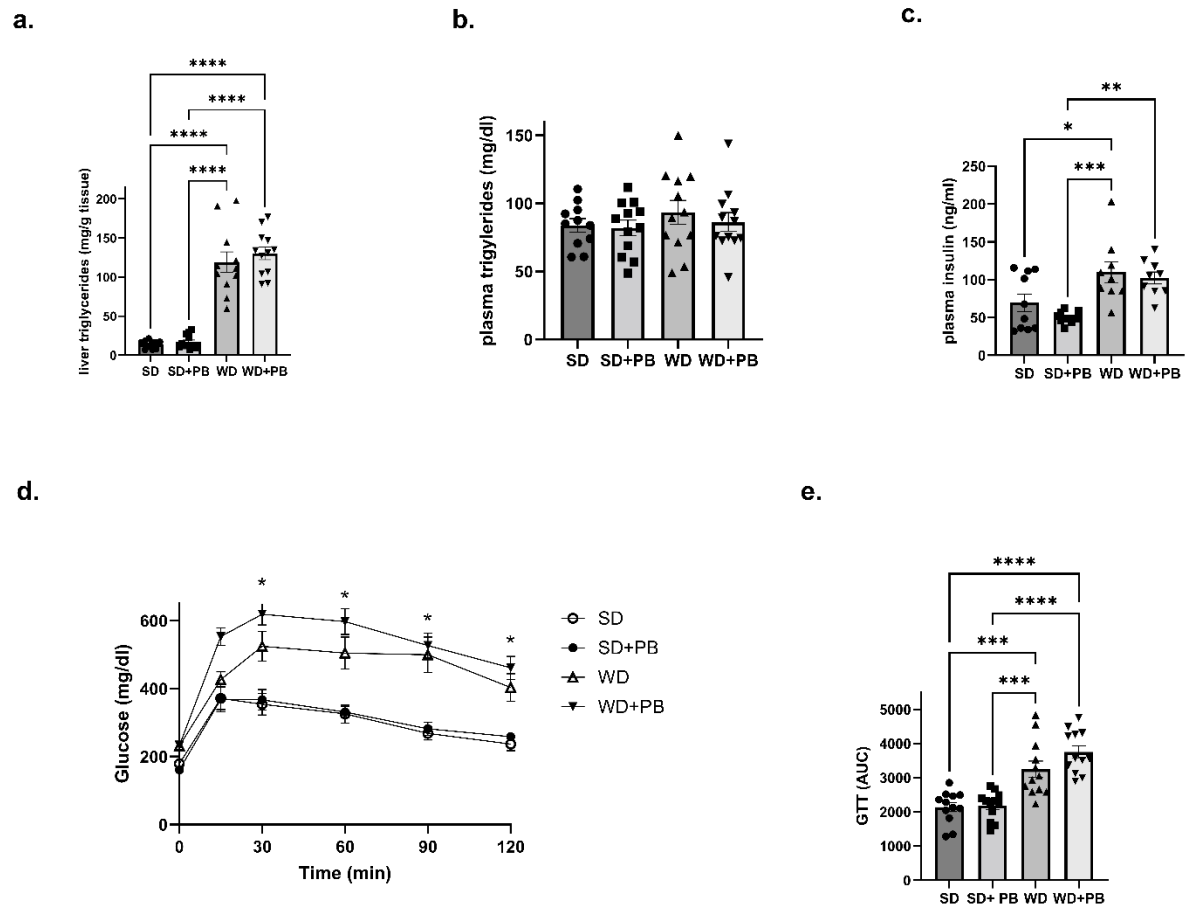

Fig. 3.3 Western diet feeding increases liver triglycerides and plasma insulin while impairing fasting glucose tolerance. **a.** Liver triglycerides expressed as mg/g of tissue **b.** Plasma triglycerides **c.** Plasma insulin **d.** Glucose tolerance test and **e.** Glucose tolerance test area under the curve (GTT AUC) at termination. Statistical analysis was performed using a mixed-effects analysis (glucose tolerance test curve) or one-way ANOVA (remaining outcomes). When a significant main effect was observed, Tukey's post-hoc test was implemented to estimate pairwise comparisons. Data expressed as mean±SEM; n=9-12; *p<0.05 WD vs. SD, ^{a,b,c}p<0.05, data with different superscript letters are significantly different.

Similar to metabolic parameters, *in vivo* intestinal permeability and circulating LBP were impaired in both WD and WD+PB compared to the two SD groups (permeability: SD; 0.40±0.7, SD+PB; 0.40±0.04, WD; 0.60±0.02, WD+PB; 0.73±0.05 µg/ml; p<0.001; Fig. 3.4a).

(circulating LBP: SD; 23519.9±54, SD+PB; 25095.4±91.4, WD; 71464.6±170.7, WD+PB; 61273.6±138 ng/ml; p<0.0001; Fig. 3.4b). There were no significant differences between groups in ileum intestinal alkaline phosphatase (IAP), an indicator to measure LPS detoxification in the intestinal lumen (SD; 14.5±1.8, SD+PB; 21.8±7.9, WD; 18.5±3.1, WD+PB; 19.3±6.3 ng/ml; p=0.82; Fig. 3.4c) or secretory immunoglobulin A (sIgA), a marker of mucosal immune activation (SD; 1057.4±93.4, SD+PB; 978.2±69.4, WD; 1055.7±74.4, WD+PB; 909.4±151.21 ng/ml; p=0.59; Fig. 3.4d).

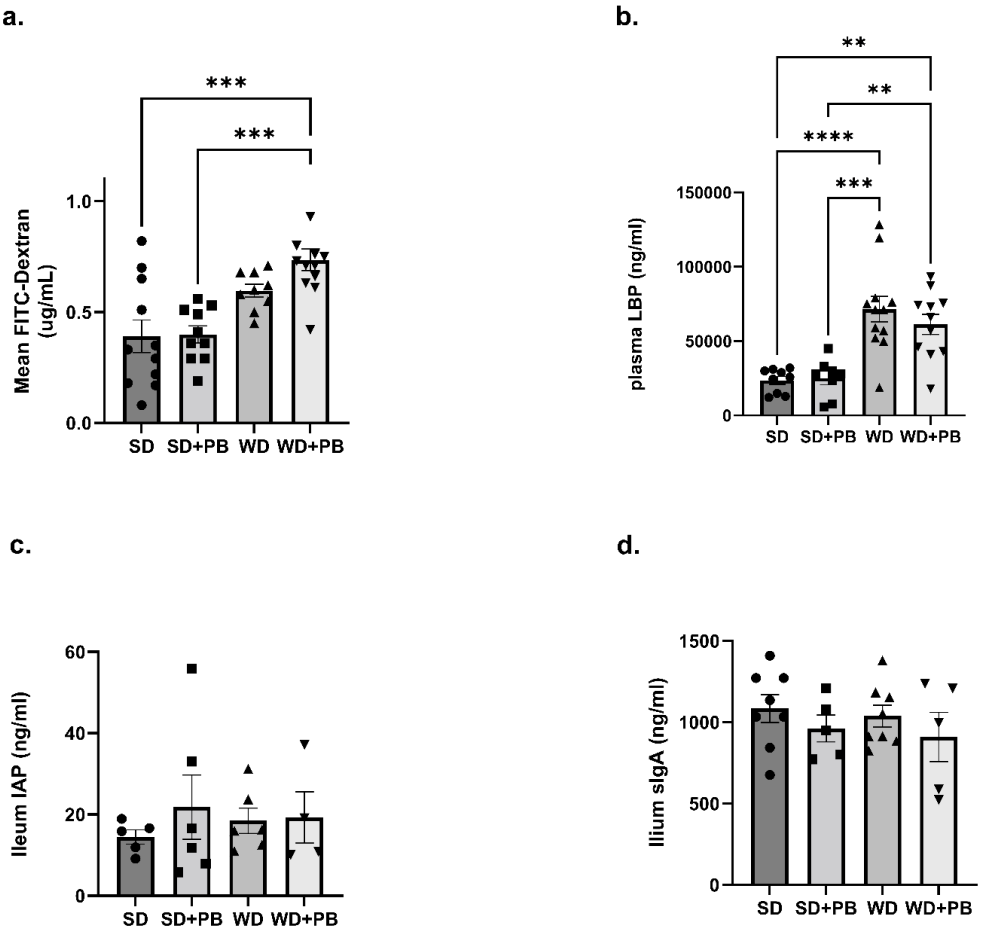

Fig. 3.4 PB treatment does not effectively moderate intestinal permeability or markers associated with lipopolysaccharide translocation. **a.** FiTC-dextran concentration **b.** Plasma lipopolysaccharide-binding protein (LBP) **c.** Ileal intestinal alkaline phosphatase (IAP) **d.** Ileal secretory immunoglobulin A (sIgA). Statistical analysis was performed using a one-way ANOVA. When a significant main effect was observed, Tukey's post-hoc test was implemented to estimate pairwise comparisons. Data expressed as mean±SEM; n=4-12; $^{a,b}p<0.05$, data with different superscript letters are significantly different.

We next analyzed the fecal microbiota to determine compositional changes due to diet and probiotic supplementation. Measuring the microbial abundance via qPCR, there was no difference in total bacterial loads detected in fecal samples between cohorts (SD; 5.72±0.12, SD+PB; 5.68±0.11, WD; 5.71±0.07, WD+PB; 5.59±0.04 log[gene copy/µl]; p=0.66; Supplemental 1a). The average number of 16s rRNA reads per sample was forty-two thousand three hundred eleven, with thirty-four features removed after filtering for low abundance and low variance. Sequences classified into five dominant phyla, with the majority being represented by *Bacillota (*formerly *Firmicutes)*, followed by *Verrucomicrobiota* and *Baceteriodota (*formerly *Bacteroidetes)*, then minor phyla consisting of *Pseudomonadota (*formerly *Proteobacteria)* and *Actinomycetota (*formerly *Actinobacteria)*. Microbiota differences were largely driven by diet, which was unaffected by PB intervention. There was a significant decrease in *Bacteriodota* in both groups of WD mice compared to SD-only mice at the phyla level ($p<0.0004$; Fig. 3.5a). Furthermore, an increase was observed in the *Bacillota* to *Bacteriodota* ratio in the WD cohorts (WD; 63:14.8, WD+PB; 63:10.5, SD; 55.2:28, SD+PB; 58.7:23; Fig. 3.5a). No significant phyla differences were observed between WD and WD+PB mice ($p>0.99$). Evaluating richness and evenness, there were no significant differences in Shannon's diversity between WD mice and WD+PB mice ($p=0.93$, $w=70.0$; Fig. 3.5b) at the genus level. However, there was significantly increased alpha diversity in WD+PB mice as compared to SD mice ($p<0.05$, $w=111.00$; Fig. 3.5 b & c) and a trend towards significance in WD mice vs SD mice ($p=0.06$, $w=104.00$; Fig. 3.5b) before FDR correction. Additionally, PCoA ordinations of Bray-Curtis distances showed a striking separation between the microbiota of mice fed the SD or WD, reflecting a 41.9% of the total variability in the dataset (PCoA; pairwise PERMANOVA F-value=6.80512, $p<0.005$, FDR adjusted $p<0.001$, Fig. 3.5c). Probiotic addition to the diet did not affect these results (PCoA; PERMDISP F-value=0.83624, $p=0.48$, Supplemental 1b). A LefSe and heat tree analysis, depicting pairwise differences of genus-level taxonomy between only SD and WD groups,

showed robust variation between the groups (Supplemental 2b & 2c). However, when analyzing the heat tree of WD vs. WD+PB mice, trending decreases in *Ruminococcaceae* and *Anaerotruncus* were observed (Fig. 3.6a; Supp. 2a). MaAslin2 multiple linear regression with covariate adjustment analysis between WD and WD+PB groups also showed a trending decrease in *Anaerotruncus* in the WD+PB mice (log2FC=1.55, p<0.05, FDR adjusted p-value=0.08; Fig. 3.6b) further confirming that the primary driver of these microbiota profiles was diet.

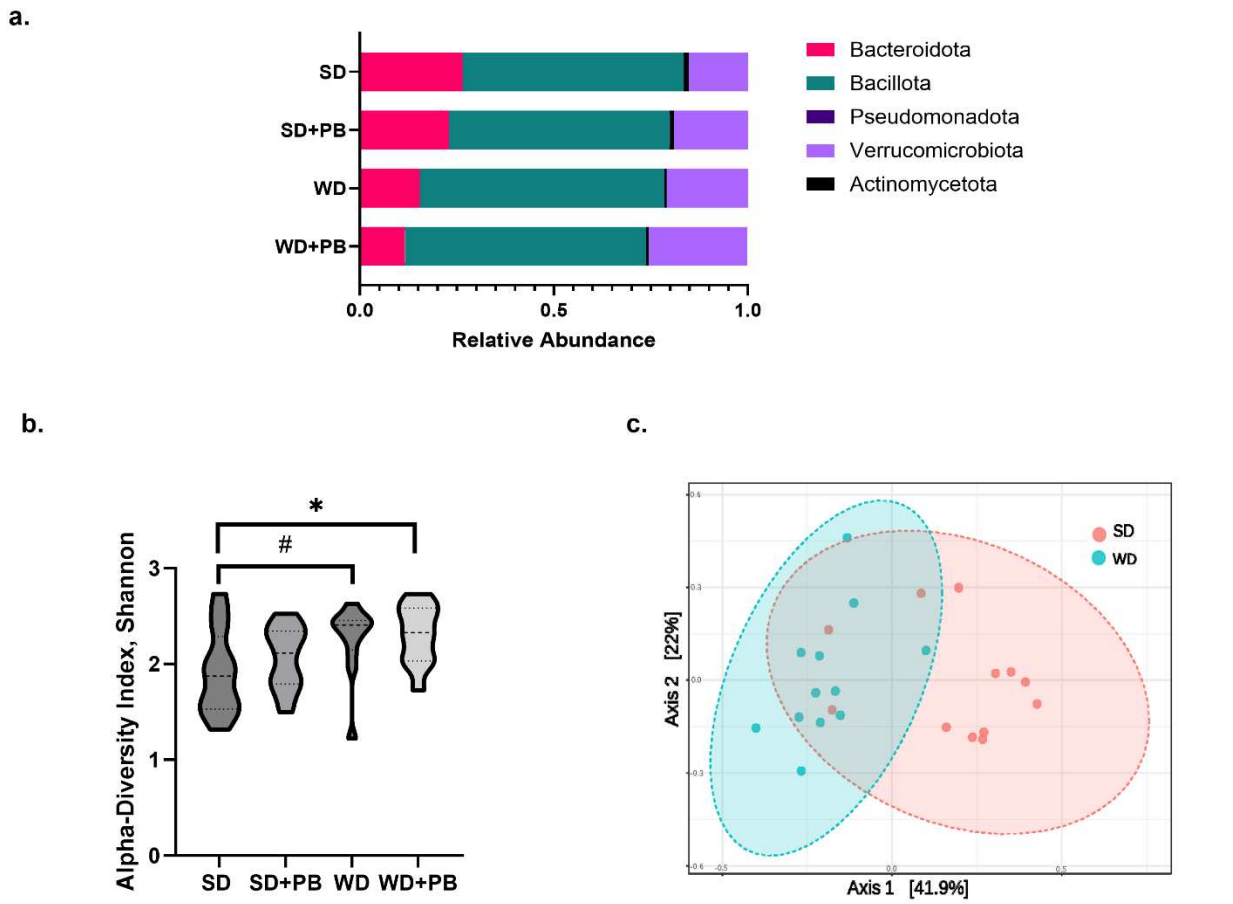

Fig. 3.5 PB treatment does not induce global microbiota alterations. **a.** Relative abundance of major bacterial phyla detected in colon contents **b.** Shannon's alpha diversity index at the genus taxonomic level **c**. Principle coordinate analysis (PCoA) of beta diversity at the phyla taxonomic level between SD and WD cohorts. The relative abundance of *Baceteriodota* between groups was calculated using a one-way ANOVA with Tukey's post-hoc test. Shannon's alpha diversity was determined using the Mann-Whitney test. P-value reported before Benjamini-Hochberg false discovery rate, W-statistic not significant. Violin plots display min, max, and 25th-75th percentile values. *p<0.05, #p=0.06. PCoA using Bray-Curtis dissimilarity index with pairwise PERMANOVA and Benjamini-Hochberg false discovery rate (SD vs WD; p<0.001), ellipses show the 95% confidence interval for each cohort.

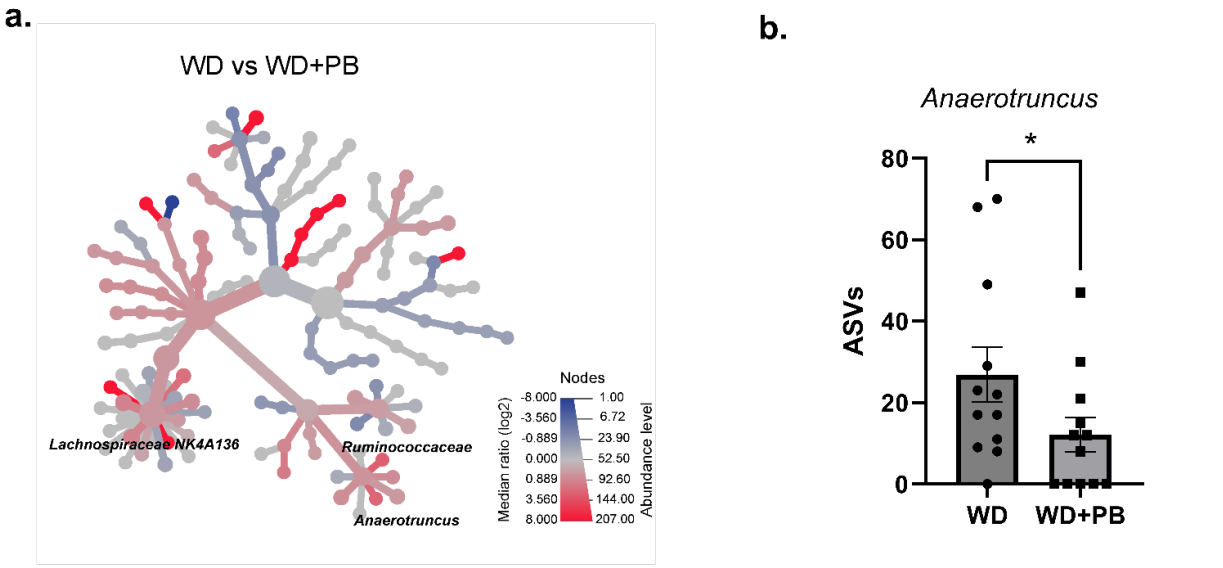

Fig. 3.6 PB intervention decreases *Anaerotruncus* presence in WD+PB mice a. Heat tree of differentially abundant taxa in WD and WD+PB groups b. *Anaerotruncus* presence between groups. Heat tree taxonomic classification was determined quantitatively using median abundance with non-parametric Mann-Whitney/Kruskal-Wallis test. *Anaerotruncus* comparison using MaAsLin2 multiple linear regression with linear adjustment using diet as the covariate between WD and WD+PB mice. *n*=12/group; *p<0.05.

As our animal data indicated that PB-induced reversal of endothelial dysfunction may have been independent of improvements in intestinal barrier function, we further tested this hypothesis which we confirmed by using trans-epithelial electrical resistance (TEER) in a Caco-2 cell model to examine intestinal barrier function. Caco-2 cells were treated with supernatant obtained from *B. subtilis* DE111 cultures or fresh LB media. They were also treated with pooled fecal waters collected from our previous human intervention[19] at baseline or after four weeks of *B. subtilis* DE111 treatment. Cells treated with LB media showed significantly improved barrier function at twenty-four hrs, while the PB-conditioned media did not significantly change. As a result, the barrier integrity was significantly greater at twenty-four hrs than those exposed to media used to grow PB cultures (Vehicle Control; +15.75±2.5, p<0.001, Probiotic Supernatant; +7.00±3.7 p=0.109; % Ωcm^2 change; Fig. 3.7a). Baseline-adjusted resistance under both conditions significantly dropped between twenty-four and forty-eight hrs (Vehicle Control; -9.10±5.3, Probiotic Supernatant; -9.45±6.3, % Ωcm^2 change; p<0.005; Fig. 3.7b). In

comparison, TEER was higher in PB-conditioned fecal waters compared to baseline fecal water samples at the twenty-four hr timepoint; however, barrier function from t=0hr to t=24hr was not significantly changed, likely due to high variability in the t=0hr measurements (Human Fecal Water Baseline; 264±3.8, Human Fecal Water After PB Treatment; 277±3.3 Ωcm2; $p<0.05$; Fig. 3.7c). Interestingly, there was no reduction in TEER over the course of forty-eight hrs after treatment with either of the human fecal water treatments (Human Fecal Water Baseline; -7.35±5.6, Human Fecal Water after PB treatment; +2.25±9.3 % Ωcm^2 change; $p=0.271$; Fig. 3.7d). As a WD is associated with inflammation of the gastrointestinal tract and elevated intestinal permeability,[31] we also tested barrier function of the fecal water conditions after addition of proinflammatory effectors and cytokines (TNF-α, LPS, IFN-γ, and IL-1β). The pro-inflammatory cocktail was added after a twenty-four hr preconditioning with the fecal water treatments. Neither of the fecal water treatments provided protection against inflammation-induced barrier disruption (Human Fecal Water; -39.25±4.7, Human Fecal Water after PB Treatment; -46.45±3.2 % Ωcm^2 change; $p<0.001$; Fig. 3.e & f).

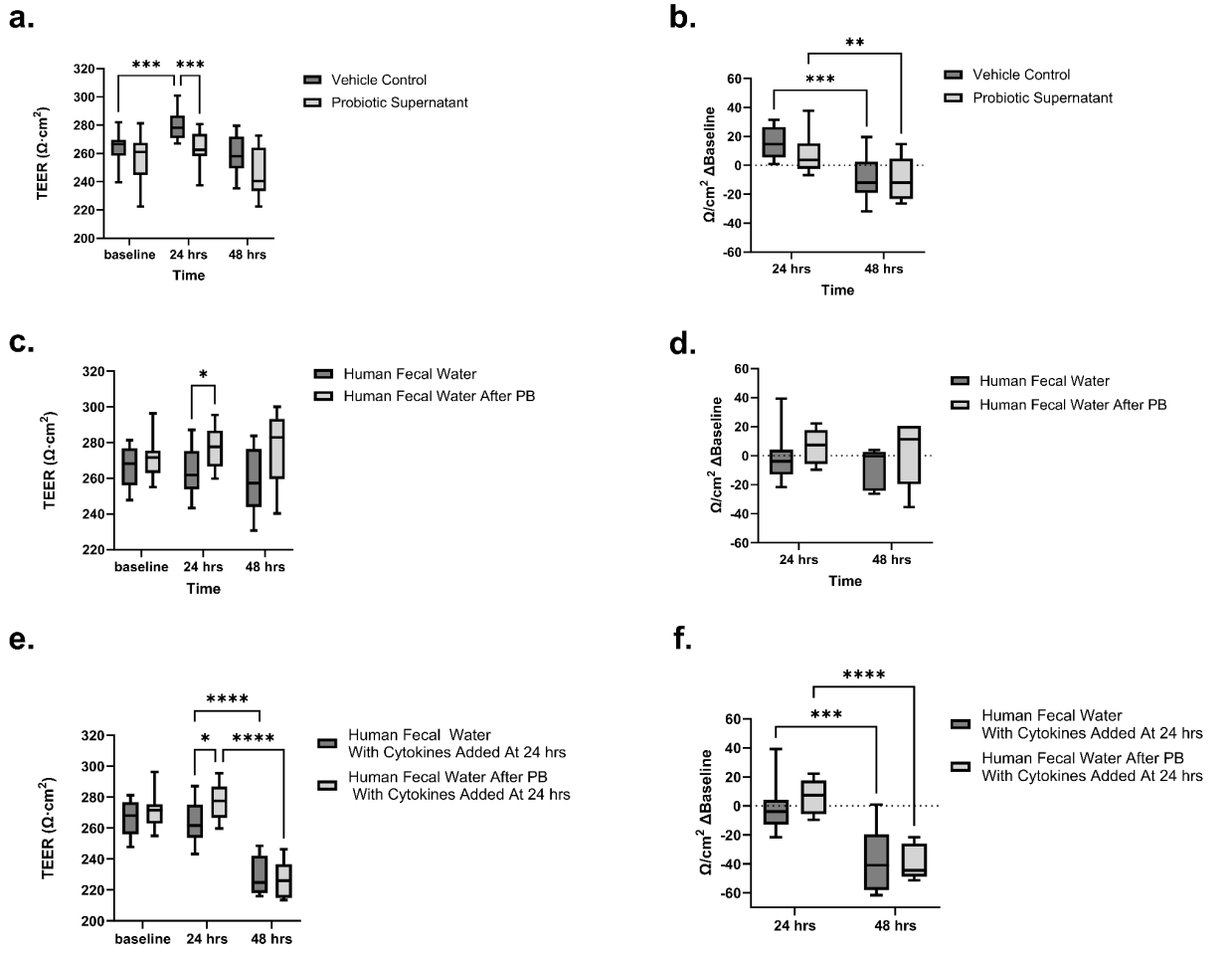

Fig. 3.7 Fecal water after PB supplementation stabilizes Caco-2 epithelial layer integrity, but not after an inflammatory insult. **a.** TEER changes at baseline, twenty-four and forty-eight hrs after probiotic supernatant conditioning **b.** Percent change in probiotic supernatant TEER from baseline **c.** TEER changes at baseline, twenty-four and forty-eight hrs after fecal water conditioning **d.** Percent change in fecal water TEER from baseline **e.** TEER changes at baseline, twenty-four and forty-eight hrs after fecal water and cytokine conditioning **f.** Percent change in fecal water TEER from baseline. To obtain TEER, the net ohms after adjusting for background resistance were multiplied by the diameter of the insert. Statistical analysis was performed using a two-way mixed effects model. When a significant main effect was observed, Tukey's post-hoc test was implemented to estimate pairwise comparisons. Data expressed as mean±SEM; *n*=6-9/group; *p<0.05, **p<0.005, ***p<0.0005, ****p<0.0001.

In spite of PB not exhibiting improvement in gut barrier function among WD+PB mice, there was a significant improvement in endothelial function. This suggests a gut-vascular connection outside gut permeability, that we further investigated using a progressive co-culture system. Following the complete treatment of Caco2 cells with PB supernatant or human fecal waters as previously described, we proceeded with co-culturing these cells with confluent

human umbilical vein endothelial cells (HUVECs) for four hours with the treated Caco2 cells and imaged after adding acetylcholine (ACh) to the HUVECs to stimulate nitric oxide (NO) release (Vehicle Control 3686±802.6, ACh 7449±784.1 RFU; p<0.005; Supp. Figure 3a). No significant differences were observed between the cells treated with PB adjuncts against the ACH control or unstimulated vehicle control (Vehicle Control 3686±802.6, ACh 7449±784.1, PB Supernatant (w/ACh) 6339±1289, Human Fecal Water After PB (w/ACH) 6230±984.5 RFU; p=0.102; Supp. Figure 3a). Yet, the cells treated with human fecal water before PB treatment showed a significant increase in NO fluorescence (Vehicle Control 3686±802.6, ACh 7449±784.1, Human Fecal Water (w/ACh) 8820±1640.0 RFU; p<0.005; Supp. Figure 3a). As ROS is associated with a WD and elevated concentrations can damage to the endothelium,[3] we tested the production of hydroxyl radicals, superoxide, hydrogen peroxide, and peroxynitrite in co-cultured HUVECs. We found that both of the human fecal waters increased ROS production (Vehicle Control 3973±404.9, Human Fecal Water 7115±646.1, Human Fecal Water After PB 7686±1083.9 RFU; p<0.05; Supp. Figure 3b). However, the probiotic supernatant did not show a significant increase in ROS fluorescence over the vehicle control (Vehicle Control 3973±404.9, PB Supernatant 4925±798.7 RFU; p=0.782; Supp. Figure 3b). It is worth noting that the viability of the HUVECs remained unchanged after co-culturing with the Caco2 cells in their respective conditions (Vehicle Control 9.12±0.76, PB Supernatant 9.05±0.77, Human Fecal Water 9.42±0.78, Human Fecal Water After PB 8.77±0.47 10^4 cells; p=0.928; Supp. Figure 4b). This observation strongly suggests that fecal water treatment did not have a toxic effect on the cells during the co-culturing process.

As there was a clear effect of human fecal water on HUVEC release of ROS, we conditioned HUVECs with plasma from a single participant both before and after supplementing with PB in our previous clinical trial, and stimulated the cells with vitamin K3 as a positive control for ROS and peroxynitrite. Our focus was to evaluate the release of general ROS and peroxynitrite, as these can inhibit endothelial-mediated dilation and lead to

endothelial dysfunction through oxidative stress signaling.[3] At basal conditions, peroxynitrite was elevated in human plasma (Negative Control 3711±67.0, Human Plasma 3758±53.3, Human Plasma After PB 4675±72.3 RFU; p<0.0001; Supp. Figure 5a) and was analogous to the K3 positive control fluorescence after stimulation (Positive Control 4794±82.4, Human Plasma (w/K3) 4174±46.1, Human Plasma After PB (w/K3) 4598±45.4 RFU; p<0.0001; Supp. Figure 5b). However, general ROS production in HUVECs treated with human plasma after PB intervention was significantly lower than the baseline human plasma (Human Plasma 2691±23.4, Human Plasma After PB 2204±21.3 RFU; p<0.0001; Supp. Figure 5c), and ~47% lower than the negative control (Negative Control 4146±57.8, Human Plasma After PB 2204±21.3 RFU; p<0.0001; Supp. Figure 5c). After K3 stimulation, ROS fluorescence in HUVECs was significantly lower human plasma both before and after PB treatment (Positive Control (K3) 5665±82.7, Human Plasma (w/K3) 4196±40.2, Human Plasma After PB (w/K3) 3678±37.4 RFU; p<0.0001; Fig. 5d).

V. DISCUSSION

This study investigated the potential of a *B. subtilis* DECA9 to counteract Western diet-induced endothelial dysfunction in experimental mice. In a previous human study, consumption of the human-compliant variation of this strain, *B. subtilis* DE111, resulted in improved endothelial function (reported as RHI) in healthy humans.[19] Inspection of individual responses in the human data suggested that RHI improvements were largely driven by individuals with a higher body mass index (BMI) or lower baseline RHI scores. A high BMI due to obesity is a risk factor for endothelial dysfunction,[6] and the development of new interventions is highly valued in reducing the progression of CVD in this demographic. In mice, obesity-associated endothelial dysfunction can reliably be induced by WD feeding. Therefore, we used this model to test the hypothesis that *B. subtilis* intervention could *reverse* endothelial dysfunction. In line with this hypothesis, our main finding was that endothelial-mediated dilation improved in Western diet mice receiving a *B. subtilis* DECA9 compared to mice solely on a Western diet.

Interestingly, improvements in endothelial function were not associated with changes in body weight or other cardiometabolic parameters, and there was no indication these improvements were due to enhancements in intestinal barrier function. Western-diet induced alterations to the gut microbiome induces intestinal inflammation, leading to increased permeability and transit of large endotoxemic molecules such as LPS through the intestinal barrier into the bloodstream that contacts the endothelium to initiate a systemic pro-inflammatory response.[32] This response, in turn, has been linked to endothelial impairments.[33,34] In the present study, plasma LBP- a surrogate marker for LPS,[35] and FiTC-dextran analysis of intestinal permeability were both significantly elevated in all WD-fed mice, with no improvements observed in the group that received PB supplementation. Neither diet nor PB treatment altered ileal IAP, a proxy of LPS neutralization in the intestine, or the mucosal immunity marker, sIgA. Despite a lack of IAP upregulation in our animal model, a study in human ileostomy patients supplemented with *Bacillus subtilis* DE111 did show increased IAP after probiotic administration.[36] These discrepancies could be due to inherent differences in the models or variability introduced by capsule versus food-based delivery of the probiotic. Other studies utilizing diet-induced obese rodents have demonstrated the ability of certain *Bacillus* strains, such as *B. subtilis* R0179 and *B. subtilis* natto JLCC513 to decrease circulating LPS[37,38] and *Bacillus licheniformis Zhengchangsheng* to improve gut barrier integrity[39]. However, Kim et al., reported that five *Bacillus* strains comprised of *B. sonorensis* JJY12-3, *B. paralicheniformis* JJY12-8*, B. sonorensis* JJY13-1, *B. sonorensis* JJY13-3, and *B. sonorensis* JJY13-8 did not appreciably lower plasma LPS concentrations in WD-fed mice, indicating that the strain of probiotic may dictate LPS neutralization.[40]

To further explore the effects of *Bacillus subtilis* DE111 on gut barrier integrity, we performed *in vitro* TEER assays using Caco-2 cells. Treatments included culture supernatants from LB-grown *B. subtilis* DE111 and fecal waters collected from human participants before and after a four-week course of *B. subtilis* DE111 supplementation. The culture supernatants showed no

beneficial effects and decreased barrier function compared to the vehicle control. However, the human fecal waters collected after DE111 supplementation showed improved barrier function at twenty-four hrs compared to the pre-probiotic controls from the same individuals. After a twenty-four-hour preconditioning with the supernatants or fecal waters, a subset of cells was exposed to a proinflammatory cytokine cocktail. Unfortunately, none of the treatments were effective in providing protection against the inflammatory insult. Yet, in the absence of the cytokines, the media-treated Caco-2 barriers also showed a significant decrease at forty-eight hrs while the fecal water treated better preserved their barrier integrity cells did not. This suggests that the metabolites and other components from the intestinal milieu could be important in preserving barrier function in this model and the benefits noted in the post-probiotic fecal waters are mediated through complex interactions between the various intestinal components. As there is considerable variation in the reported effects of *B. subtilis*[18,41,42] on gut barrier integrity, further research is warranted to understand whether these differences are due to experimental inconsistencies or influenced by probiotic strain and host factors, such as composition of the commensal gut microbes.

Numerous studies have confirmed that obesity and a WD alters gut microbiome composition.[43–45] For example, Turnbaugh et al. have observed that a genetically obese rodent microbiome harvests more energy from the diet, and confers phenotype to naïve germ-free recipients along with increases in *Bacillota*:*Bacteriodota* ratios as compared to lean controls.[44] Additionally, others have found that similar changes occur in the same microbial phyla in wild-type mice fed a WD.[45] Consistent with previous reports, we saw reduced *Bacteroidota* resulting in an increased ratio of *Bacillota* to *Bacteroidota*, which has been linked to elevated circulating LPS.[46] Our data suggest increased circulating LPS, as indicated by the reduced barrier function and increased LBP observed with WD feeding. Compared to SD-fed mice, the WD+PB group had increased Shannon's diversity. Although increased microbial diversity is often associated with improved health outcomes this association in both the animal and human microbiota

literature is inconsistent.[47,48] It is important to note that most of the microbiota differences we observed were due to diet, and that addition of *B. subtilis* DECA9 did not appreciably alter microbiota composition. These results concur with observations from our previous clinical trial in humans, where supplementation with 1x10^9 CFU/d of *B. subtilis* DE111 for four weeks had a negligible impact on global microbiota composition.[19] Similar observations have also been made in other studies incorporating *B. subtilis* strains,[49] suggesting that even though *B. subtilis* is a highly adaptable and ubiquitous microorganism, it does not induce perturbations to gut ecology. Instead, subtle and limited interactions such as a decrease in *Anaerotruncus* in WD+PB mice compared to WD mice were observed. *Anaerotruncus* is a member of the LPS-producing *Bacillota* phylum and is commonly associated with digestive discomfort,[50] and often associated with a high-fat Westernized diet.[51,52] These indices suggest that *B. subtilis* DECA9's effects are outside the scope of global microbiome revision, but may subtly alter the relative abundance of specific bacteria associated with diet-induced perturbations.

There are noteworthy limitations to the current study. First, although we validated the viability of the probiotic for a therapeutic dose upon consumption, we cannot confirm whether each mouse ingested a consistent amount daily. Nevertheless, we did not observe significant differences in weekly body weight changes among co-housed mice with an estimated daily intake of 1x10^9 CFU/d. Second, we examined only male mice, and thus, the findings should not be assumed to be similar in female mice. However, our previous work in humans did suggest that PB may be efficacious in both sexes in a healthy cohort.[19] Lastly, although endothelial function improved in PB-treated WD mice, we cannot translate these results to an obese human population at risk for endothelial dysfunction. Future clinical studies, including both obese males and females, will be needed to address these questions further.

VI. CONCLUSIONS

In conclusion, we found that diet-induced obese mice fed a commonly recommended dose of *B. subtilis* exhibited partial reversal of endothelial dysfunction. These improvements do

not appear to be mediated by weight loss effects or improved gut barrier integrity, at least in this rodent model. Additional mechanisms, such as microbial metabolites interacting with the vascular endothelium or modulating inflammatory molecules, may also be involved. These results extend our previous work in healthy humans by suggesting that *B. subtilis* may improve existing vascular function to support general cardiovascular health. Taken together, these findings emphasize the intricate interplay between gut microbiota and endothelial function. Future research should prioritize unraveling the mechanisms through which *B. subtilis* enhances endothelial improvements, and determining whether it can support cardiovascular health in human populations with vascular dysfunction who are at risk for developing cardiovascular disease.

REFERENCES

1. Coronado F, Melvin SC, Bell RA, Zhao G. Global responses to prevent, manage, and control cardiovascular diseases. *Prev Chronic Dis*. 2022;19(220347):E84.

2. Rajendran P, Rengarajan T, Thangavel J, et al. The vascular endothelium and human diseases. *Int J Biol Sci*. 2013;9(10):1057-1069.

3. Poredos P, Poredos AV, Gregoric I. Endothelial dysfunction and its clinical implications. *Angiology*. 2021;72(7):604-615.

4. Zuchi C, Tritto I, Carluccio E, Mattei C, Cattadori G, Ambrosio G. Role of endothelial dysfunction in heart failure. *Heart Fail Rev*. 2020;25(1):21-30.

5. Qin Y, Wade PA. Crosstalk between the microbiome and epigenome: messages from bugs. *J Biochem*. 2018;163(2):105-112.

6. Engin A. Endothelial dysfunction in obesity. *Adv Exp Med Biol*. 2017;960:345-379.

7. Battson ML, Lee DM, Jarrell DK, et al. Suppression of gut dysbiosis reverses Western diet-induced vascular dysfunction. *Am J Physiol Endocrinol Metab*. 2018;314(5):E468-E477.

8. Trikha SRJ, Lee DM, Ecton KE, et al. Transplantation of an obesity-associated human gut microbiota to mice induces vascular dysfunction and glucose intolerance. *Gut Microbes*. 2021;13(1):1940791.

9. Lee DM, Battson ML, Jarrell DK, et al. SGLT2 inhibition via dapagliflozin improves generalized vascular dysfunction and alters the gut microbiota in type 2 diabetic mice. *Cardiovasc Diabetol*. 2018;17(1). doi:10.1186/s12933-018-0708-x

10. Brunt VE, Gioscia-Ryan RA, Richey JJ, et al. Suppression of the gut microbiome ameliorates age-related arterial dysfunction and oxidative stress in mice. *J Physiol*. 2019;597(9):2361-2378.

11. Hill C, Guarner F, Reid G, et al. Expert consensus document. The International Scientific Association for Probiotics and Prebiotics consensus statement on the scope and appropriate use of the term probiotic. *Nat Rev Gastroenterol Hepatol*. 2014;11(8):506-514.

12.Tam NKM, Uyen NQ, Hong HA, et al. The intestinal life cycle of Bacillus subtilis and close relatives. *J Bacteriol*. 2006;188(7):2692-2700.

13.Colom J, Freitas D, Simon A, et al. Presence and germination of the probiotic Bacillus subtilis DE111® in the human small intestinal tract: A randomized, crossover, double-blind, and placebo-controlled study. *Front Microbiol*. 2021;12:715863.

14.Jeżewska-Frąckowiak J, Seroczyńska K, Banaszczyk J, Jedrzejczak G, Żylicz-Stachula A, Skowron PM. The promises and risks of probiotic Bacillus species. *Acta Biochim Pol*. 2018;65(4):509-519.

15.Williams N, Weir TL. Spore-based probiotic Bacillus subtilis: Current applications in humans and future perspectives. *Fermentation*. 2024;10(2):78.

16.Paytuví-Gallart A, Sanseverino W, Winger AM. Daily intake of probiotic strain Bacillus subtilis DE111 supports a healthy microbiome in children attending day-care. *Benef Microbes*. 2020;11(7):611-620.

17.Cuentas AM, Deaton J, Khan S, Davidson J, Ardita C. The effect of Bacillus subtilis DE111 on the daily bowel movement profile for people with occasional gastrointestinal irregularity. *J Probiotics Health*. 2017;05(04). doi:10.4172/2329-8901.1000189

18. Freedman KE, Hill JL, Wei Y, et al. Examining the gastrointestinal and immunomodulatory effects of the novel probiotic Bacillus subtilis DE111. *Int J Mol Sci*. 2021;22(5). doi:10.3390/ijms22052453

19.Trotter RE, Vazquez AR, Grubb DS, et al. Bacillus subtilis DE111 intake may improve blood lipids and endothelial function in healthy adults. *Benef Microbes*. 2020;11(7):621-630.

20. The ARRIVE guidelines 2.0. ARRIVE Guidelines. Accessed June 17, 2024. https://arriveguidelines.org/arrive-guidelines

21.Ecton KE, Graham EL, Risk BD, et al. Toll-like receptor 4 deletion partially protects mice from high fat diet-induced arterial stiffness despite perturbation to the gut microbiota. *Front Microbiomes*. 2023;2. doi:10.3389/frmbi.2023.1095997

22. 16S Illumina Amplicon Protocol : earth microbiome. Accessed June 14, 2024. https://earthmicrobiome.org/protocols-and-standards/16s/

23. Hamady M, Knight R. Microbial community profiling for human microbiome projects: Tools, techniques, and challenges. *Genome Res*. 2009;19(7):1141-1152.

24. Hamady M, Walker JJ, Harris JK, Gold NJ, Knight R. Error-correcting barcoded primers for pyrosequencing hundreds of samples in multiplex. *Nat Methods*. 2008;5(3):235-237.

25. Bolyen E, Rideout JR, Dillon MR, et al. Author Correction: Reproducible, interactive, scalable and extensible microbiome data science using QIIME 2. *Nat Biotechnol*. 2019;37(9):1091.

26. Callahan BJ, McMurdie PJ, Rosen MJ, Han AW, Johnson AJA, Holmes SP. DADA2: High-resolution sample inference from Illumina amplicon data. *Nat Methods*. 2016;13(7):581-583.

27. Robeson MS II, O'Rourke DR, Kaehler BD, et al. RESCRIPt: Reproducible sequence taxonomy reference database management for the masses. *bioRxiv*. Published online October 5, 2020. doi:10.1101/2020.10.05.326504

28. Bokulich NA, Kaehler BD, Rideout JR. Optimizing taxonomic classification of marker-gene amplicon sequences with QIIME 2's q2-feature-classifier plugin. Microbiome. 2018;6:1-17.

29. sepp: Insert fragment sequences using SEPP into reference phylogenies. — QIIME 2

2022.2.0 documentation. Accessed March 31, 2024. https://docs.qiime2.org/2022.2/plugins/available/fragment-insertion/sepp/

30. Chong J, Liu P, Zhou G, Xia J. Using MicrobiomeAnalyst for comprehensive statistical, functional, and meta-analysis of microbiome data. *Nat Protoc*. 2020;15(3):799-821.

31. Malesza IJ, Malesza M, Walkowiak J, et al. High-Fat, Western-Style Diet, Systemic Inflammation, and Gut Microbiota: A Narrative Review. *Cells*. 2021;10(11). doi:10.3390/cells10113164

32. Harris K, Kassis A, Major G, Chou CJ. Is the gut microbiota a new factor contributing to obesity and its metabolic disorders? *J Obes*. 2012;2012:879151.

33. Choy KW, Lau YS, Murugan D, Vanhoutte PM, Mustafa MR. Paeonol attenuates LPS-induced endothelial dysfunction and apoptosis by inhibiting BMP4 and TLR4 signaling simultaneously but independently. *J Pharmacol Exp Ther*. 2018;364(3):420-432.

34. Coquerel D, Neviere R, Delile E, et al. Gene deletion of protein tyrosine phosphatase 1B protects against sepsis-induced cardiovascular dysfunction and mortality. *Arterioscler Thromb Vasc Biol*. 2014;34(5):1032-1044.

35. Li C, Gao M, Zhang W, et al. Zonulin regulates intestinal permeability and facilitates Enteric bacteria permeation in coronary artery disease. *Sci Rep*. 2016;6:29142.

36. Colom J, Freitas D, Simon A, et al. Acute physiological effects following Bacillus subtilis DE111 oral ingestion - a randomised, double blinded, placebo-controlled study. *Benef Microbes*. 2023;14(1):31-43.

37. Huang J, Huang J, Yin T, Lv H, Zhang P, Li H. Enterococcus faecium R0026 combined with Bacillus subtilis R0179 prevent obesity-associated hyperlipidemia and modulate gut Microbiota in C57BL/6 mice. *J Microbiol Biotechnol*. 2021;31(2):181-188.

38. Li Y, Liu M, Liu H, et al. Oral supplements of combined Bacillus licheniformis Zhengchangsheng® and xylooligosaccharides improve high-fat diet-induced obesity and modulate the gut Microbiota in rats. *Biomed Res Int*. 2020;2020:9067821.

39. Sun R, Niu H, Sun M, et al. Effects of Bacillus subtilis natto JLCC513 on gut microbiota and intestinal barrier function in obese rats. *J Appl Microbiol*. 2022;133(6):3634-3644.

40. Kim B, Kwon J, Kim MS, et al. Protective effects of Bacillus probiotics against high-fat diet-induced metabolic disorders in mice. *PLoS One*. 2018;13(12):e0210120.

41. Lefevre M, Racedo SM, Ripert G, et al. Probiotic strain Bacillus subtilis CU1 stimulates immune system of elderly during common infectious disease period: a randomized, double-blind placebo-controlled study. *Immun Ageing*. 2015;12(1):24.

42. Garvey SM, Mah E, Blonquist TM, Kaden VN, Spears JL. The probiotic Bacillus subtilis BS50 decreases gastrointestinal symptoms in healthy adults: a randomized, double-blind, placebo-controlled trial. *Gut Microbes*. 2022;14(1):2122668.

43. Ley RE, Turnbaugh PJ, Klein S, Gordon JI. Microbial ecology: human gut microbes associated with obesity. *Nature*. 2006;444(7122):1022-1023.

44. Turnbaugh PJ, Ley RE, Mahowald MA, Magrini V, Mardis ER, Gordon JI. An obesity-associated gut microbiome with increased capacity for energy harvest. *Nature*. 2006;444(7122):1027-1031.

45. Murphy EF, Cotter PD, Healy S, et al. Composition and energy harvesting capacity of the gut microbiota: relationship to diet, obesity and time in mouse models. *Gut*. 2010;59(12):1635-1642.

46. Caricilli AM, Saad MJA. The role of gut microbiota on insulin resistance. *Nutrients*. 2013;5(3):829-851.

47. Pinart M, Dötsch A, Schlicht K, et al. Gut microbiome composition in obese and non-obese persons: A systematic review and meta-analysis. *Nutrients*. 2021;14(1):12.

48. Hills RD Jr, Pontefract BA, Mishcon HR, Black CA, Sutton SC, Theberge CR. Gut microbiome: Profound implications for diet and disease. *Nutrients*. 2019;11(7):1613.

49. Hanifi A, Culpepper T, Mai V, et al. Evaluation of Bacillus subtilis R0179 on gastrointestinal viability and general wellness: a randomised, double-blind, placebo-controlled trial in healthy adults. *Benef Microbes*. 2015;6(1):19-27.

50. Nouvenne A, Ticinesi A, Tana C, et al. Digestive disorders and Intestinal microbiota. *Acta Biomed*. 2018;89(9-S):47-51.

51.Kong C, Gao R, Yan X, Huang L, Qin H. Probiotics improve gut microbiota dysbiosis in obese mice fed a high-fat or high-sucrose diet. *Nutrition*. 2019;60:175-184.

52. Bailén M, Bressa C, Martínez-López S, et al. Microbiota features associated with a high-fat/low-fiber diet in healthy adults. *Front Nutr*. 2020;7:583608.

CHAPTER 5: FUTURE PERSPECTIVES-AN ARGUMENT FOR MICROBIAL METABOLOMICS

Throughout this dissertation, the connection between the microbiome and the health of the vascular endothelium have been examined. It has been demonstrated through various trials involving human subjects, mice, and cell culture that dietary interventions contribute to reducing endothelial dysfunction across a range of health conditions, gender, species, and age. These findings support other research that nutritional modifications extend beyond the digestive system in managing vascular health.[1] More specifically, the microbiome as a consortium of microorganisms, its genes, and metabolites impact endothelial function via liberation of bioactive metabolites via mechanisms outside intestinal barrier modulation. The implications of this research may serve as a catalyst for future research, and for developing microbiome-targeted interventions in the prevention and treatment of endothelial dysfunction.

Despite a limited understanding of bioavailability and bioactivity, stark contrast exist in the microbiome and its metabolite profile in healthy versus diseased states.[1,2] This underscores the role of microbe-derived metabolites in processes related to human health, with compelling evidence pointing to the study of microbial metabolites, known as metabolomics, as a promising new frontier in medicine.[3] The ratio of bacterial to human cells is approximately 1:1, yet the microbiome genome dwarfs the human genome of >22 million genes to 23,000 genes.[4] This inequality in genomic disparity highlights the potential of harnessing the microbiome, which far surpasses that of the human genome for targeted therapies.

Nutritional interventions, such as the Mediterranean diet high in SCFA-producing fiber and polyphenols, are currently being studied for their cardioprotective effects.[5,6] Probiotics have been found to effectively modulate the microbiome to improve endothelial function[7,8] and partially reverse this condition in diet-induced obesity. Lastly, fecal stool transplant from a donor to a recipient completely restructures the microbiome, offering a new avenue to study the

intestinal environment and endothelial function. Yet, the question remains whether it is the microbiota or the metabolites they produce that contribute to disease or homeostasis.

Given that metabolomics provides a snapshot into microbiome metabolism at any point in time, the clinical significance of microbial metabolites may surpass that of microbial diversity.[4] A single microbial metabolite can be toxic (ie. PAGln) or beneficial (ie. butyrate) depending on the concentration of the metabolite and the health state of targeted tissues.[4] The burgeoning field of metabolomic research presents the opportunity to classify and quantify metabolites to identify their origin, biotransformation, transport systems, effective concentrations, and interaction with the host.[9] Integrating knowledge regarding the metabolic products of microorganisms and their impact on host physiology has emerged as a transformative avenue in advancing therapeutic approaches to CVD. This represents a significant paradigm shift in the field of medical science, with the potential to revolutionize the way we approach the treatment of various ailments. In the coming years, it will be imperative that rigorous studies determine how the enrichment or depletion of microbiota with their metabolites can impact CVD. Only by tracking changes over time can we comprehensively understand the complex interplay between the human body and the microbiome and pave the way for more effective treatments and improved cardiovascular outcomes.

REFERENCES

1. Rahman MM, Islam F, -Or-Rashid MH, et al. The Gut Microbiota (Microbiome) in Cardiovascular Disease and Its Therapeutic Regulation. *Front Cell Infect Microbiol*. 2022;12:903570.

2. Chen X, Zhang H, Ren S, et al. Gut microbiota and microbiota-derived metabolites in cardiovascular diseases. *Chin Med J* . 2023;136(19):2269-2284.

3. Zhang LS, Davies SS. Microbial metabolism of dietary components to bioactive metabolites: opportunities for new therapeutic interventions. *Genome Med*. 2016;8(1):46.

4. Krautkramer KA, Fan J, Bäckhed F. Gut microbial metabolites as multi-kingdom intermediates. *Nat Rev Microbiol*. 2021;19(2):77-94.

5. Yubero-Serrano EM, Fernandez-Gandara C, Garcia-Rios A, et al. Mediterranean diet and endothelial function in patients with coronary heart disease: An analysis of the CORDIOPREV randomized controlled trial. *PLoS Med*. 2020;17(9):e1003282.

6. Wang DD, Nguyen LH, Li Y, et al. The gut microbiome modulates the protective association between a Mediterranean diet and cardiometabolic disease risk. *Nat Med*. 2021;27(2):333-343.

7. Trotter RE, Vazquez AR, Grubb DS, et al. Bacillus subtilis DE111 intake may improve blood lipids and endothelial function in healthy adults. *Benef Microbes*. 2020;11(7):621-630.

8. Szulińska M, Łoniewski I, Skrypnik K, et al. Multispecies Probiotic Supplementation Favorably Affects Vascular Function and Reduces Arterial Stiffness in Obese Postmenopausal Women-A 12-Week Placebo-Controlled and Randomized Clinical Study. *Nutrients*. 2018;10(11). doi:10.3390/nu10111672

9. Sharon G, Garg N, Debelius J, Knight R, Dorrestein PC, Mazmanian SK. Specialized metabolites from the microbiome in health and disease. Cell Metab. 2014;20(5):719-730.

Supplementary Figures

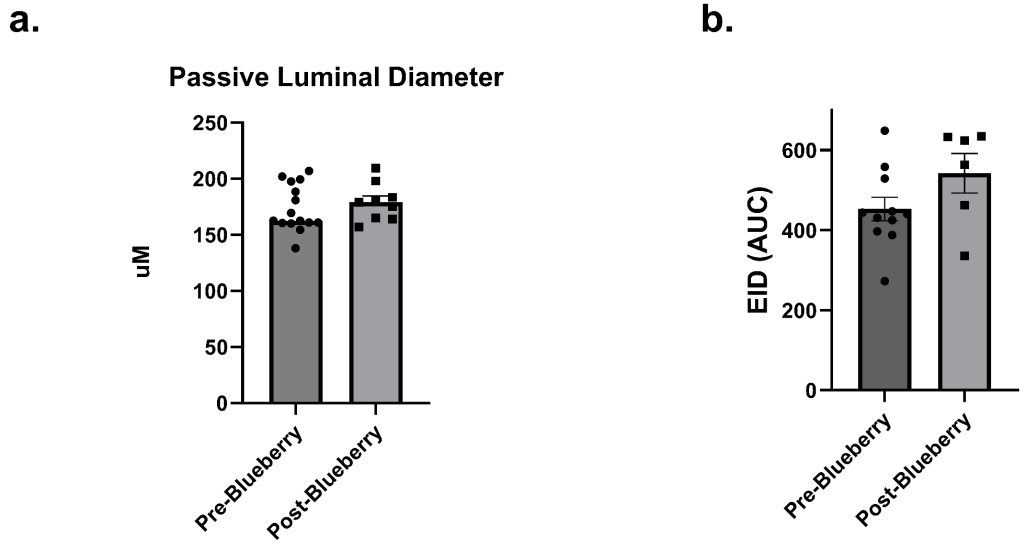

Supp. Figure 1: a.Passive luminal diameter of secondary mesenteric arteries.**b.** Endothelial-independent dilation area under the curve (EID-AUC). Statistical analysis was performed using an unpaired Student's t-test Data expressed as mean±SEM; *n*=8-13/group.

Supplementary Figures

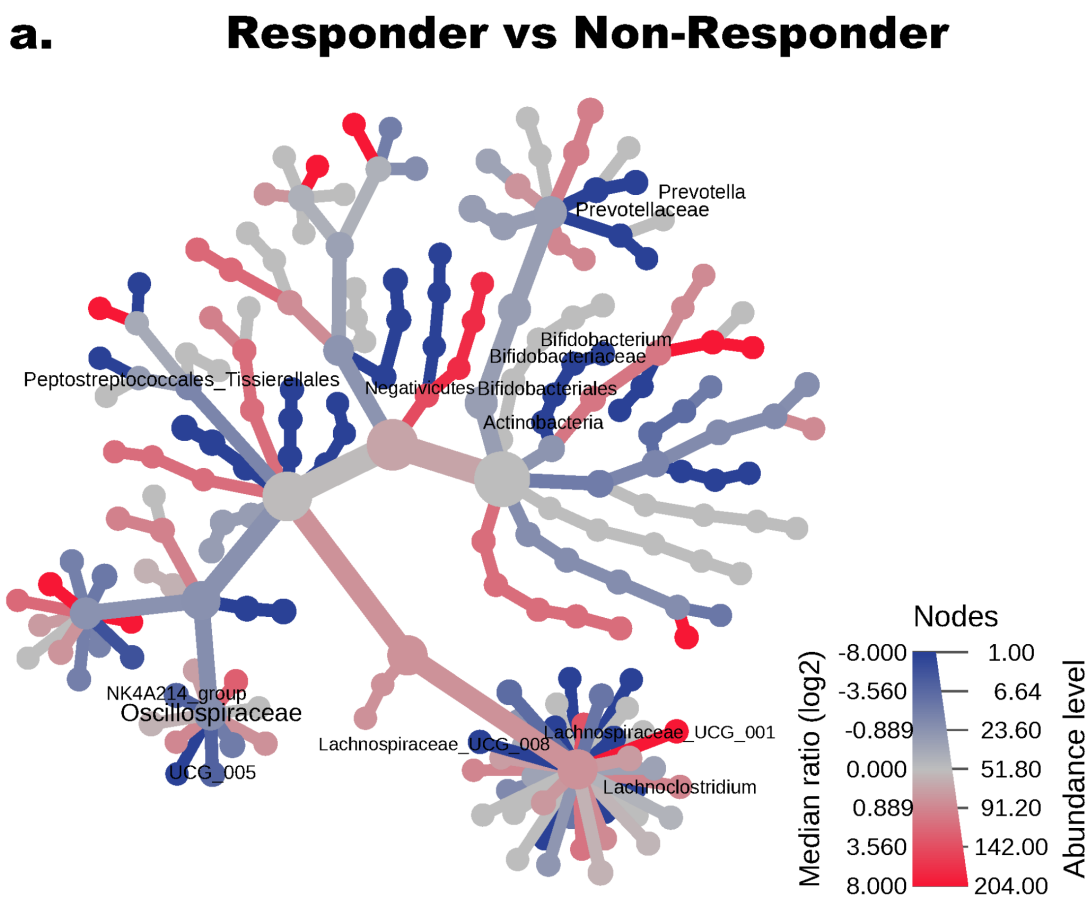

Supp. Figure 1a. Genera heat tree between responders and non-responders

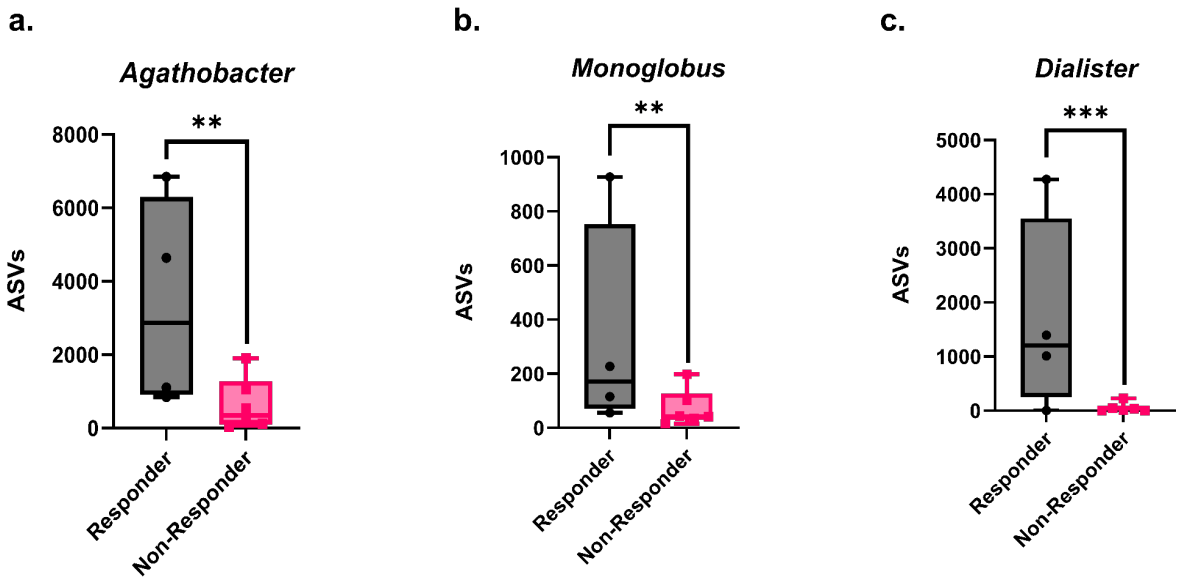

Supp. Figure 2. Polyphenol degrading bacterial genera higher in responders **a.** *Agathobacter* **b.** *Monoglobus* **c.** *Dialister* Statistics performed using EDGER single factor analysis in Microbiomeanalyst from 16s rRNA data to identify statistically significant genera. **p<0.005, ***p<0.0005. *n*=4-6/group.

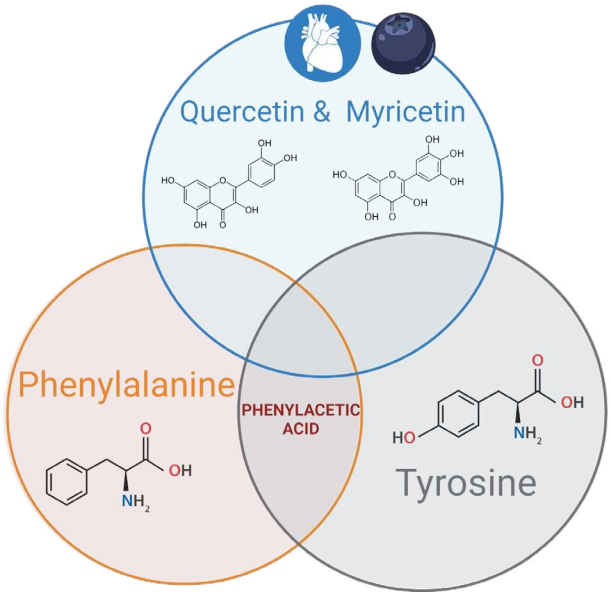

Supp. Figure 3a. Metabolism of quercetin, myricetin, phenylalanine, and tyrosine converge into phenylacetic acid.

Supplementary Figures

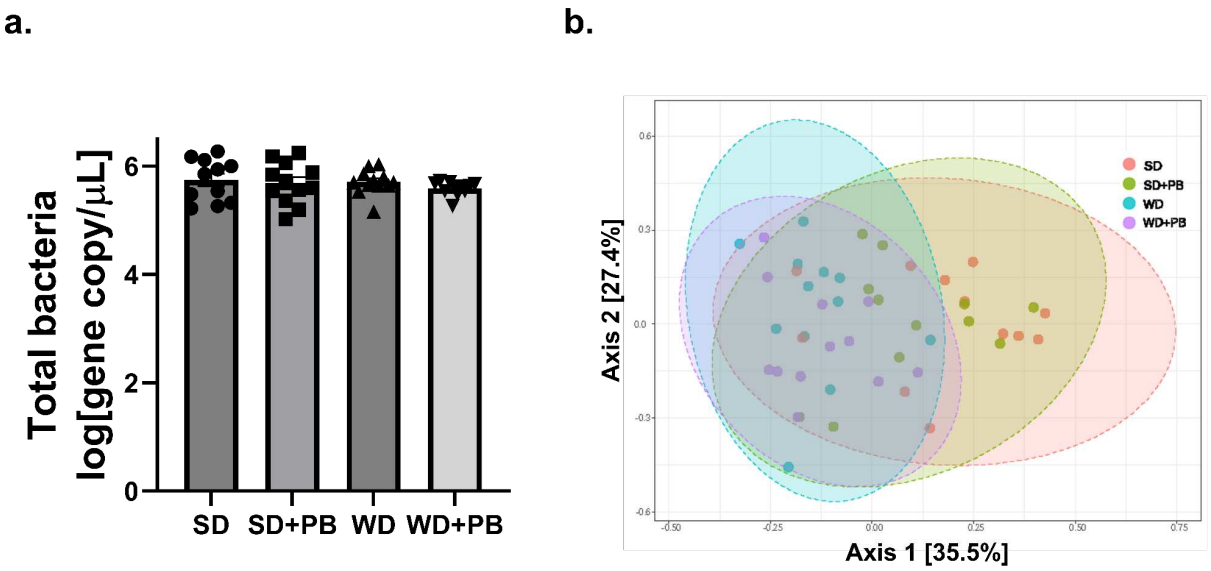

Supp. Figure 1 PB intervention does not alter fecal microbial content or beta diversity **a.** Total fecal bacterial count via qPCR **b.** Principle coordinate analysis (PCoA) of beta diversity at the phyla taxonomic level between all cohorts. Statistical analysis was performed using a one-way ANOVA (Supp. Figure 1a). PCoA using Bray-Curtis dissimilarity index with pairwise PERMANOVA and Benjamini-Hochberg false discovery rate, ellipses show the 95% confidence interval for each cohort (Supp. Figure 1b).

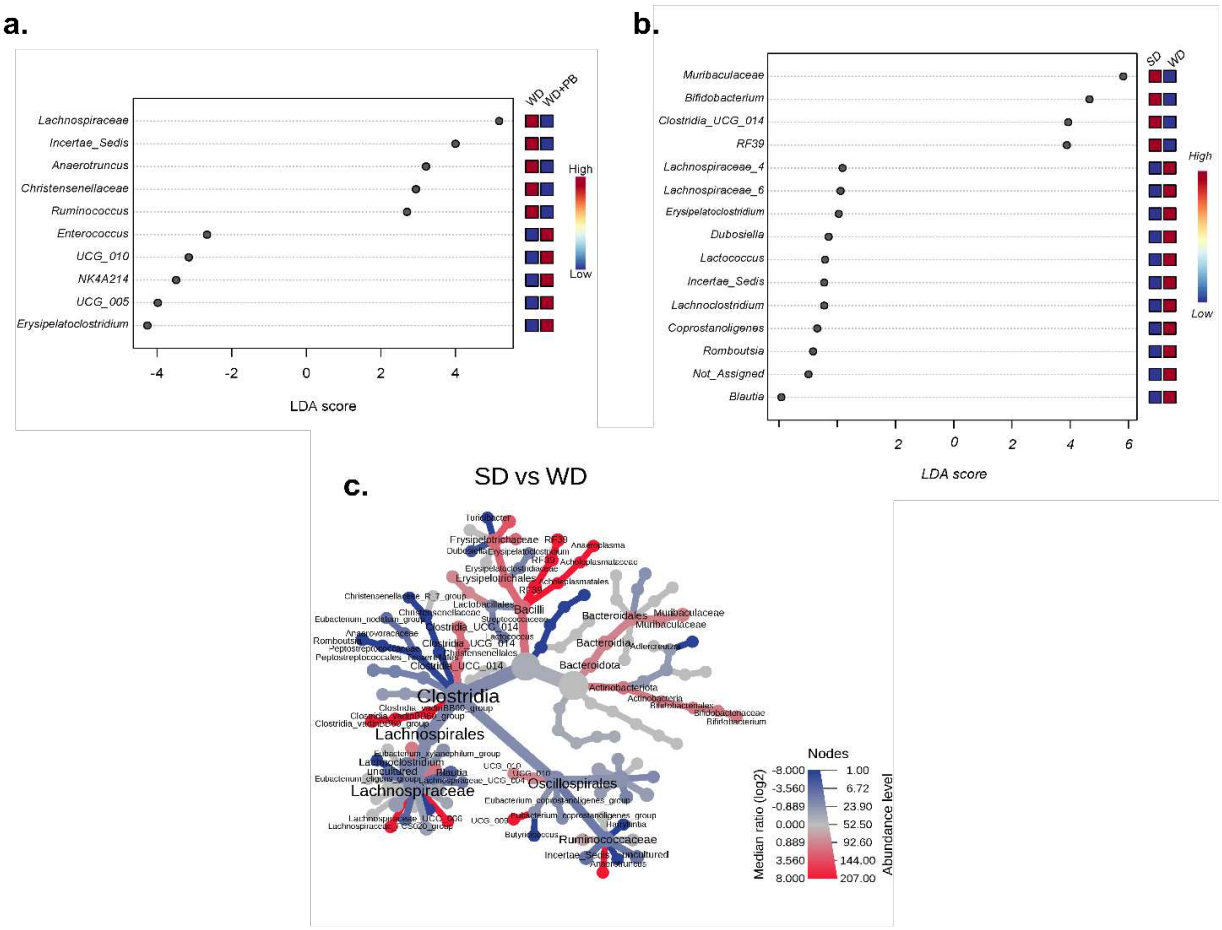

Supp. Figure 2 Diet, not PB treatment drives changes in microbial taxa. **a.** Heat tree of differentially abundant genera of WD vs WD+PB groups **b.** Heat tree of differentially abundant genera of SD vs WD groups **c.** Heat tree of differentially abundant taxa in SD and WD groups. Heat tree taxonomic classification was determined quantitatively using median abundance with non-parametric Mann-Whitney/Kruskal-Wallis test.

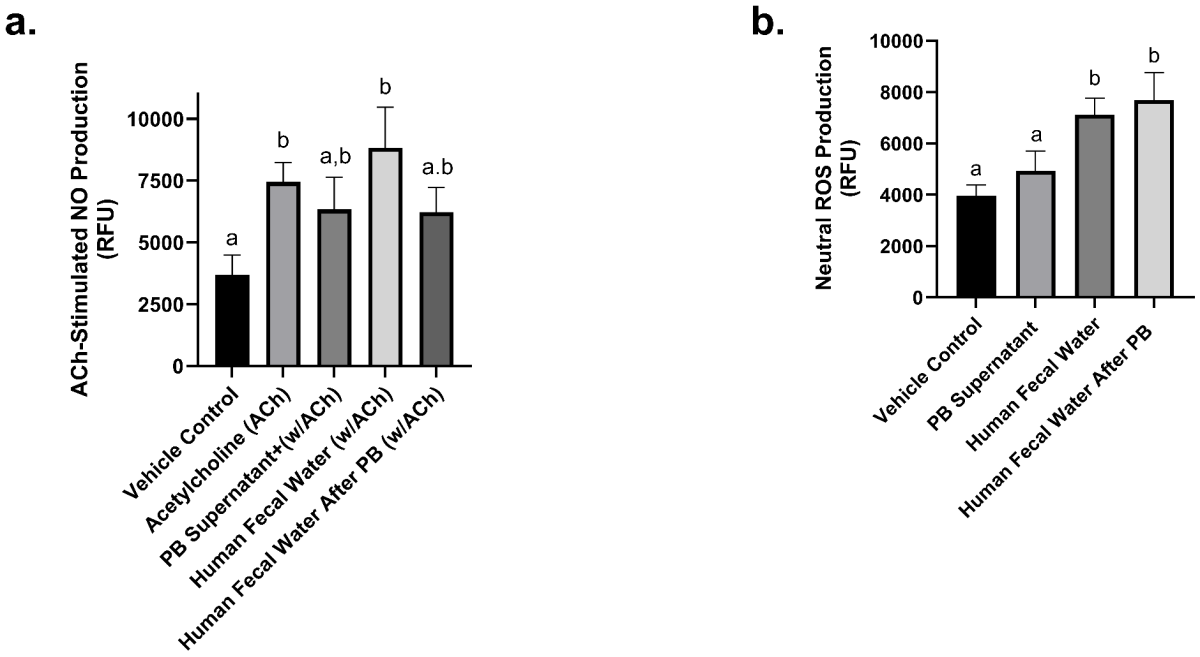

Supp. Figure 3 Fecal water increases ROS release in HUVECs when co-cultured with Caco2 cells. **a.** Nitric oxide (NO) production in PB supernatant, human fecal water, and human fecal water after PB treatment with acetylcholine (ACh) stimulation **b.** Reactive oxygen species (ROS) production in PB supernatant, human fecal water, and human fecal water after PB treatment Statistical analysis was performed using a one-way ANOVA either against ACh (Supp. Figure 3a) or the vehicle control (Supp. Figure 3b). When a significant main effect was observed, Tukey's post-hoc test was implemented to estimate pairwise comparisons. Data expressed as mean±SEM; *n*=8-12/group; *p<0.05, **p<0.005; RFU=relative fluorescence units

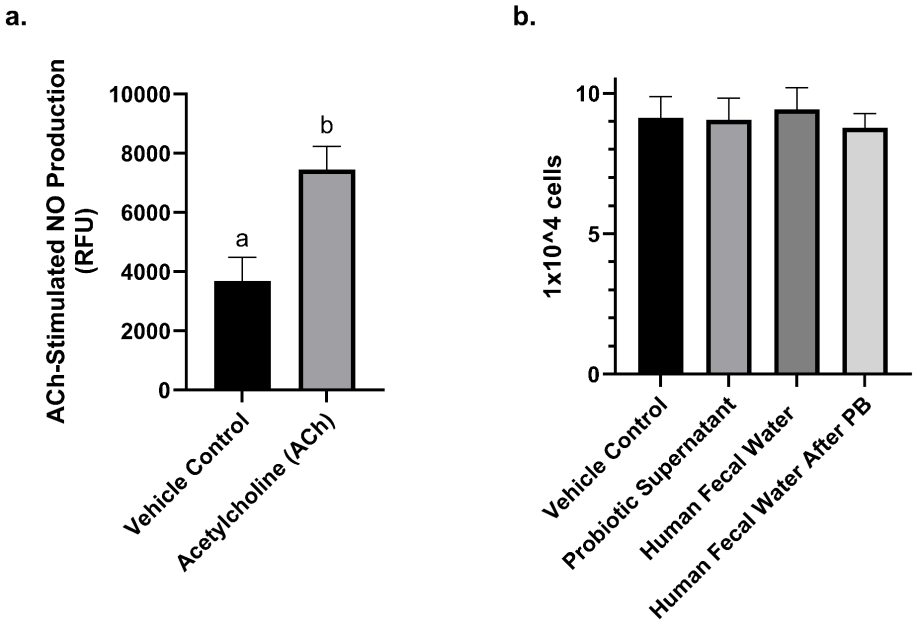

Supp. Figure 4 PB and fecal water treatments do not alter HUVEC cell viability **a.** ACh positive control increases NO detection in the HUVEC endothelium **b.** HUVEC cell viability. Statistical analysis was performed using an unpaired student's t-test (Supp. Figure 4a) or one way ANOVA (Supp. Figure 4b). Data expressed as mean±SEM; *n*=8-12/group; [a,b]p<0.005; RFU=relative fluorescence units

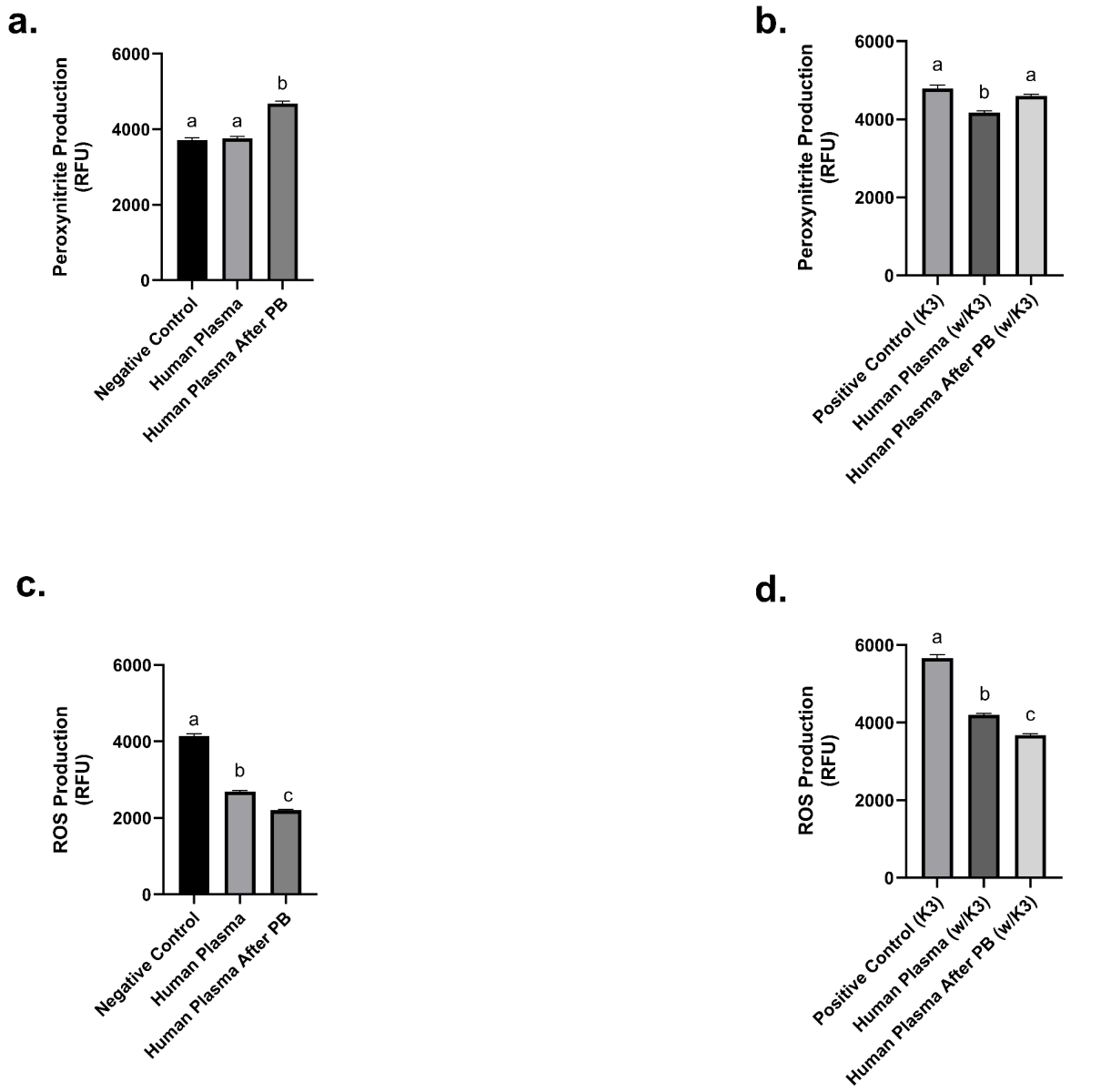

Supp. Figure 5 PB treatment in humans decreases ROS but not peroxynitrite release in plasma-conditioned HUVECs. **a.** Peroxynitrite release in basal conditions **b.** Peroxynitrite release after K3 stimulation **c.** General ROS release in basal conditions **d.** General ROS release after K3 stimulation. Statistical analysis was performed using a one-way ANOVA. When a significant main effect was observed, Tukey's post-hoc test was implemented to estimate pairwise comparisons. Data expressed as mean±SEM; *n*=3-7/group; K3=Vitamin K3 (menadione), RFU=relative fluorescence units. Plasma was from a single individual before and after a forty-five day PB intervention.